https://doi.org/10.1070/RCR5016

Coordination compounds of biogenic metals as cytotoxic agents in cancer therapy

Dmitry A. Guk, Olga O. Krasnovskaya, Elena K. Beloglazkina

Department of Chemistry, Lomonosov Moscow State University, Leninskie Gory 1, stroenie 3, 119991 Moscow, Russian Federation

The review summarizes the data on the structures and methods for the synthesis of compounds with anticancer activity based on biogenic metals, which can replace platinum drugs prevailing in cytotoxic therapy. The main focus is given to the comparison of the mechanisms of the cytotoxic action of these complexes, their efficacy and prospects of their use in clinical practice. This is the first systematic review of cytotoxic zinc, iron, cobalt and copper compounds. The structure – activity relationships and the mechanisms of antitumour action are formulated for each type of metal complexes.
The bibliography includes 181 references.

Contents

1. Introduction 1566
2. Zinc coordination compounds as cytotoxic agents 1568
2.1. Octahedral, square-pyramidal and tetrahedral zinc(II) coordination compounds 1568
2.2. Square-planar zinc(II) compounds 1577
2.3. Effect of ligand structure on cytotoxicity 1577
2.4. Prospects of the development of anticancer agents based on zinc ions 1578
3. Iron coordination compounds as cytotoxic agents 1578
3.1. Cytotoxic ferrocene derivatives 1584
3.2. Cytotoxic half-sandwich iron complexes 1586
3.3. Classical iron coordination compounds with cytotoxic activity 1586
3.3.1. Octahedral iron(II and III) coordination compounds 1586
3.3.2. Square-pyramidal iron(III) coordination compounds 1588
3.3.3. Bipyramidal iron(II) coordination compounds 1588
3.3.4. Tetrahedral iron(III) coordination compounds 1589
3.3.5. Trigonal-prismatic iron(II) coordination compounds 1589
3.4. Prospects of the development of anticancer agents based on iron ions 1590
4. Cobalt coordination compounds as cytotoxic agents 1590
4.1. Octahedral cobalt(III) coordination compounds 1596
4.2. Octahedral cobalt(II) coordination compounds 1597
4.3. Tetrahedral cobalt(II) coordination compounds 1599
4.4. Bipyramidal cobalt(II) coordination compounds 1600
4.5. Square-planar cobalt(II) coordination compounds 1601
4.6. Prospects of the development of anticancer agents based on cobalt ions 1602
5. Copper coordination compounds as cytotoxic agents 1602
5.1. Square-pyramidal copper(II) coordination compounds 1602
5.2. Square-planar copper(II) coordination compounds 1612
5.3. Octahedral copper(II) coordination compounds 1613
5.4. Tetrahedral copper(II) coordination compounds 1614
5.5. Trigonal-bipyramidal copper(II) coordination compounds 1614
5.6. Tetrahedral copper(I) coordination compounds 1615
5.7. Triangular and trigonal-pyramidal copper(I) coordination compounds 1615
5.8. Prospects of the development of anticancer agents based on copper ions 1616
6. Conclusion 1617
7. List of acronyms and abbreviations 1617

D.A.Guk. Junior Researcher at the Division of Organic Chemistry of the Department of Chemistry of MSU.
E-mail: dmh200949@gmail.com
Current research interests: anticancer agents, chemistry of coordination compounds, organic synthesis, chemistry of organoelement compounds.
O.O. Krasnovskaya. Ph.D. in Chemistry, Researcher at the same Division.
E-mail: krasnovskayao@gmail.com
Current research interests: anticancer agents, chemistry of coordination compounds, organic synthesis.
E.K. Beloglazkina. Doctor of Chemical Sciences, Professor at the same Division.
E-mail: beloglazki@mail.ru
Current research interests: synthesis and reactivity of organonitrogen and organosulfur compounds, organic ligands, coordination chemistry, nanomaterials.

Translation: T.N.Safonova

1. Introduction

The diagnosis and treatment of malignant tumours are challenges for modern medicine. Cancer is the second most common cause of death after cardiovascular diseases. The development of new effective anticancer drugs is a significant research area of medicinal chemistry. By 2017, the US Food and Drug Administration (FDA) approved 150 anticancer drugs, about 2/3 of them being approved in the past two decades.[1]

Anticancer drugs containing metal ions play an important role in cancer chemotherapy. Since the discovery of anticancer activity, cisplatin (*cis*-$[Pt(NH_3)_2Cl_2]$) has been and remains one of the most common chemotherapeutic drugs for the treatment of a number of different types of cancer.[2] Second- and third-generation platinum agents,

Received 16 February 2020
© 2021 Uspekhi Khimii, ZIOC RAS, Russian Academy of Sciences and IOP Publishing Limited

such as carboplatin, oxaliplatin and picoplatin, have been developed and introduced into clinical practice.[3]

However, the therapeutic application of Pt drugs has disadvantages, such as severe side effects related to the abiogenic nature of platinum and its accumulation in patients because of the absence of naturally occurring mechanisms of excretion of this metal from the body. The most common adverse effects negating the positive effect of chemotherapy are nephrotoxicity,[4] neurotoxicity,[5] as well as ototoxicity and myelosuppression.[3] Therefore, the research attention is increasingly focused not on the modification of platinum compounds but on the search for new cytotoxic coordination compounds of biogenic transitions metals, which should have lower overall toxicity and should be easily excreted from the body.[4]

Biogenic metals include zinc, iron, cobalt and copper, as nutritionally essential trace elements in the human body, which can potentially replace platinum drugs prevailing in cytotoxic therapy. According to the *Web of Science* database (Fig. 1), the past five years have witnessed an explosive growth of the number of publications on coordination compounds of these metals as anticancer agents.

The biological role of zinc was described in detail. This element is the sixth most abundant metal in the human body (behind calcium, sodium, potassium, magnesium and iron). Zinc is involved in cell metabolism and is present in the active sites of more than 200 metalloenzymes.[6,7] Zinc(II) complexes with different organic ligands were successfully tested *in vitro* for anti-inflammatory,[8] antibacterial,[9] antioxidant [10] and antiproliferative activity (see Section 2.3).

Iron has important functions in mammalian cells. Iron ions ensure the correct functioning of essential enzymes containing either free iron or the haem, in particular mitochondrial enzymes involved in cellular respiration, enzymes necessary for DNA synthesis and the cell cycle, enzymes of the antioxidant system, such as peroxidase and catalase, and many other.[11] Consequently, iron is required for DNA replication, cell viability and cell growth. However, the ability of iron to accept and donate electrons makes iron ions a critical component of the active site of enzymes and allows iron to participate in the production of free radicals potentially harmful for the body. These processes include the Fenton reaction of divalent iron with hydrogen peroxide, in which iron donates an electron, resulting in the formation of a hydroxyl radical and reactive oxygen species (ROS). These species not only damage lipids and proteins but also cause oxidative damage to DNA, including base modification in double-stranded DNA and DNA interstrand crosslinks,[12,13] which can be mutagenic.[14] Consequently, iron in the human body is not only an indispensable element but is also potentially toxic.

Cobalt is an essential redox trace element highly abundant in mammalian cells. In the body, it exists in three relatively stable (which are often converted into each other) oxidation states: Co^{I}, Co^{II} and Co^{III}. This metal plays an important role in the chemistry of vitamin B_{12} (cobalamin) and is involved in redox processes, alkylation and the free radical generation (destruction) in the living cell.[15] Cobalt ions actively participate in the maintenance of homeostasis of reactive oxygen species and radicals, thereby making it simultaneously indispensable in the cell and potentially toxic.

Copper ions play an important role in the metabolism of the human body due to the involvement in different physiological processes (the development of connective, bone and nerve tissues, angiogenesis) and the participation in the functioning of a number of redox metalloenzymes.[16,17] A number of copper coordination compounds are currently in different phases of clinical trials as anticancer agents (*e.g.*, first- and second-generation Casiopeinas [18]). Some known copper-containing derivatives exhibited significant cytotoxic activity in *in vitro* assays (see Section 5.8).

This review summarizes the data on the structures, mechanisms of action and the efficiency and prospects of further studies of cytotoxic coordination compounds based on biogenic metals such as Zn, Fe, Co and Cu. The published data are divided into sections. Each section is devoted to the analysis of scientific publications over the

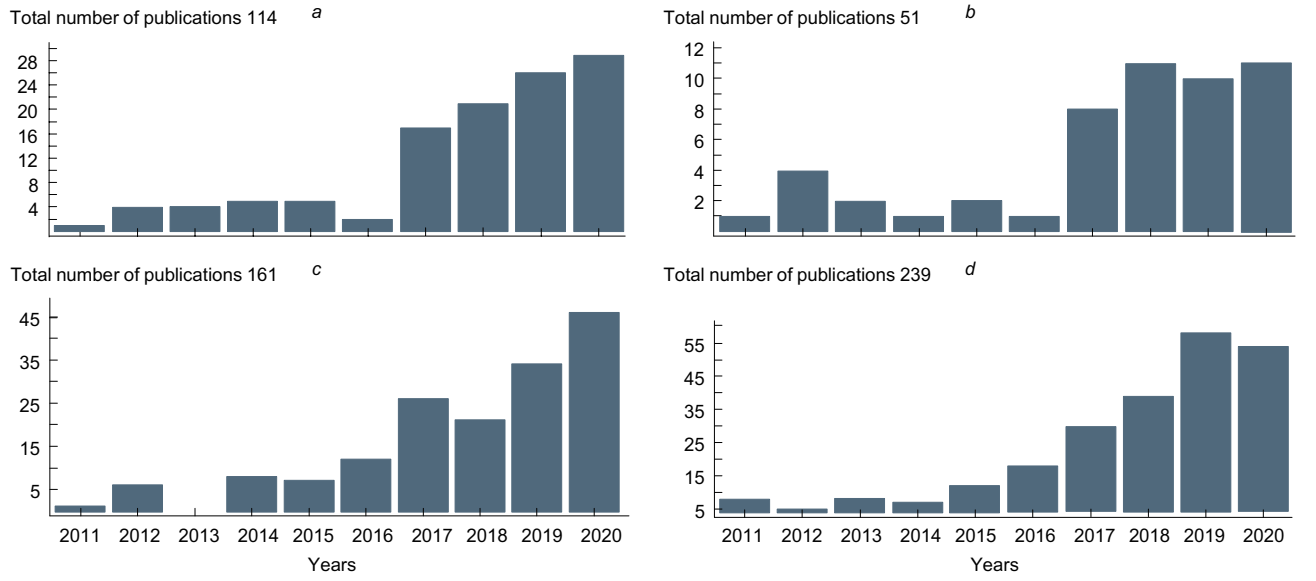


Figure 1. Number of publications on zinc (*a*), iron (*b*), cobalt (*c*) and copper (*d*) coordination compounds with anticancer activity over the period from 2011 to 2020 (the search by key words 'coordination compound', 'anticancer' and the chemical symbol of the corresponding metal) found in *Web of Science* of April 2021.

past decade on complexes of a particular metal exhibiting the proven anticancer activity. The main goal of the review is to reveal the dependence of the mechanism of cytotoxic activity on the oxidation state of the metal in the coordination compound and on the geometry and chemical nature of the ligand environment. Hence, we selected mainly the publications concerning the mechanisms of cytotoxic activity. The exceptions are studies of coordination compounds having a rare geometry, in which only putative mechanisms of their action or molecular targets are suggested because of an insufficient number of representatives. The final section of the review presents a comparative analysis of the advantages and drawbacks of coordination compounds of the metals under consideration, the mechanisms of their cytotoxic activity and prospects of application for the further development of anticancer agents.

It is worth noting that most of the recent literature reviews on the use of metal complexes as cytotoxic agents focus on the analysis of coordination compounds of only one transition metal, most often platinum,[19–21] or, in one case, of platinum group metals.[22] This review is the first to bring together the data on cytotoxic compounds of different biogenic metals and to compare them in terms of the mechanisms of action. It should also be noted that there are a few Russian reviews on this issue that summarize the data on individual classes of platinum coordination compounds[23] and different dosage forms of platinum drugs.[24] Besides, there are reviews on cytotoxic coordination compounds based on gold[25] rather than on platinum group metals and on a small number of coordination compounds with one ligand.[26] The recent review[27] devoted to the analysis of individual mechanisms of action of different compounds includes a small Section on transition metal complexes, in particular biogenic metals. Meanwhile, reviews concerned with the cytotoxic and anticancer activity of coordination compounds of biogenic metals were lacking at the time of the writing of this review.

2. Zinc coordination compounds as cytotoxic agents

Among oxidation states characteristic of zinc, the oxidation state 2+ is the most stable under physiological conditions. Hence, in studies aimed at searching for cytotoxic zinc coordination compounds, the researchers varied the ligand environment of zinc(II) ions, which are abundant in living organisms. The published data on Zn^{II} complexes with proven cytotoxicity are summarized in Table 1.†

An analysis of the publications on the synthesis of zinc coordination compounds with cytotoxic activity shows that the tetrahedral (17 examples in 35 publications, the proportion is 48%), octahedral (11 examples, 31%) and square-pyramidal (6 examples, 17%) geometries of the coordination sphere are the most typical of Zn^{II} ions, although rare examples of square-planar ligand environment are also known (5 examples, four of which refer to substituted zinc porphyrinates, 14%). In the case of bulky and polydentate ligands, the coordination polyhedra can be significantly distorted, although they are not transformed into each other and differ according to the X-ray diffraction data.

To establish the dependence of the mechanisms of cytotoxic activity on the geometry and chemical nature of the ligand environment, this Section focuses on mononuclear Zn^{II} coordination compounds exhibiting significant cytotoxicity against cancer cell lines. An analysis of the structure–activity relationships for dinuclear and polynuclear structures is often a complicated issue because different metal ions have different coordination geometry and it is often difficult to distinguish the contributions of each structure to the cytotoxicity, evaluate the synergistic effect, *etc*.

The consideration of the chemical nature of ligands of cytotoxic zinc complexes (see Table 1 and references therein) shows that the coordination environment of the metal ion in the majority of the characterized complexes involves two or more oxygen atoms. This is attributed to high oxophilicity of the zinc atom and its tendency to form bonds with charged chalcogens atoms (primarily with oxygen and sulfur). The vacancies of the zinc coordination sphere are filled by donor ligands, most often by those containing nitrogen atoms or halide ions and polar solvent molecules, which do not leave the coordination sphere upon the interaction of an inorganic zinc salt with an organic ligand. Besides, it is worth noting that the small size of the zinc ion has stimulated researchers to look for coordination compounds stable under physiological conditions using polydentante and chelating ligands (30 out of 35 papers), which are less prone to exchange with solvent molecules or polar moieties of cellular proteins.

In some of these studies, the authors attempted to elucidate the mechanism of cytotoxic activity of the synthesized compounds and concluded that zinc complexes are characterized by a wide spectrum of the possible mechanisms of action. These mechanisms involve those common to all metal coordination compounds (DNA intercalation and binding, the generation of reactive oxygen species, the induction of apoptosis *via* the mitochondrial pathway) and also the possibility of inhibition of haem oxygenase-1 (HO-1) unique for zinc compounds and the Wnt signaling pathway. However, a comparison of the data on the putative mechanism of cytotoxic activity in representative samples of biologically active zinc compounds with different coordination geometry makes it possible to reveal a number of general patterns.

2.1. Octahedral, square-pyramidal and tetrahedral zinc(II) coordination compounds

Zinc(II) coordination compounds with octahedral, square-pyramidal and tetrahedral geometry were characterized in most detail. These compounds have a common mechanism of action but differ in interactions with the same molecular targets, affecting the overall IC_{50} values. Thus, a comparison of the interactions of different Zn complexes with DNA shows that the intercalation is most typical of the octahedral coordination compounds $[Zn(dppt)_2Cl_2]$ (**1**),[36] $[Zn_3(fen)_6(MeOH)_2]$ (**2**), $[Zn(fen)_2(tmen)]$ (**3**), [Zn(bapen)(fen)]fen (**4**) and $[Zn(cyclam)(fen)_2]$ (**5**).[48]

Meanwhile, square-pyramidal complexes **6**–**13** bind to DNA *via* two pathways — by intercalating into DNA[60,61] or electrostatically binding to the minor groove.[43]

Tetrahedral structures **14**–**27** bind to double-stranded DNA mainly through electrostatic interactions,[32] occupying the major or minor groove.[46,49,58]

† In this review, the references in all tables are given in chronological order (according to the publication date of the original paper beginning from 2010), the serial numbers of the compounds are given in accordance with the numbers of their structures in the respective subsections, and the names of the cell lines are decoded in the List of acronyms and abbreviations (Section 7).

Table 1. Cytotoxic zinc coordination compounds.

No.	Complex (serial number of the compound)	Coordination sphere	Binding mode	Metal coordination geometry	Mechanism of cytotoxic activity	IC_{50} max (cell line)	Ref.
1	$[Zn(AcPipPheF)_2]$ (**36**), $[Zn(OAc)(AcPipPheF)]_2$ (**37**)	ZnN_2O_2S	Tridentate chelate with a bridging acetate anion	Square-pyramidal or octahedral	Arrest of the cell cycle at the S phase	25.5 ± 6 nM (K562)	28
2	$[Zn(R\text{-}DT)_2]$ (**38**–**41**, **45**)	ZnS_4	Bidentate	Tetrahedral	Induction of apoptosis (also active against Pt-resistant cell lines)	0.1 – 1 μM (A431, A431Pt)	29
3	ZnPP (**48**)	ZnN_4	Chelate	Square-planar	Inhibition of haem oxygenase-1 (HO-1)	3.1 μM (MCF-7), the toxicity against a number of cell lines is ~10 μM	30
4	ZnPP (**48**)	ZnN_4	Chelate	Square-planar	Inhibition of the Wnt/b signaling pathway	~10 μM	31
5	α,ω-Bis{diacetyl-2-(4-*N*-thio-semicarbazone)-3-(4-*N*-thio-semicarbazone)zinc(II)}alkanes (**14**–**17**)	ZnN_2S_2	Chelate	Tetrahedral	Binding to DNA (electrostatic)	< 0.1 μM (MCF-7, HepG2)	32
6	$[Zn(L^1)_2 \cdot 2\,H_2O](AcO)_2$ (see [a])	$ZnN_2S_2(H_2O)_2$	Bidentate	Distorted octahedral	Unknown	97% Inhibition at C = 100 μM (HT-29)	33
7	Zn bis(pyrazolyl)acetamide complexes (**26**–**29**)	ZnN_4O_2	Tridentate chelate	Octahedral	Induction of apoptosis through caspase-7 activation	18 ± 5 μM (MCF-7)	34
8	$[Zn(pysR)_2]$, $[Zn(pysR)_2)(AcO)]_2$ (R = Me, Bn)	ZnN_4S_2	Tridentate chelate	Distorted octahedral	Unknown, substituents in the ligand have no effect on IC_{50}	0.39 – 0.84 μM (HeLa, HL-60)	35
9	$[Zn(dppt)_2Cl_2]$ (**1**)	ZnN_4Cl_2	Bidentate chelate	Octahedral	Intercalation into DNA	10.44 ± 0.52 μM (MCF-7)	36
10	$[Zn(AP)_2I_2]$ (**46**)	ZnO_2I_2	Monodentate	Tetrahedral	Inhibition of caspase-3; not apoptosis	100 μM (NCTC L929)	37
11	ZnPP (**48**)	ZnN_4	Chelate	Square-planar	Unknown	~10 μM (HeLa)	38
12	Zn 2-(2-pyridyl)imidazo[1,2-*a*]-pyridine complexes (**30**–**34**)	ZnN_2O_2	Bidentate chelate	Tetrahedral	Unknown; related Cu complexes are more cytotoxic	13.2 μM (HT-29)	39
13	$Zn(N\text{-}R\text{-}chtsc)_2$ (R = Me (**50**), Ph (**51**))	ZnN_2S_2	Bidentate chelate	Distorted square	Inhibition of topoisomerase 1, binding to the minor groove of DNA followed by oxidative DNA cleavage	2 – 3 μM (Caki-2, MCF-7, CaSki, NCI-H322M, Co-115)	40

Table 1 (continued).

No.	Complex (serial number of the compound)	Coordination sphere	Binding mode	Metal coordination geometry	Mechanism of cytotoxic activity	IC_{50} max (cell line)	Ref.
14	Zn^{II}-Cyclen-$(Trp)_2$ (**49**)	ZnN_4	Chelate	Distorted square	Binding to the minor groove of DNA, DNA damage, induction of caspase-3-dependent apoptosis	25 μM (U-87 MG), toxicity against normal cells is six times lower	41
15	$Zn_2(L^2)_2$ (see [b])	$ZnSNO_2$	Tridentate chelate + H_2O	Distorted tetrahedral	ROS-Mediated induction of apoptosis	50 μM (CEM/ADR5000), 500 μM against normal cells	42
16	[Zn(TTA)(bipy)Cl] (**12**), [Zn(TTA)(phen)Cl] (**13**)	ZnN_2O_2Cl	Bidentate	Square-pyramidal	Electrostatic binding to the minor groove of DNA followed by the induction of apoptosis	1 – 1.5 μM (MKN-45, MCF-7)	43
17	$Zn(AcTsc)_2$ (**25**)	ZnN_2S_2	Bidentate chelate	Distorted tetrahedral	Intercalation into DNA	36 μM (HepG-2, IM-9)	44
18	$[Zn(AP)_2I_2]$ (**46**), $[Zn(Caf)(H_2O)I_2]$ (**47**)	ZnN_2I_2	Bidentate chelate	Tetrahedral	Unknown	50 – 70 μM (PC3, MCF-7)	45
19	$[Zn(L^{Thio}SN)_2]$ (**18**), $[Zn(L^{Br}SN)_2]$ (**19**), $[Zn(L^{DiOMe}SN)_2]$ (**20**) [c]	ZnN_2S_2	Bidentate chelate	Tetrahedral	Non-covalent binding to the groove of DNA	~20 μM (HeLa, MCF-7)	46
20	$[ZnL](ClO_4)_2$ (L is *N*,*N*′-bis-(salicylidene)-4R-phenylene-1,2-diamine (R = H (**52**), F (**53**), CF_3 (**54**)))	ZnN_2O_2	Tetradentate chelate	Square-planar	Selective binding to G4-DNA	Not measured	47
21	$[Zn_3(fen)_6(MeOH)_2]$ (**2**), $[Zn(fen)_2(tmen)]$ (**3**), [Zn(bapen)(fen)]fen (**4**), [Zn(cyclam)(fen)$_2$] (**5**)	ZnO_4, ZnN_2O_2, ZnN_4O_2, ZnN_4O_2	Monodentate with additional N ligands	Tetrahedral, distorted octahedral, octahedral	Intercalation only of the octahedral complex into DNA; in other cases, weak binding to the groove	Not measured	48
22	$[Zn(3\text{-}FC_6H_4CH_2CO_2)_2]$ (**21**), $[Zn_3(3\text{-}FC_6H_4CH_2CO_2)_6(phen)_2]$ (**22**), $[Zn_3(3\text{-}FC_6H_4CH_2CO_2)_6(bipy)_2]$ (**23**)	ZnO_4, ZnO_6, ZnO_6	Monodentate	Tetrahedral, octahedral, octahedral	Binding to the groove; intercalation is impossible because the complexes are polynuclear. The binding of the tetrahedral complex to the groove is stronger compared to the octahedral complexes	Not measured	49
23	$[Zn_2(azil)_2(H_2O)_4]\cdot 2\,H_2O$ (**35**)	$ZnNOO_2(H_2O)$	Bidentate chelate	Tetrahedral	Generation of ROS leading to the induction of apoptosis *via* the mitochondrial pathway through caspase-9 activation	155 ± 12 μM (A549), non-toxic up to 250 μM against normal cells (MRC5)	50

Table 1 (continued).

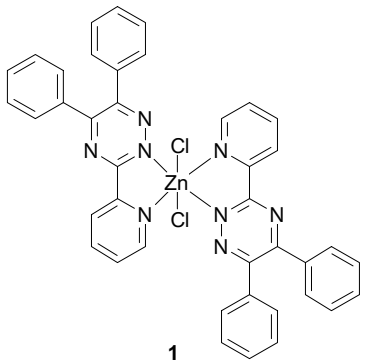
No.	Complex (serial number of the compound)	Coordination sphere	Binding mode	Metal coordination geometry	Mechanism of cytotoxic activity	IC_{50} max (cell line)	Ref.
24	$[Zn(L^3)Cl]$ [d]	ZnN_4Cl	Tetradentate chelate	Distorted square-pyramidal	Putative ROS generation	10 – 11 μM (MCF-7)	51
25	$Zn(Caf)(H_2O)Hal_2$ (Hal = Cl (**47**), I (**55**))	$ZnNOHal_2$	Monodentate	Tetrahedral	Activation of necrosis-associated genes mainly in MCF-7	10^{-4} M (MCF-7)	52
26	Dichlorobis[1-(4-bromobenzyl)-2-phenyl-1*H*-benzimidazole-κN^3]zinc(II)	ZnN_2Cl_2	Monodentate	Tetrahedral	Unknown	0.05 μM (A2780)	53
27	[Zn(Sal-Gly)(NN)(H_2O)] (NN = Clphen, amphen, epoxyphen, 4,7-diphenyl-1,10-phenanthroline)	ZnN_3O_3	Chelate + bidentate N,N ligand	Octahedral	Induction of apoptosis *via* the mitochondrial pathway (probably through ROS generation)	1.73 – 5.8 μM (A2780) with SI(V79) 2.3 – 6.0 μM	54
28	$[ZnHal_2L]$ (Hal = Br, I; (L are 4-(*o*-, *m*-, *p*-hydroxyphenyl)-terpyridines)	ZnN_3Hal_2	Chelate	Square-pyramidal	Putative binding to heat shock protein Hsp90	0.116 – 0.201 μM (HCT-8), 0.519 – 2.039 μM (A549), 0.899 – 3.049 μM (MCF-7)	55
29	$Zn(Caf)(H_2O)Br_2$ (**56**)	$ZnNOBr_2$	Monodentate	Tetrahedral	Activation of necrosis-associated genes mainly in MCF-7	10^{-4} M (MCF-7)	56
30	Bis{(*E*)-2-[(1*H*-indol-3-yl)methylene]-R-hydrazinecarbothioamide}zinc(II) (R = H (**57**), Me (**58**), Et (**59**), Hex (**60**))	ZnN_2S_2	Bidentate chelate	Intermediate between tetrahedral and planar-square	Induction of apoptosis in the A549 and MCF-7 cell lines, can intercalate into DNA	37.9 – 100 μM (A549), 60.3 – 88.1 μM (MCF-7); 20 – 30% less active against normal MCF-10A, HEK-293, L929 cell lines	57
31	$Zn(HL^4)$ (**24**) [e]	ZnN_2O_2	Tetradentate chelate	Distorted tetrahedral	Induction of necrosis and apoptosis in an equal ratio. Binding to the minor groove of DNA	6.4 μM (K562)	58
32	$[Zn(Hal\text{-}Q)_3]$, $K[Zn(Hal\text{-}Q)_2H_2O]$ (Hal-Q = dClQ, dBrQ, 7-BrQ, CQ)	ZnN_2O_4	Bidentate	Octahedral	Unknown, non-selective against normal cells, similar toxicity against bacteria	1.8 – 7.1 μM (HCT 116)	59
33	$[\{Zn(L^5)(DMSO)_2\}_2]\cdot$ DMSO (**6**), $[\{Zn(L^6)Cl\}_2]$ (**7**), $[(Zn_2(L^7))_2(\mu\text{-}OAc)_2(\mu^3\text{-}O)_2]$ (**8**) [f]	$ZnO_2NSO(DMSO)$, ZnN_2S_2Cl, ZnO_5	Chelate	Square-pyramidal	Intercalation into DNA, intercalation of dimers is more efficient compared to the tetramer. Chromatin condensation followed by the induction of apoptosis	16.26 – 53.8 μM (HeLa)	60

Table 1 (continued).

No.	Complex (serial number of the compound)	Coordination sphere	Binding mode	Metal coordination geometry	Mechanism of cytotoxic activity	IC_{50} max (cell line)	Ref.
34	$[Zn(L^8)_2(phen)]$ (**9**), $[Zn_2(L^9)_4(bipy)_2]$ (**10**), $[Zn(L^9)_2(bipy)H_2O]$ (**11**) [g]	ZnO_4N_2, ZnO_3N_2, ZnO_3N_2	Bidentate	Octahedral, pseudooctahedral, square-pyramidal	Intercalation into DNA; in similar systems, the intercalation of the octahedral complex is more efficient compared to the pseudo-octahedral complex, the intercalation of the square-pyramidal complex is the least efficient	Not measured	61
35	$[Zn(Caf)(H_2O)Hal_2]$ (Hal = Cl, Br, I)	ZnN_2Hal_2	Monodentate	Square-planar	Unknown	$\sim 5 \times 10^{-4}$ M (MCF-7)	62

Note. The following abbreviations are used: IC_{50} is the half-maximal inhibitory concentration, in mol L^{-1} (M); HAcPipPheF is 2-acetylpyridine N^4-1-(4-fluorophenyl)piperazinolthiosemicarbazone, R-DT is R-substituted dithiocarbamate, PP is protoporphyrin IX, HpysR is Schiff base of pyridine-2-carboxaldehyde and S-substituted dithiocarbazate (R = Me, Bn), dppt is 3-(2-pyridyl)-5,6-diphenyl-1,2,4-triazine, AP is antipyrine, chtsc is cyclohexanone thiosemicarbazone, cyclam is 1,4,8,11-tetraazacyclotetradecane, Cyclen is 1,4,7,10-tetraazacyclododecane, Trp is tryptophan, TTA is 4,4,4-trifluoro-1-(2-furyl)butane-1,3-dione, bipy is 2,2′-bipyridine, phen is 1,10-phenanthroline, AcTsc is 3-acetylcoumarin thiosemicarbazone, Caf is caffeine, Hfen is fenamic (2-phenylaminobenzoic) acid, tmen is *N*,*N*,*N*′,*N*′-tetramethylethylenediamine, bapen is *N*,*N*′-bis(3-aminopropyl)ethylenediamine, azil is azilsartan, Sal is salicylate, Gly is glutamate, Clphen is 5-chloro-1,10-phenanthroline, amphen is 5-amino-1,10-phenanthroline, epoxyphen is 5,6-epoxy-5,6-dihydro-1,10-phenanthroline, Hex is n-hexyl, dClQ is 5,7-dichloroquinolin-8-ol, dBrQ is protonated 5,7-dibromoquinolin-8-ol, 7-BrQ is 7-bromoquinolin-8-ol, CQ is 5-chloro-7-iodoquinolin-8-ol. [a] L^1 is 4-[(5-bromo-2-hydroxybenzylidene)amino]-3-methyl-1,2,4-triazole-5-thione; [b] H_2L^2 is 2-[(2-hydroxy-3-methoxybenzylidene)amino]-3-sulfanylpropionic acid; [c] $L^{Thio}SN$ is (*E*)-[2-(2-thienylmethyleneamino)phenylsulfanyl, $L^{Br}SN$ is (*E*)-[2-(4-bromophenylmethyleneamino)phenylsulfanyl, $L^{DiOMe}SN_2$ is (*E*)-[2-(3,4-dimethoxyphenylmethyleneamino)phenylsulfanyl; [d] L^3 is *N*,*N*′-bis[1-(2-pyridyl)ethylidene]-2,2-dimethylpropane-1,3-diamine; [e] H_3L^4 is 2-hydroxy-1,3-bis{2-[(2-hydroxy-5-nitrophenylmethylene)aminomethyl]phenyloxy}propane; [f] H_2L^5 is hydroxynaphthaldehyde 4-(*p*-methoxyphenyl)thiosemicarbazone, H_2L^6 is benzoylpyridine 4-(*p*-methoxyphenyl)thiosemicarbazone, H_2L^7 is vanillin 4-(*p*-chlorophenyl)thiosemicarbazone; [g] HL^8 is 4-(*o*-toluidino)-4-oxobutanoic acid, HL^9 is 4-(4-nitrophenylamino)-4-oxobut-2-enoic acid.

Structure 1



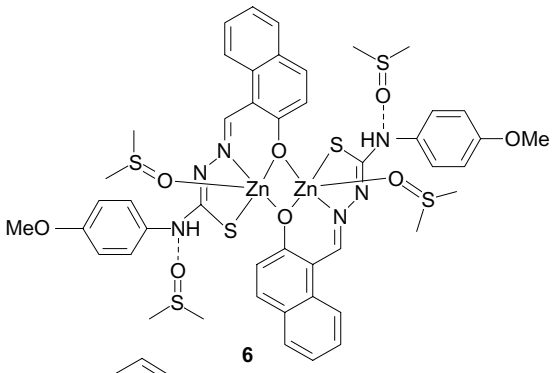
1

It was demonstrated that the constants of DNA binding *via* the intercalation mechanism are, on the average, higher for octahedral complexes compared to square-pyramidal complexes. Although the volume of the octahedron is larger than that of the square pyramid, it can be suggested that the binding in the former case is more efficient due to the easier exchange of axial ligands for electron-donating groups of nitrogenous bases of DNA. This exchange is hindered for square-pyramidal complexes and is impossible for tetrahedral complexes, which do not contain explicitly axial ligands. The investigation of the binding of a series of zinc complexes to double-stranded DNA [61] provided additional evidence in favour of this hypothesis. This study showed that the change in the geometry from square-pyramidal to octahedral leads to an increase in the DNA binding constant.

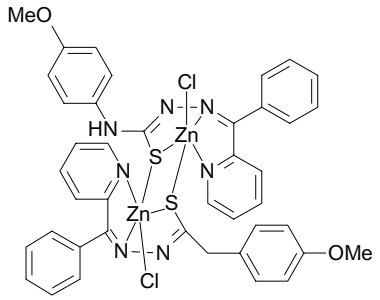
Mehr-un-Nisa *et al.*[61] synthesized three zinc coordination compounds **9** – **11** with ligands of similar chemical nature, such as the 4-(*o*-toluidino)-4-oxobutanoate and 4-(4-nitrophenylamino)-4-oxobut-2-enoate anions, and found that complex **9** has non-distorted octahedral geometry, complex **10** is a dinuclear pseudooctahedron consisting of two square pyramids, and complex **10** has non-distorted square-pyramidal geometry (Fig. 2). The investigation of their intercalation into double-stranded DNA by viscosimetry and UV spectroscopy led to the conclusion that the octahedral complex has better intercalation properties compared to the pseudooctahedral complex and both these complexes are characterized by more efficient intercalation compared to the square-pyramidal complex even despite very similar nature, close sizes and similar binding modes of the organic ligands; the binding constants (K_b) are 7.05×10^4, 6.3×10^4 and 1.6×10^4 L mol^{-1} for complexes **9** – **11**, respectively. The distortion of the octahedral geometry of coordination compounds, resulting in a decrease in the angle between the axial substituents from 180° to 167 – 160°, does not cause significant changes in cytotoxicity.[35] On the contrary, strong distortions of the geometry of coordination compounds from octahedral towards bipyramidal (an increase in the bond lengths between zinc ions and axial ligands) can lead not only to the loss of the binding to DNA but also to a significant reduction of cytotoxicity (an increase in IC_{50}).[33] Octahedral coordination compounds containing planar aromatic ligands, hydroxyquinolines, showed the highest activity (IC_{50} = 1.1 – 0.9 μM in the HCT-116 cell line).[59]

In the study of the interactions of tetrahedral zinc coordination compounds **18** – **20** with the DNA double strand,[46] it was demonstrated that the binding of complexes of this structural type occurs *via* an electrostatic mechanism. Only in the case of the coordination compound [Zn($L^{DiOMe}SN)_2$] (**20**) with the most freely rotating phenyl moieties (their conformational freedom is evidenced by the disorder in the X-ray crystal structure), there is a possibility of weak intercalation and the displacement of a small portion of ethidium bromide from the complex with DNA. The validity of these conclusions was confirmed by the molecular docking results, according to which the binding of all coordination compounds to the minor groove of double-stranded DNA is characterized by the highest binding energy. The docking also showed that the intercalation of conformationally flexible phenyl moieties of the compound [Zn($L^{DiOMe}SN)_2$] (**20**) is also possible, but the intercalation only additionally stabilizes the complex of the coordination compound with DNA and does not lead to the displacement of the tetrahedrally coordinated zinc ion from the minor groove (Fig. 3).

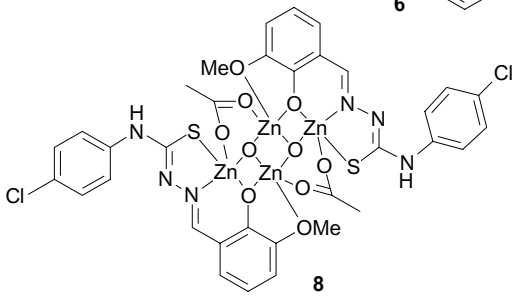
Structures 6 – 13



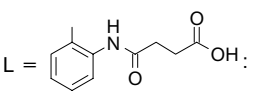
6



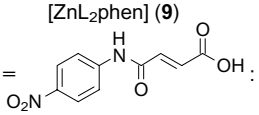
7



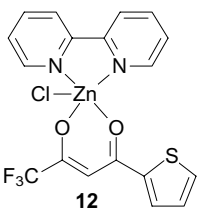
8

L =  :

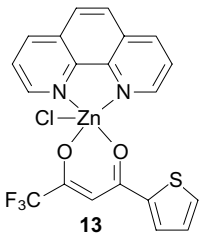
[ZnL_2phen] (**9**)

L =  :

[$Zn_2L_4(bipy)_2$] (**10**),
[$ZnL_2(bipy)(H_2O)$] (**11**)

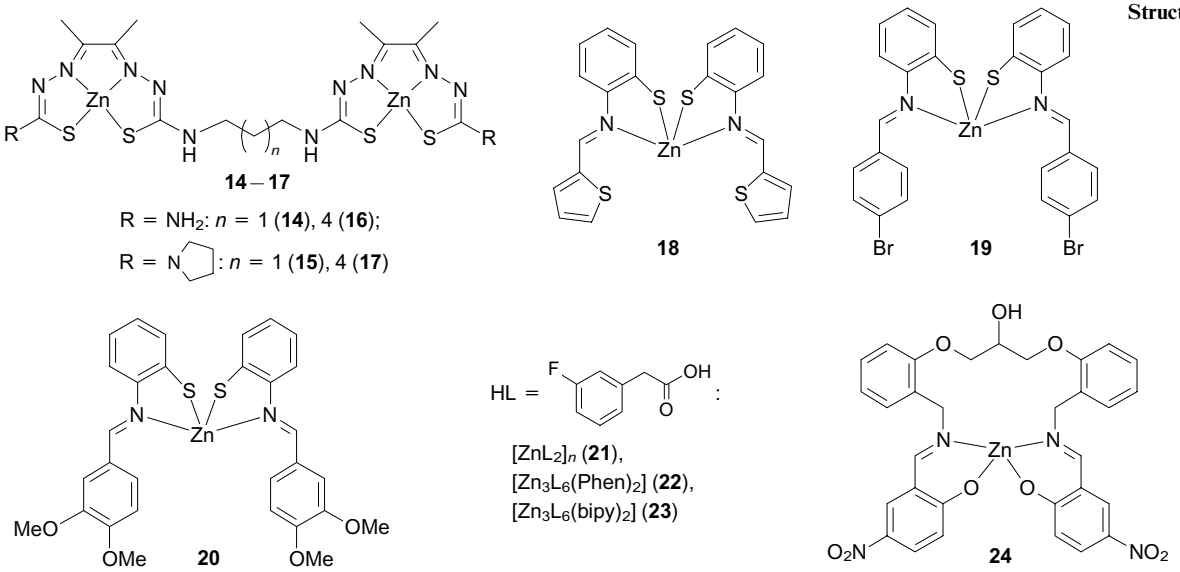


12



13

Structures 14 – 24



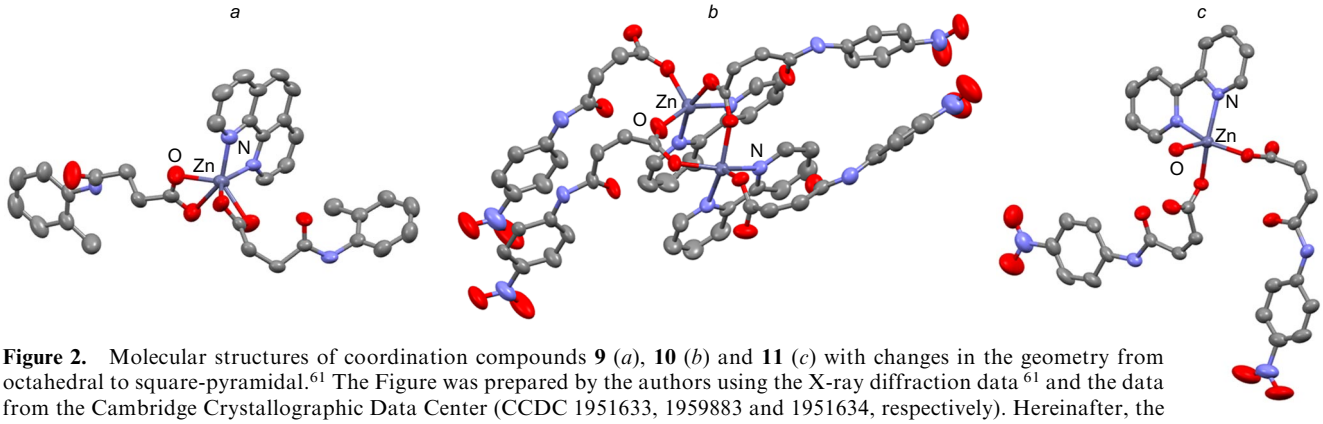


Figure 2. Molecular structures of coordination compounds **9** (*a*), **10** (*b*) and **11** (*c*) with changes in the geometry from octahedral to square-pyramidal.[61] The Figure was prepared by the authors using the X-ray diffraction data [61] and the data from the Cambridge Crystallographic Data Center (CCDC 1951633, 1959883 and 1951634, respectively). Hereinafter, the hydrogen atoms are omitted for clarity.

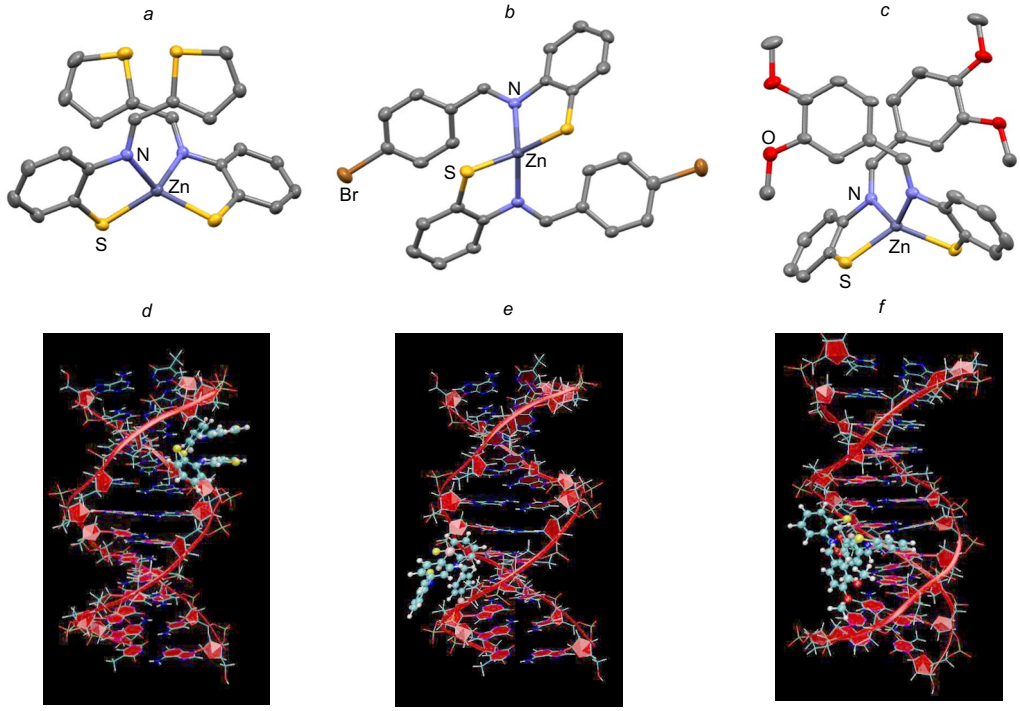


Figure 3. Molecular structures of tetrahedral zinc(II) coordination compounds **18** – **20** (*a* – *c*, respectively) and the results of molecular docking into G2-DNA (*d* – *f*).[46] Reproduced with the permission of Elsevier.

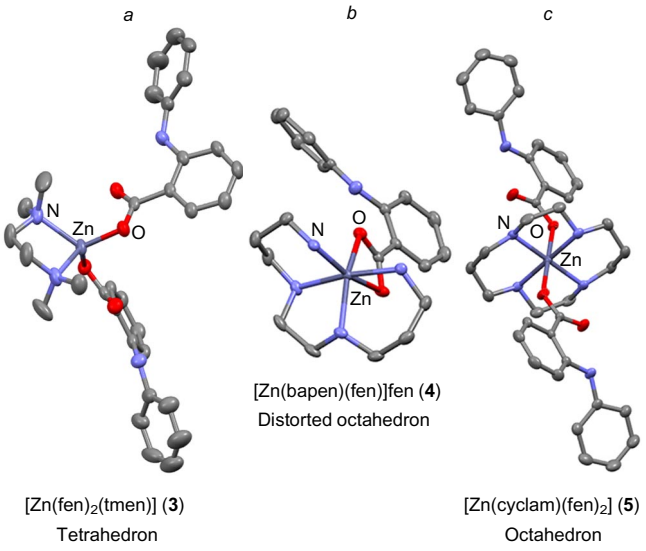
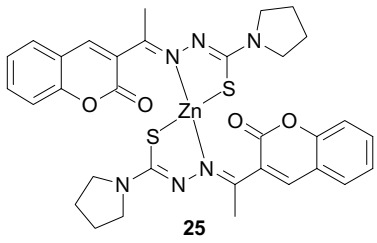


Figure 4. Molecular structures of zinc coordination compounds **3**–**5** (*a*–*c*, respectively) based on fenamic acid.[48] The Figure was prepared by the authors using the X-ray diffraction data [48] and the data from the Cambridge Crystallographic Data Center (CCDC 1561622, 1561623 and 1561624, respectively).

Structure 25



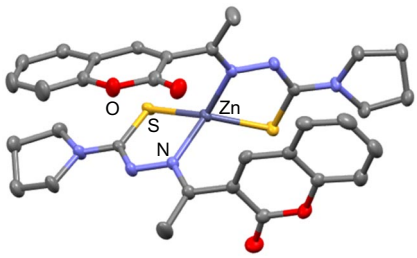


Figure 5. Molecular structure of zinc coordination compound **25** with thiosemicarbazone and coumarin ligands having tetrahedral geometry strongly distorted towards a square.[44] The Figure was prepared by the authors using the X-ray diffraction data [44] and the data from the Cambridge Crystallographic Data Center (CCDC 1425154).

A direct comparison of octahedral, distorted octahedral and tetrahedral complexes **3**–**5** with ligands of similar nature and with the same binding mode (Fig. 4) was performed in a single study.[48] The authors came to similar conclusions that the intercalation is possible only for the octahedral complex, whereas the distorted octahedral and tetrahedral complexes bind to the minor groove of DNA *via* electrostatic interactions.

In rare cases, where the interaction of a tetrahedral zinc(II) coordination compound with DNA occurs *via* an intercalation mechanism, this interaction is also due to the ligand effect. Thus, Rahman *et al.* [44] reported the intercalation of the tetrahedral complex $Zn(AcTsc)_2$ (**25**) into double-stranded DNA (Fig. 5). They demonstrated that the tetrahedral geometry is strongly distorted towards square-planar geometry and that the coumarin-based planar aromatic ligand makes a major contribution to stacking interactions between the coordination compound and nitrogenous base pairs.

The induction of apoptosis is the second most important mechanism of cytotoxic activity of Zn^{II} complexes after the interaction with DNA. This mechanism is typical of coordination compounds with all geometry types: octahedral

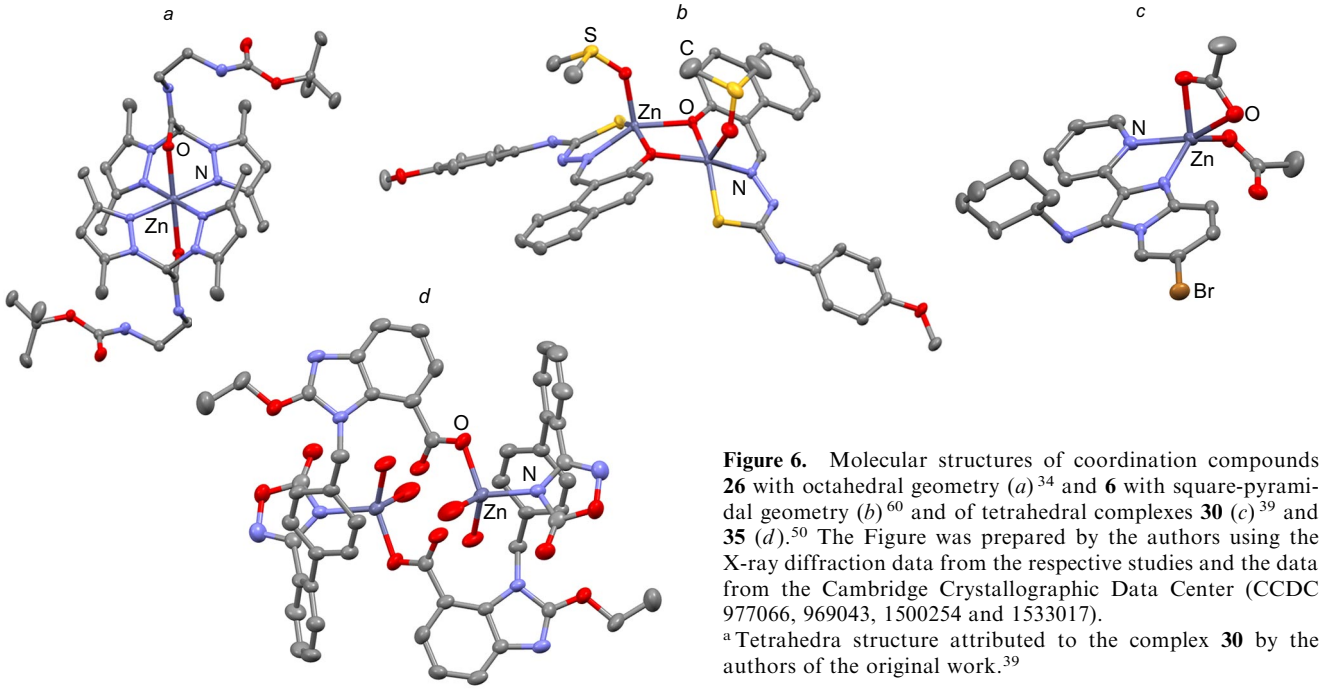
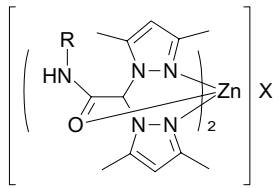
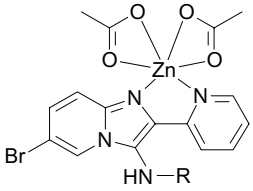


Figure 6. Molecular structures of coordination compounds **26** with octahedral geometry (*a*) [34] and **6** with square-pyramidal geometry (*b*) [60] and of tetrahedral complexes **30** (*c*) [39] and **35** (*d*).[50] The Figure was prepared by the authors using the X-ray diffraction data from the respective studies and the data from the Cambridge Crystallographic Data Center (CCDC 977066, 969043, 1500254 and 1533017).
[a] Tetrahedra structure attributed to the complex **30** by the authors of the original work.[39]

Structures 26 – 35

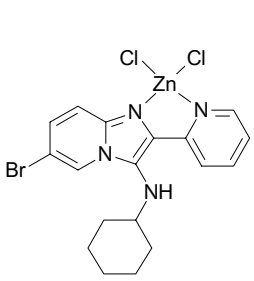


26 – 29

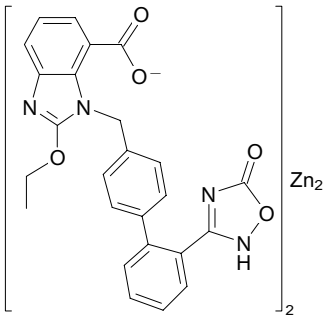


30 – 33

26 – 29: R = $(CH_2)_2NHBoc$: X = $[ZnCl_3(MeOH)]_2$ (**26**), $(ClO_4)_2$ (**27**);
R = (*S*)-$CH(CO_2Me)(CH_2)_2SMe$, X = $(ClO_4)_2$ (**28**);
R = 1,3,4,6-$(OAc)_4$-2-deoxy-β-D-glucopyranos-2-yl,
X = $(ClO_4)Cl$ (**29**);
30 – 33: R = Cy (**30**), Bn (**31**), CH_2CO_2Et (**32**), 1-Ad (**33**);
Boc is *tert*-butoxycarbonyl, Cy is cyclohexyl, As is adamantyl



34



35

(**26 – 29**),[34] square-pyramidal (**6 – 8**)[60] and tetrahedral (**30 – 35**).[39, 50] Examples of molecular structures of these compounds are shown in Fig. 6.[39, 50] Based on the available data, it is impossible to draw conclusions about the structural features of coordination compounds necessary for the efficient induction of apoptosis, because only morphological changes in the cells, indicative of the onset of apoptosis, were reported in many studies, but the factors responsible for the induction of apoptosis were not additionally studied.[29, 57, 58, 60] It can also be stated that in most cases, increased levels of reactive oxygen species[42, 50, 51, 54] or the activation of caspases-3(7,9)[34, 50] were observed in apoptotic cells.

Stanojkovic *et al.*[28] demonstrated that the monomeric octahedral coordination compounds $[ZnL_2]$ (**36**) and $[Zn(OAc)L]_2$ (**37**), where HL is 2-acetylpyridine N^4-1-(4-fluorophenyl)piperazinethiosemicarbazone, are less toxic and less efficient in the induction of apoptosis in the HeLa, MDA-MB-361, MDA-MB-453 and K562 cell lines compared to dinuclear square-pyramidal complexes (Fig. 7). This synergistic effect of two coordinated zinc ions provides indirect evidence that the induction of apoptosis is associated with the generation of reactive oxygen species (a larger amount of ROS is generated at two metal ions) rather than with the inhibition or activation of enzymes (in this case, the synergistic effect is rarely observed and only with multidomain proteins). Meanwhile, for tetrahedral coordination compounds there is evidence in favour of the caspase-dependent induction of apoptosis. The average IC_{50} values of tetrahedral coordination compounds **38 – 45**, which trigger apoptosis, are 0.1 – 1.0 μM against the A431, A431Pt, MCF-7 and HepG2 cell lines[29, 32] and 0.05 μM against the A2780 cell line.[53] However, if a compound is a caspase-3 inhibitor, its toxicity decreases and IC_{50} increases to 100 μM, while no morphological features of apoptotic cell death typical of apoptosis being observed.[37] This fact, most likely, accounts for low toxicity of the tetrahedral zinc coordination compounds with antipyrine and caffeine $[Zn(AP)_2I_2]$ (**46**) and $[Zn(Caf)(H_2O)I_2]$ (**47**), which varies in the range of 70 – 100 μM against the A549, MCF-7 and PC-3 cell lines.[45, 62]

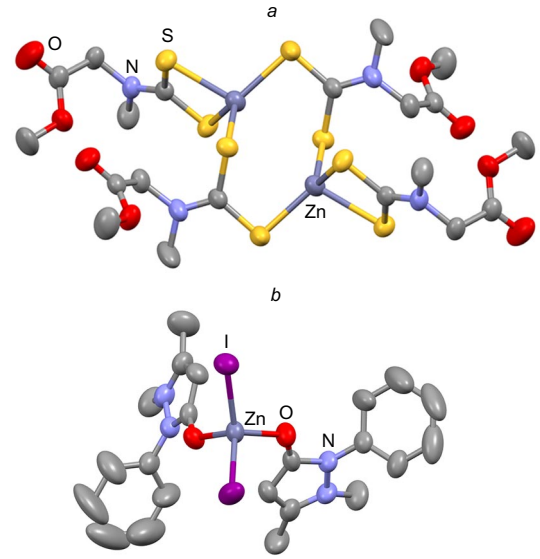
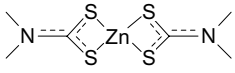


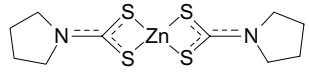
Figure 7. Molecular structures of tetrahedral coordination compounds **45** (*a*) and **46** (*b*) capable and incapable of inhibiting caspase-3.[37, 45] The Figure was prepared by the authors using the X-ray diffraction data[37, 45] and the data from the Cambridge Crystallographic Data Center (CCDC 832168 and 1417284).

Structures 38 – 46

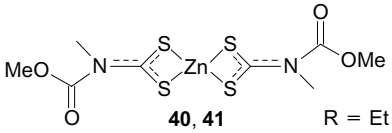
Does not inhibit caspases — high toxicity:



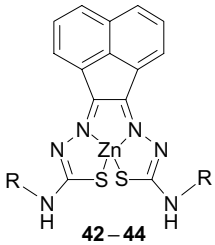
38



39

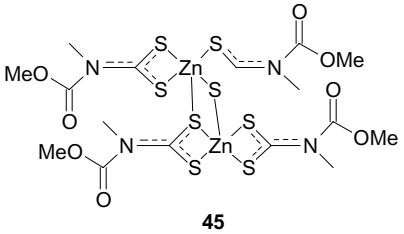


40, 41 R = Et (**40**), Bu^t (**41**)



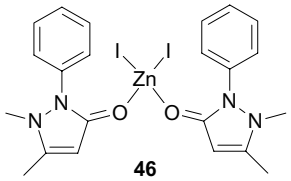
42 – 44

R = Me (**42**), Et (**43**), Ph (**44**)



45

Inhibits caspases — low toxicity:



46

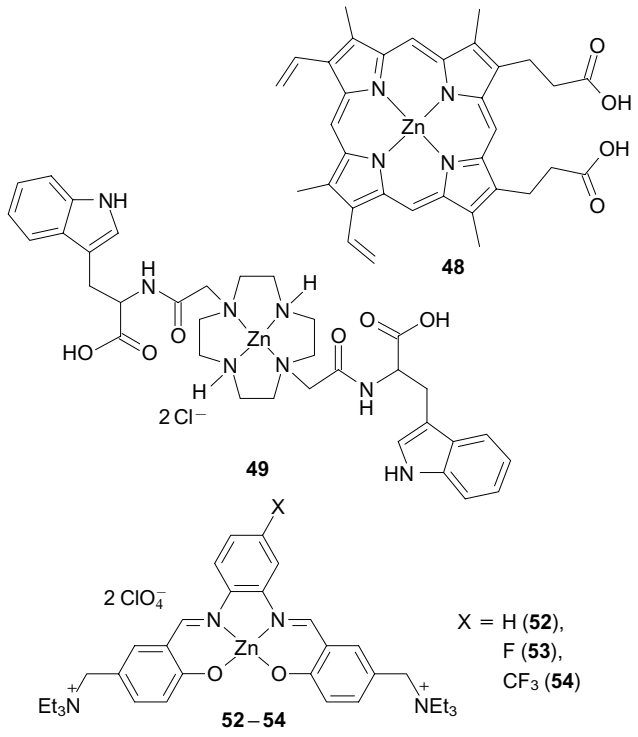
In some cases, the apoptosis is accompanied by tumour cell necrosis.[56, 58] Although a few studies demonstrated the possibility of the induction of cell necrosis through activation of a number of specific genes upon the interaction of zinc(II) complexes with DNA, a sufficient number of representatives required for the construction of the relationship between the structure of coordination compounds and the efficiency of the induction of necrosis is lacking in the literature.[52]

The binding to the heat shock protein Hsp90, which stabilizes some enzymes essential for carcinogenesis, is the most recently described mechanism of the anticancer effect of square-pyramidal Zn^{II} complexes. In the only study,[55] in which the authors showed that the function of the chaperone Hsp90 can by impaired by zinc(II) hydroxyterpyridinate, they concluded that Hsp90 is involved in the mechanism of cytotoxic activity of coordination compounds based on the results of molecular docking. However, this fact was not confirmed experimentally.

2.2. Square-planar zinc(II) compounds

The individual Section deals with rarely occurring square-planar zinc coordination compounds typical of ligands of the protoporphyrin (ZnPP, **48**)[30, 31, 38] and cyclene series [Zn^{II}-Cyclen-$(Trp)_2$, **49**][41] and also with rare compounds bearing substituted Schiff bases **50** – **54**.[40, 47] The interaction between square-planar Zn^{II} complexes and DNA have attracted the most attention of researchers. In the only study[47] concerned with the interaction between coordination compounds of this class and different DNA secondary structures, it was shown that a number of coordination compounds have significant selectivity towards G4-quadruplexes, non-canonical three-dimensional structures of DNA.[27] While being weakly bound to double-stranded DNA, zinc(II) complexes **52** – **54** with ligands as Schiff bases, which were prepared from substituted salicylaldehydes and *o*-phenylenediamines, bind to G4-DNA with $K_b = (3-5) \times 10^4$ L mol^{-1}.

Structures 48 – 54



48

49

52 – 54

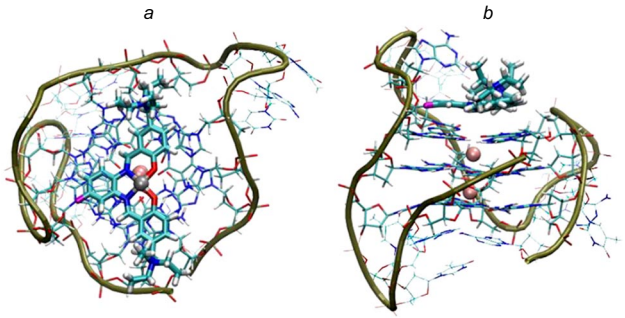


Figure 8. Binding of complex **52** to G4-DNA according to the molecular docking results: the top view (*a*) and the side view (*b*).[47] Reproduced with the permission of Elsevier.

It was shown that this property, promising for the development of cytostatic agents, is due to the presence of Zn^{II} ions in the coordination compounds; Ni^{II} complexes with the same ligands and a similar geometry are three orders of magnitude less selective towards G4-DNA. The experimental data were confirmed by the molecular docking calculations of their binding energies to the duplex and G4-DNA (Fig. 8).[47]

The mechanism of cytotoxic activity through the induction of apoptosis was revealed only for square-planar cyclene-based coordination compound **49**. It was shown that the interaction of this complex with DNA leads to its damage, which causes the activation of caspase-3 followed by the induction of apoptosis through a caspase-dependent pathway.[41]

It was found that haem oxygenase-1 inhibitors based on zinc protoporphyrinates **48** exhibit cytotoxicity of about 10 μM.[30, 31, 38] In one of the first cited studies, Fang *et al.*[30] showed that the toxicity is associated with the inhibition of the enzyme HO-1; however, there is also another mechanism because the toxicity is retained in the cells in the absence of overexpression of HO-1. Wang *et al.*[31] reported that zinc protoporphyrinates can exhibit a cytotoxic effect, by blocking the Wnt signaling pathway of the cell characteristic of most of cell lines. The inhibition constants of the enzymes under consideration correlate with the IC_{50} values. Hence, it can be suggested that, due to the structural features, planar coordination compounds (*e.g.*, ZnPP) do not prone to DNA intercalation and binding, ROS generation and the induction of apoptosis and act *via* these specific mechanisms.

2.3. Effect of ligand structure on cytotoxicity

Apart from the geometry of the metal coordination sphere, the influence of the chemical nature and the donor ability (acceptor ability) of the ligand should be taken into account when considering relationships between the structure of zinc(II) coordination compounds and the mechanism of cytotoxic activity. A comparison of the cytotoxicity in series of zinc complexes with the same coordination geometry shows that the cytotoxic activity differs in this series and the IC_{50} values vary in a wide range. For example, the cytotoxicity of tetrahedral complexes (see Table 1) against the breast adenocarcinoma cell line (MCF-7) varies from 0.1 to 100 μM. The difference in the cytotoxicity by three orders of magnitude indicates that not only the geometry but also

the structure and chemical nature of the organic ligand play an important role in the antiproliferative activity.

The elucidation of the effect pattern of the ligands on cytotoxicity is complicated by the fact that coordination compounds with the same geometry and a similar mechanism of action should be compared using the same cell line. A series of octahedral coordination compounds with toxicity evaluated against the MCF-7 cell line (2 studies, see Refs 34 and 36) and a series of tetrahedral coordination compounds, the toxicity of which was evaluated against the MCF-7 (6 studies, see Refs 32, 45, 46, 52, 56 and 58) and Hep-G2 cell lines (2 studies, see Refs 32 and 44) are representative samples corresponding to these selection criteria and allowing an educated guess of the effect of the chemical structure of the ligand on cytotoxicity.

Let us compare octahedral coordination compounds **26** and **1** bearing two equatorial bidentate nitrogen-containing ligands [bis(3,5-dimethylpyrazol-2-yl)acetamide derivatives in the former compound [34] and 3-(2-pyridyl)-1,2,4-triazine derivatives in the latter compound [36]] in the metal coordination sphere. The coordination spheres of complexes **26** and **1** differ only in that the amide oxygen atoms linked to equatorial ligands serve as axial ligands in the case of bispyrazole, whereas Cl^- ions are in axial positions in the case of 3-(2-pyridyl)-1,2,4-triazine. The replacement of oxygen ligands strongly coordinated to zinc by easily dissociating chloride ions leads to an expected decrease in the IC_{50} value (increase in the cytotoxicity) from 18 ± 5 to 10.44 ± 0.52 μM. This difference between the IC_{50} values of compounds **26** and **1**, which is significantly larger than the standard deviations reported in this study, is an additional evidence that the loss of axial ligands followed by the intercalation of the resulting square-planar complex into DNA is the main mechanism of cytotoxic activity of octahedral zinc coordination compounds.

A comparison of the IC_{50} values of tetrahedral coordination compounds **14** – **17**,[32] **18** – **20**,[46] **47**,[45, 52] **55**,[52] **56** (Ref. 56) and **57** – **60** (Ref. 57) evaluated against the MCF-7 cell line suggests that sulfur-containing ligands favour higher cytotoxicity of the Zn complex, whereas the presence of easily dissociating halide ions leads, on the contrary, to the reduction of cytotoxicity. This is indirect evidence that tetrahedral coordination compounds exhibit cytotoxic activity in the undissociated state and, consequently, they should have the most stable structure. For example, complexes **57** – **60** with thiosemicarbazones conjugated with the aromatic system, which are stable under physiological conditions and do not undergo ligand exchange, have IC_{50} values of 60.3 – 88.1 μM even in the case of a significantly distorted tetrahedral geometry of the coordination sphere.[57] Mononuclear complexes **19** and **20** with a more rigid sulfur-containing organic ligand bearing the thiophenolate moiety and with less distorted geometry have cytotoxicity of 20 μM.[46]

Besides, the study [32] of tetrahedral dinuclear zinc thiosemicarbazone coordination compounds **14** – **17** showed that IC_{50} of the complexes, in which the tetrahedra are coupled through a flexible organic linker, was 0.1 μM against the same MCF-7 cell line. This is evidence of the synergistic effect characteristic of inhibition of multidomain proteins by structurally related inhibitors. However, this statement is ambiguous because of the small number of representatives. Therefore, further studies are required.

Meanwhile, the cytotoxicity of complexes **47**, **55** and **56**, which do not contain sulfur atoms in the ligand environment and bear halide ligands, is two orders of magnitude lower ($IC_{50} \approx 1000$ μM). It is worth noting that, according to the results of the studies,[52, 56] the mechanism of their action also differs from the mechanism of action of other stable tetrahedral coordination compounds and leads mainly to the induction of cell death *via* a necrotic rather than an apoptotic pathway.

2.4. Prospects of the development of anticancer agents based on zinc ions

The above data on the structures and mechanisms of cytotoxic activity of zinc coordination compounds demonstrate that octahedral zinc compounds were studied in most detail. For these complexes, the main mechanism of cytotoxic activity (intercalation into double-stranded DNA) was determined and comprehensively analyzed. The following structural motifs of the ligands allowing the improvement of cytotoxicity were revealed: axial ligands weakly coordinated to zinc in the case of octahedral complexes and polydentate ligands strongly coordinated to zinc in the case of tetrahedral complexes, as well as sulfur-containing ligands. Meanwhile, tetrahedral zinc coordination compounds exhibiting relatively higher toxicity are less well studied. For these compounds, the main mechanism of cytotoxic activity is not ultimately determined. It is known that this mechanism is associated with the induction of apoptosis and necrosis and, according to some indirect evidence, it can be suggested that it includes the inhibition of cellular respiration enzymes or enzymes involved in cell cycle regulation (telomerase, *etc.*).

Square-pyramidal zinc coordination compounds are scarce in the literature, being intermediate in the degree of evaluation of cytotoxic activity between octahedral and tetrahedral coordination compounds. Probably, these complexes combine the mechanisms of cytotoxic activity through DNA intercalation and the interaction with cellular enzymes.

Rare examples of square-planar zinc(II) coordination compounds were described in a few studies. However, these studies offer significant prospects for the development of a new class of anticancer drugs exhibiting selective cytotoxic activity through the interaction with G4-DNA and, probably, with other non-classical secondary chromatin structures characteristic of cancer cells.

3. Iron coordination compounds as cytotoxic agents

Iron is one of the most important redox-active elements in the body. In both characteristic oxidation states, Fe^{II} and Fe^{III}, iron ions are stable under physiological conditions and are abundant in the body; they are involved in many metabolic processes within mitochondria (the electron transport chain), cells (DNA synthesis and repair) and the body as a whole (transport of oxygen and carbon dioxide).[63 – 65]

The recently obtained data on the changes in the morphology of cells (the cell nucleus and other organoids) and the chemical structure of chromatin (a nucleoprotein complex as the fundamental structural unit of chromosomes) caused by iron coordination compounds revealed a specific cell death pathway. This pathway is emerged through the influence of iron coordination compounds and salts on dividing cells and is called ferroptosis due to its similarity to apoptosis.[66]

Table 2. Cytotoxic iron coordination compounds.

No.	Complex (serial number of the compound)	Coordination sphere	Binding mode	Metal coordination geometry	Mechanism of cytotoxic activity	IC_{50} max (cell line)	Ref.
1	$Fe^{III}LCl_3$ (**148**–**153**) (L are substituted 6-benzylamino-9-isopropylpurines)	$FeNCl_3$	Monodentate	Tetrahedral	Inhibition of E/Cdk2 kinases after cellular hydrolysis	4–135 μM (G-361, HOS, K-562, MCF-7)	67
2	$[Fe^{III}$(salophene)Cl] (**129**)	FeN_2O_2Cl	Tetradentate chelate	Distorted square-pyramidal	Induction of apoptosis *via* the mitochondrial pathway through ROS generation and oxidative DNA damagē	0.07 μM (BJAB), 2.5 μM (Nalm-6), 1.5 μM (Jurkat), 3 μM (MelHO), 5 μM (MCF-7)	68
3	Ferrocenyl–thymine conjugate	$FeCp_2$	π-Complex	Sandwich complex	Unknown, but not the interaction with DNA	20–30 μM (MCF-7). Thymine reduces toxicity	69
4	s-$[Fe^{II}L_2]X_2$ (**116**–**121**) (L are 4-substituted terpyridines; $X = ClO_4^-$ or Cl^-)	FeN_6	Tridentate chelate	Distorted octahedral	Intercalation into DNA followed by photoactivated ROS-mediated DNA damage	7–11 μM (HeLa) in the light; 87–90 μM (HeLa) in the dark	70
5	$Fe^{II}(phen)_3(BF_4)_2$ (**106**)	FeN_6	Bidentate	Octahedral	Binding to the groove of DNA and ROS-mediated double-strand breaks	Not measured	71
6	$[CpFe^{II}$(dppe)L][OTf] (**89**–**92**) (L are 1-substituted imidazoles)	$FeCpP_2N$	Monodentate for imidazole, bidentate for diphosphine and π-complex for Cp	Half-sandwich complex	Putative ROS generation	0.22–0.43 μM (A2780), 0.81–3.10 μM (MCF7), 1.40–6.30 μM (HeLa)	72
7	Ferrocenylpyrimidines (**69**–**74**)	$FeCp_2$	π-Complex	Sandwich complex	Involvement in DNA synthesis, impairment of DNA replication and the arrest of the cell cycle at the S phase	52–64 μM against ovarian cancer cells (surgical material)	73
8	$[Fe^{II}$(Pamp)(MeOH)$Cl_2]$	FeN_3OCl_2	Tridentate	Distorted octahedral	ROS-Mediated DNA damage without DNA binding (weak electrostatic binding)	Not measured	74
9	$Fe^{II}(Bd)_2$(XGm(morph))$(BF)_2$ (**154**–**157**)	FeN_6	Polydentate chelate	Distorted trigonal-prismatic	Inhibition of DNA and RNA transcription	Not measured	75

Table 2 (continued).

No.	Complex (serial number of the compound)	Coordination sphere	Binding mode	Metal coordination geometry	Mechanism of cytotoxic activity	IC_{50} max (cell line)	Ref.
10	Plumbagin *N′*-(Ferrocenylcarbonyl)-hydrazone (**75**)	$FeCp_2$	π-Complex	Sandwich complex	Intercalation into DNA, damage of DNA structure (detected by EMSA) and the arrest of the cell cycle at the G2/M phase	0.5 ± 0.1 μM (518A2), 4.7 ± 1.8 μM (HCT-116), 1.1 ± 0.1 μM (KB-V1/Vbl)	76
11	[FeCp(dppe)(L)][PF_6] (L is quinoline-2-carbonitrile (**93**), quinoline-3-carbonitrile (**94**), pyrazine-2-carbonitrile (**95**), pyrazine-2,3-carbodinitrile (**96**))	$FeCpP_2N$	Monodentate for imidazole, bidentate for diphosphine and π-complex for cyclopentadienyl	Half-sandwich complex	Intercalation into DNA accompanied by multiple breaks in supercoiled plasmids (detected by atomic force microscopy), induction of apoptosis	0.77 – 5.05 μM (HL-60)	77
12	[Fe^{III}(BHA)LCl]Cl (L = phdpa (**114**), pydpa (**115**))	FeN_3O_2Cl	Tridentate and bidentate	Distorted octahedral	Binding to the groove of DNA stabilized by partial intercalation; DNA breaks upon irradiation	14.6 μM (HeLa) in the light, 77 μM (HeLa) in the dark	78
13	$Fe^{II}L_3SO_4$ (L = bipy (**123**), phen (**124**), ip (**125**), pip (**126**), me-pip (**127**))	FeN_6	Bidentate	Octahedral	All complexes enter cells through endocytosis to form secondary lysosome, then hydrophilic complexes are translocated to the cell nucleus, where they damage DNA and induce S-phase cell cycle arrest (p53-dependent). Hydrophobic complexes are localized in the cell cytoplasm and inhibit the protein kinase B signaling cascade, arresting the cell cycle at the G0/G1 phase and triggering apoptosis	0.5 – 1.7 μM (MCF-7), 1 – 30 μM (A375, HeLa, HepG2, PC-12, RHepG2, A549)	79
14	[Fe^{III}(salophen)L] (HL is imidazole (**130**), 1,2,4-triazole (**131**), benzo[*d*][1,2,3]triazole (**132**), 5-amino- (**133**) and 5-phenyltetrazoles (**134**))	FeN_3O_2	Tetradentate chelate + monodentate ligand L	Square-pyramidal	Intercalation into DNA, the DNA binding affinity increases by two orders of magnitude in the presence of a planar and unhindered substituent in the ligand L; apparently, only the ligand L intercalates into DNA	0.38 – 0.70 μM (MCF-7), 0.058 μM (A2780), 0.4 – 5.0 μM (HOS, A549, HeLa, G-361, LH32)	80

Table 2 (continued).

No.	Complex (serial number of the compound)	Coordination sphere	Binding mode	Metal coordination geometry	Mechanism of cytotoxic activity	IC_{50} max (cell line)	Ref.
15	$[Fe^{III}(sal)LCl]$ (L = phdpa, andpa)	FeN_3O_2Cl	Tridentate amine, bidentate salicylic acid and monodentate chloride ion	Distorted octahedral	Binding to DNA followed by photocleavage, presumably mitochondrial DNA is cleaved	8.6 μM (HeLa) in the light, > 100 μM (HeLa) in the dark; 3.4 μM (MCF-7) in the light, > 100 μM (MCF-7) in the dark	81
16	$[(m\text{-}BDA)Fe^{III}Cl_3]$	FeN_3Cl_3	Tridentate	Distorted octahedral	Localized in mitochondria and, when irradiated, causes membrane depolarization and mitochondrial DNA damage	15.56 μM (HepG-2) in the dark, 6.25 μM (Hep-G2) in the light	82
17	$[FeL_2]NO_3$ (**128**) (L is (*E*)-*N*-phenyl-2-(quinolin-2-ylmethyl)diazenecarbothioamide)	FeN_4S_2	Bidentate	Distorted octahedral	Binds to DNA, causes DNA damage *via* ROS generation and leads to the induction of apoptosis *via* the mitochondrial pathway through activation of the protein p53	0.23 μM (HepG2), 0.46 μM (HeLa), 1.62 μM (HL-7702), 1.1 μM (MCF-7), 1.38 μM (MCF-7/ADR)	83
18	$[\{FeL(cur)\}_2(\mu\text{-}O)](ClO_4)_2$ (L is bis(2-pyridylmethyl)benzylamine)	FeN_3O_3	Tridentate + bidentate	Distorted octahedral	ROS photogeneration causing DNA damage and the induction of apoptosis	3.1 μM (HeLa) in the light, > 50 μM (HeLa) in the dark; 4.9 μM (MCF-7) in the light, > 50 μM (MCF-7) in the dark	84
19	4-Azidobenzylferrocenylcarbamate (**80**)	$FeCp_2$	π-Complex	Sandwich complex	Toxicity correlates with the ROS level in the cell, ROS generation begins after the activation by glutathione or blue light	16–28 μM (HL-60); the higher the glutathione level, the higher activity	85
20	$[Fe^{III}_2(\mu\text{-}O)(L\text{-}His)_2(B)_2](ClO_4)_2$ (**104a–c**) and $[Fe^{III}_2(\mu\text{-}O)(\mu\text{-}O_2CMe)_2(B)_4](ClO_4)_3$ (**105b,c**) (B = bipy (**a**), phen (**b**), dipyrido[3,2-*d*:2′,3′-*f*]quinoxaline (**c**))	FeN_4O_2	Tridentate + bidentate	Distorted octahedral	Generate ROS in the dark and in the light inducing cell apoptosis. In the light, these complexes undergo decarboxylation and ROS is generated even more rapidly	30 μM (HeLa), 36 μM (MCF-7); in the light, IC_{50} is two times lower. Increase in the volume or lability of the nitrogen-containing ligand leads to a decrease in the activity. Non-toxic against MCF-10	86
21	$[Fe^{III}L^1(SCN)_2]X \cdot 2H_2O$ [a] (X = SCN (**141**), $Fe(SCN)_5$ (**142**))	$FeN_3O_2(SCN)_2$	Pentadentate	Pentagonal-bipyramidal	Very weak binding to DNA (not intercalation); apparently cause the induction of apoptosis	75–172 μM (HeLa, MDA-MB-453, K562, LS174, A549, MRC-5)	87

Table 2 (continued).

No.	Complex (serial number of the compound)	Coordination sphere	Binding mode	Metal coordination geometry	Mechanism of cytotoxic activity	IC_{50} max (cell line)	Ref.
22	3-Amino- (**81**, **82**) and 3-nitro-phenylferrocenes (**83**, **84**)	$FeCp_2$	π-Complex	Sandwich complex	Electrostatic binding to DNA, not studied in detail	1.55 – 4.72 μM (MCF-7); 1.5 – 2 times higher against normal cells 3.76 – 4.92 μM (HeLa)	88
23	$[CpFe^{II}(CO)(PR_3).(4\text{-}NCC_6H_4NH_2)]PF_6$ (R_3P = Ph_3P (**97**), 4-$Ph_2PC_6H_4CO_2H$-4 (**98**), $(4\text{-}FC_6H_4)_3P$ (**99**) $[CpFe^{II}(CO)(PPh_3)I]$ (**100**))	FeCpCOPN	Monodentate ligand + Cp	Half-sandwich complex	Induction of apoptosis. Complexes with asymmetric charge distribution are more cytotoxic than those with symmetric charge distribution		89
24	$[Fe^{II}(L^2)(cur)]Cl$ (**101**), $[Fe^{III}(L^3)(cur)]Cl$ (**102**), $[Fe^{III}(L^4)(cur)]$ (**103**)[b]	FeN_4O_2, FeN_3O_3, FeN_2O_4	Tetradentate + bidentate	Distorted octahedral, octahedral, octahedral	Mitochondrial localization of complexes. Generation of ROS; for Fe^{II}, in the light and in the dark, whereas for Fe^{III} only in the light	**101**: ~20 μM; **102**: ~90 μM; **103**: ~90 μM (LN-229, MCF-7, HaCaT). In the light, the toxicity of Fe^{III} increases by a factor of 2 – 5	90
25	*N*-R-4-(Ferrocenylcarbamato)-phenylboronic acid pinacol ester (R = All (**76**), prop-2-enyl (**77**), propargyl (**78**), prop-2-ynyl (**79**))	$FeCp_2$	π-Complex	Sandwich complex	Generation of ROS, oxidative stress and DNA damage	15 – 30 μM (BL-2, A2780, Jurkat)	91
26	Fe^{III} monochloro-N^1-acetylacetone-N^4-(4-methoxysalicylidene)-*S*-alkylthio-semicarbazidates (**135 – 140**)	FeN_2O_2Cl	Tetradentate	Distorted square-pyramidal	Antioxidant properties	Not measured	92
27	R-Phenylimidazophenanthrolines Fe^{III} (R = H, Me, NO_2)	FeN_6	Bidentate	Octahedral	Arrest of the cell cycle at the G0/G1 phase and the induction of apoptosis *via* the mitochondrial pathway	2 – 4 μM (ECA109, TE-1)	93
28	Hydroxyferrocifens (**61 – 68**)	$FeCp_2$	π-Complex	Sandwich complex	Generation of ROS	Not measured	94
29	$[Fe^{III}L(NN)]PF_6$) (NN = bipy (**107**), phen (**108**), amphen (**109**), Clphen (**110**), epoxyphen (**111**)); $[Fe^{III}L(EtOH)]NO_3$ (**112**) (H_2L is bis(2-hydroxy-4,5- dimethyl-benzyl)(2-pyridylmethyl)amine)	FeN_4O_2	Tetradentate + bidentate	Distorted octahedral	Electrostatic localization at the sugar phosphate backbone of DNA; ROS generation; DNA damage leading to the induction of apoptosis through caspase activation	2.2 – 7.8 μM (HeLa)	95

Table 2 (continued).

No.	Complex (serial number of the compound)	Coordination sphere	Binding mode	Metal coordination geometry	Mechanism of cytotoxic activity	IC_{50} max (cell line)	Ref.
30	$[Fe^{III}$(salophene)Cl] (**129**)	FeN_2O_2Cl	Tetradentate	Distorted square-pyramidal	Unknown, stability in solution was evaluated	Not measured	96
31	Fe^{III} Complexes with 2,6-diacetyl-pyridine bis(acylhydrazones) (**143 – 147**)	$FeN_3O_2Cl_2$	Pentadentate	Pentagonal-bipyramidal	Ligands and, to a lesser extent, complexes inhibit ribonucleotide reductase. Ligands are 4 – 5 times more cytotoxic than the complexes	33 – 73 μM (MCF-7, A549, NCI-H460)	97
32	$Fe^{III}L_3$ (HL is 8-hydroxyquinoline)	FeN_3O_3	Bidentate	Octahedral	Generation of ROS and the induction of apoptosis *via* the mitochondrial pathway	1.9 – 2.5 μM (A431, SCC9, SCC25, BCC, A375, HaCaT)	98
33	$Fe^{III}(L)(NO_3)_2 \cdot 2H_2O$ (L is triarylimidazole (**122**))	$FeNO(H_2O)_2(NO_3)_2$	Bidentate	Octahedral	Intercalation into DNA	60 μM (MCF-7, Hep-G2)	99
34	1,1′-Bis(4-aminomethylphenyl)-ferrocenes (**85 – 88**)	$FeCp_2$	π-Complex	Sandwich complex	Generation of ROS, transport to the cell through transferrin receptors	2.4 – 6.1 μM (SK-OV-3)	100
35	Fe^{III} Complex with rifampicin	$FeO_3(H_2O)_3$	Tridentate	Octahedral	Induction of apoptosis *via* the mitochondrial pathway	Suppression of solid tumour growth is two times stronger compared to the effect of the ligand	101
36	$[Fe^{III}(L^5)Cl_3]L^6$ (**158**) (L^5 is 2,4,6-tris(2-pyridyl)-1,3,5-triazine, L^6 is thiourea)	FeN_3Cl_3	Tridentate	Octahedral	Unknown	6.59 ± 0.5 μM (Hep-G2), 13.07 ± 1.1 μM (HeP2), 9.38 ± 1.0 μM (MCF-7), 8.24 ± 0.9 μM (HeLa)	102
37	$[Fe^{III}(L^7)(NO_3)_2(H_2O)_2] \cdot 0.5H_2O$ (**113**)[c]	$FeNO(NO_3)_2(H_2O)_2$	Bidentate	Octahedral	Electrostatic binding to the minor groove of DNA	38 – 91 μM (Hep-G2, MCF-7, HCT-116)	103

Note. The following abbreviations are used: salophene is *N*,*N*′-bis(salicylidene)-1,2-phenylenediamine, Cp is cyclopentadienyl, Tf is trifluoromethanesulfonyl (triflyl), Pamp is pyridine-2-carboxylic acid *N*′-phenyl-*N*′-(2-pyridyl)hydrazide, H_2Bd is α-benzyl dioxime, H_2Gm(morph) is morpholinoglyoxime, BHA is benzhydroxamate, phdpa is benzylbis(2-pyridylmethyl)amine, pydpa is (1-pyrenylmethyl)bis(2-pyridylmethyl)amine, ip is imidazo[4,5-*f*][1,10]phenanthroline, pip is 2-phenylimidazo[4,5-*f*][1,10]phenanthroline, me-pip is 2-(4-methylphenyl)-1*H*-imidazo[4,5-*f*][1,10]phenanthroline, m-BDA is 4,4-difluoro-1,3,5,7-tetramethyl-8-[3-bis(2-pyridylmethyl)aminobenzyl]-4-bora-3a,4a-diaza-*s*-indacene, cur is curcumin (bis(4-hydroxy-3-methoxyphenyl)-1,6-diene-3,5-dione), His is histidine. [a] L^1 is 2,2′-[pyridine-2,6-diylbis(ethylidene-1-hydrazinyl-2-ylidene)]bis[*N,N,N*-trimethyl-2-oxoethaneamine], [b] L^2 is tris(2-pyridylmethyl)amine, HL^3 is (2-hydroxybenzyl)bis(2-pyridylmethyl)amine, H_2L^4 is *N*,*N*-bis(4,6-di-*tert*-butyl-2-hydroxybenzyl)-*N*′,*N*′-dimethylethylenediamine, [c] HL^7 is 1-(2-hydroxyethyl)-2-(3-bromo-6-hydroxyphenyl)-4,5-diphenyl-1*H*-imidazole.

The key differences between ferroptosis and apoptosis are that the ferroptosis is not accompanied by nuclear disintegration and chromatin degradation and, in the early stage, the process is irreversible in the presence of caspase inhibitors (ferroptosis is not a caspase-dependent process). The ferroptosis involves the cell shrinkage followed by its swelling. The formation of apoptotic bodies and cell fragmentation are not observed during ferroptosis. The main morphological markers of ferroptosis are the reduction of the mitochondrial volume with condensed mitochondrial membrane density and the reduction/vanishing of mitochondrial cristae, as well as an increase in the lipid bilayer density. From the biochemical viewpoint, ferroptosis is characterized by a significant decrease in the glutathione level and dysfunction of glutathione-dependent peroxidase, resulting in a considerable increase in the ROS level in the cell.[66]

Taking into account the involvement of iron ions in key biochemical processes, iron coordination compounds hold promise for the development of anticancer agents. It is known that during many metabolic processes, iron ions change the oxidation state. This makes it possible not only to search for cytotoxic iron coordination compounds but also to design prodrugs, which differ from the available drugs by the degree of oxidation.

Abundant data on the cytotoxic activity of iron complexes against a large number of cell lines are scattered. This makes it difficult to evaluate the effect of the structure of the substituent on cytotoxic activity within individual classes of compounds. However, common mechanisms of action for different structural types of iron-containing complexes can be revealed and the ranges of IC_{50} values against cancer and normal cells can be evaluated.

Iron coordination compounds with confirmed cytotoxic activity can be divided into two main structural classes, which differ in the ligand environment and the coordination geometry of the iron ion: classical iron coordination compounds with N,O-donor ligands and substituted ferrocenes. The principal data on these compounds are summarized in Table 2.

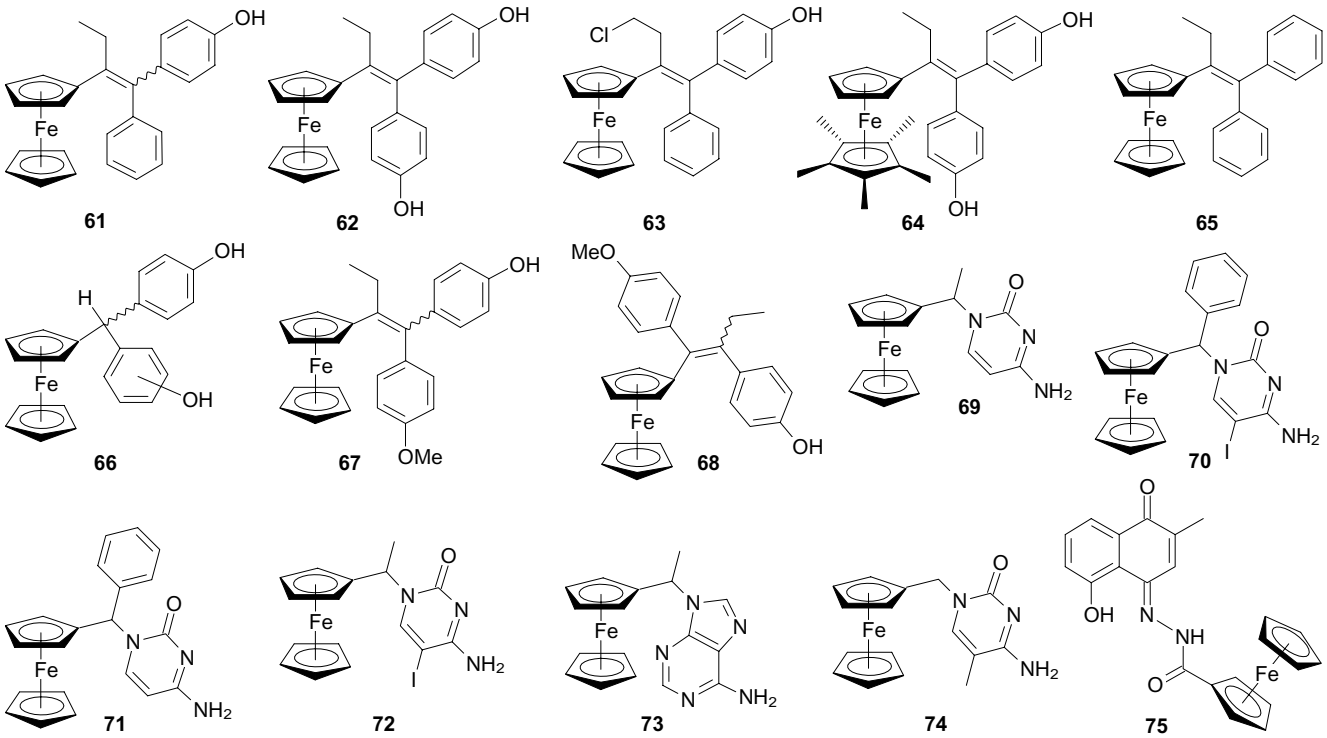
3.1. Cytotoxic ferrocene derivatives

Ferrocene was historically the first organometallic compound tested for antiproliferative activity in 1984.[104] The main advantages of ferrocene, which were mentioned in the cited study and in most of the subsequent studies, are its low toxicity against normal cells, high stability under physiological conditions and the ability to undergo one-electron oxidation to form a stable Fe^{III}-containing ferrocenium salt.[105]

The ferrocenium cation is quite stable, and the redox reaction giving this cation is reversible for most ferrocene derivatives. Ferrocenium salts (picrate and trichloroacetate) exhibited significant anticancer activity. Thus, the tumour growth retardation, which was evaluated in laboratory mice bearing transplantable Ehrlich ascites carcinoma (EAC), was 60 – 100%.[106]

The synthesis of ferrocifens, which are analogues of tamoxifen (the non-steroidal antiestrogen drug used to treat breast cancer, in which one phenyl substituent is replaced by ferrocene) was for a long time the main approach to the targeted search for cytotoxic ferrocene derivatives. In particular, it was found the ferrocene-containing hydroxytamoxifen derivatives **61** – **68** exhibit the highest activity, the hydroxyl group playing a key role in the generation of reactive oxygen species.[94] Consequently, the hydroxyl group is necessary for the manifestation of cytotoxicity. According to the results of this study, the presence of the tamoxifen moiety facilitates the intercalation of the molecule into DNA, and the ferrocene phenol system can generate reactive oxygen species only in the

Structures 61 – 75



presence of appropriate nitrogenous bases, in particular DNA nucleotides.

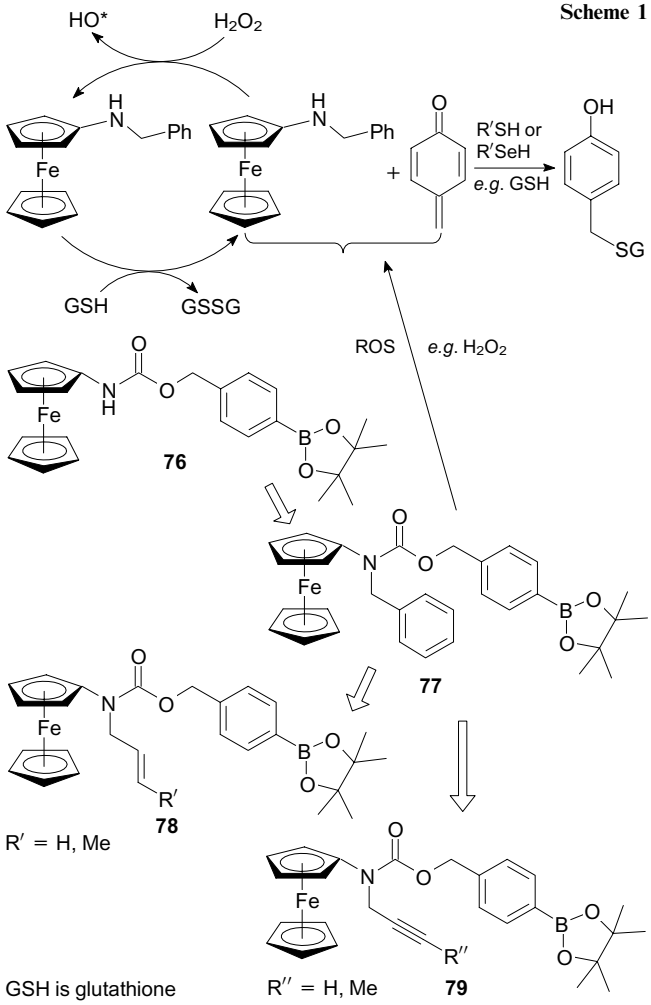
Meanwhile, an attempt to directly introduce a nitrogenous base instead of the tamoxifen moiety into the structure of the conjugate led to a significant decrease in the cytotoxicity of these compounds.[69] More detailed studies demonstrated that the replacement of the tamoxifen moiety by a nitrogenous base, in particular by pyrimidine or adenine derivatives, results in a change in the mechanism of cytotoxic activity. For example, conjugates **69**–**74** inhibit DNA synthesis and do not generate reactive oxygen species in the cell.[73]

Similar characteristics of the ROS generation and even higher cytotoxicity were achieved by replacing the tamoxifen moiety in the coordination compound by a simple quinoid structure.[76] Thus, plumbagin *N*′-(ferrocenylcarbonyl)hydrazone (**75**), a natural naphthoquinone, exhibits cytotoxicity of about 1 μmol L^{-1} against a number of cell lines (518A2, HCT-116, KB-V1/Vbl), shows 50 times lower toxicity compared to ferrocene-containing tamoxifen derivatives against normal fibroblasts (CHF) and has a similar mechanism of action causing DNA damage in the cell by reactive oxygen species.

Independently of the above studies on the optimization of the ferrocifen structure, Daum *et al.*[91] concluded that the ferrocene-containing cytotoxic conjugate should contain the quinoid moiety. They synthesized N-substituted 4-(ferrocenylcarbamato)phenylboronic acid pinacol esters **76**–**79**. These compounds are decomposed in the cell and release ferrocene-containing secondary amine and 4-methylenecyclohexadienone in the pseudo-quinoid form, which react with each other giving reactive oxygen species (Scheme 1). Besides, it was shown that a decrease in the lipophilicity of conjugates in the case of compounds **76**–**79** leads to an increase in both the efficiency of ROS generation and the improvement of cytotoxicity: for the BL-2, A2780 and Jurkat cell lines, IC_{50} are 15–30 μM.

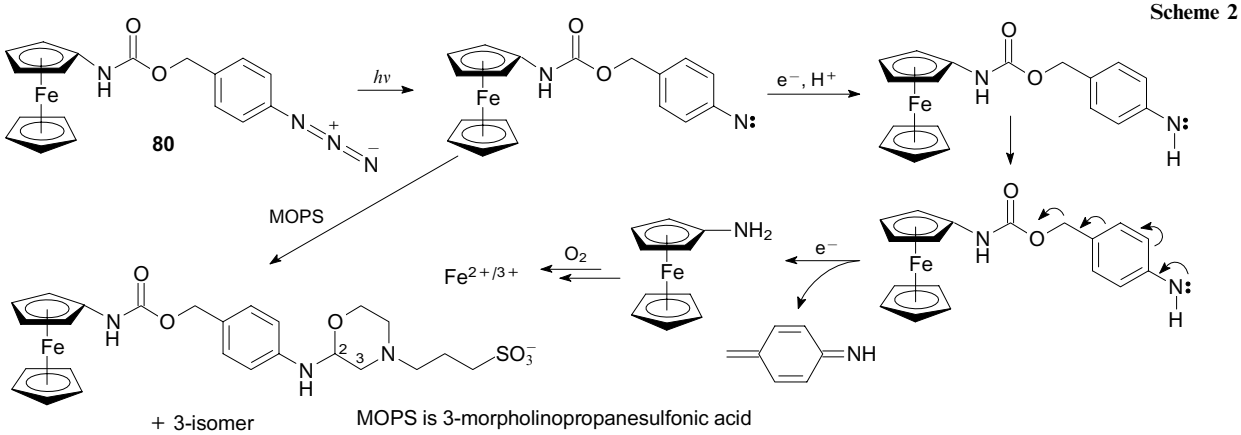
Other aminoferrocene-based carbamates, *e.g.*, 4-azidobenzyl ferrocenylcarbamate **80**,[85] have IC_{50} values against the HL-60 cell line in the same range (16–28 μM). In this case, low lipophilicity is achieved due to the presence of the polar azido group, and the metabolism of the conjugate occurs in a similar way leading to the release of free aminoferrocene and 4-methylenecyclohexadienone imine (Scheme 2). Therefore, any ferrocene conjugate with a quinoid structure in the active or latent form is apparently suitable for the manifestation of cytotoxicity *via* ROS generation.

Scheme 1

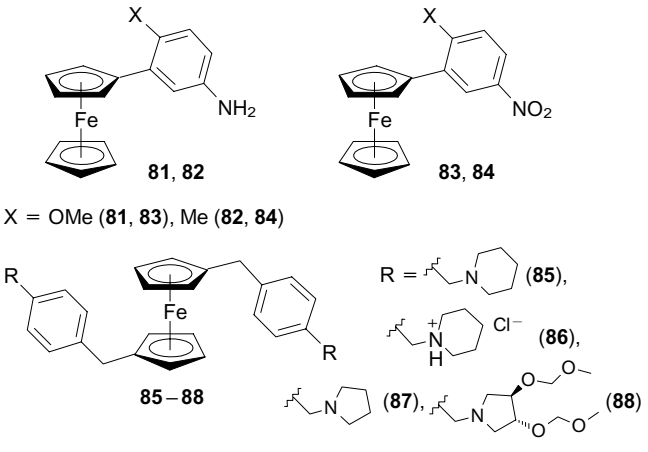


These data suggest that aminophenyl- and nitrophenyl-substituted ferrocenes,[88,100] which also exhibit cytotoxic activity through generation of reactive oxygen species, undergo a similar metabolism to form quinoid structures in a ferrocene-containing agent–DNA molecule complex. According to Asghar *et al.*,[88] these compounds bind to DNA in the cationic form *via* electrostatic interactions and cause DNA damage through the production of reactive oxygen species. The relatively lower IC_{50} values of compounds **81**–**84** and **85**–**88** (2.4–6.1 μM against the SK-OV-3 cell line and 1.55–4.72 μM against the MCF-7,

Scheme 2



Structures 81 – 88



respectively)[88, 100] compared to more complex conjugates **75** – **80** are attributed to the fact that the former compounds have higher affinity for transferrin and exhibit easier cellular uptake *via* receptor-mediated endocytosis.

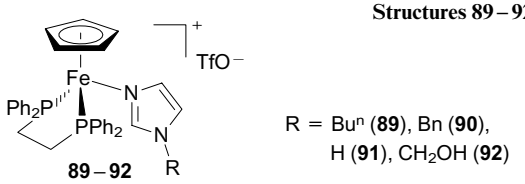
3.2. Cytotoxic half-sandwich iron complexes

A small subclass of cytotoxic ferrocene derivatives comprises half-sandwich coordination compounds, in which an iron atom is coordinated by one cyclopentadienyl ligand and the other coordination sites are occupied by N-, O- or P-donor ligands. The successful completion of the first stage of preclinical trials of the complex Cp_2TiCl_2 in 1988 [107] and the more recent data on cytotoxic activity of ferrocene derivatives were the impetus for the extensive research on the synthesis of these compounds and their evaluation for anticancer pharmaceuticals.

An analysis of the published data shows that soft ligands, such as phosphines, nitriles [77] or carbonyls,[89] capable of strong π-back donation, are more suitable for the stabilization of unsymmetrical iron coordination compounds. According to the results of the study,[89] a bifunctional ligand bearing amino and cyano groups is coordinated to the iron ion exclusively through the softer cyano moiety.

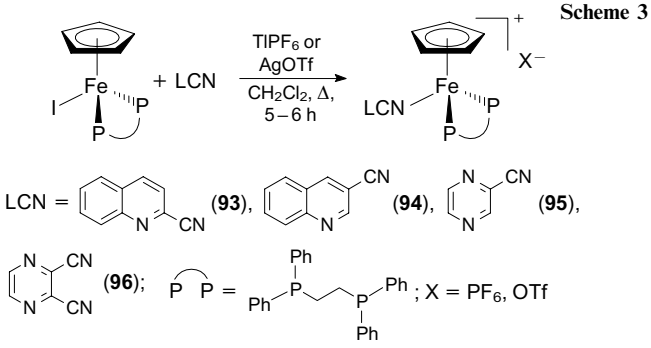
All coordination compounds **89** – **100** tested in the studies [72, 77, 89] exhibit cytotoxicity with IC_{50} values of a few μmol L^{-1} against the HL-60 and HeLa cell lines, causing the induction of apoptosis through DNA damage.

Structures 89 – 92

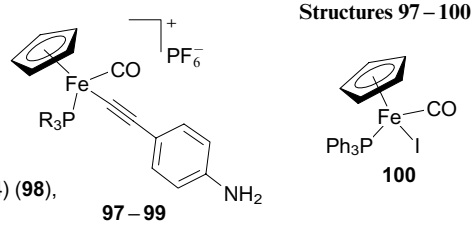


Valente *et al.* [77] demonstrated that half-sandwich coordination compounds **93** – **96** (Scheme 3), like ferrocene derivatives, can strongly bind to DNA and cause its damage. Pilon *et al.*[89] came to the same conclusions about the mechanism of action of coordination compounds **97** – **100** and additionally stated that the complexes with asymmetric charge distribution display comparatively higher cytotoxicity.

Scheme 3



Structures 97 – 100



These conclusions provide indirect evidence that complexes with a half-sandwich structure, like the ferrocene derivatives considered above, cause DNA damage through the production of reactive oxygen species. The charge distribution between the ligands in coordination compounds plays a key role in this redox process.

3.3. Classical iron coordination compounds with cytotoxic activity

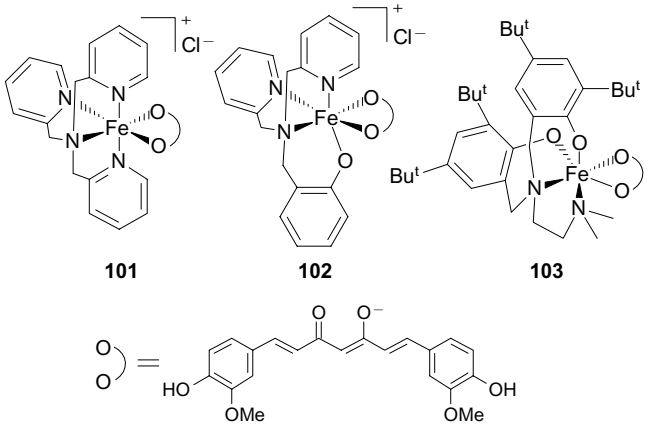
Iron ions in oxidation states +2 and +3 are characterized by coordination numbers 4, 5 and 6. Iron complexes bearing organic ligands with all possible coordination geometries were described (see Table 2): tetrahedral (1 example out of 27 characterized compounds), trigonal-prismatic (1 example), square- and triangular-prismatic (2 examples), square-pyramidal (4 examples) and octahedral (19 examples). As is seen in Table 2, the metal ion coordination environment in the overwhelming majority of cytotoxic iron coordination compounds has an octahedral geometry, the oxidation state of the iron ion placing no limitations on the possible geometry of coordination compounds. Thus, Fe^{II} and Fe^{III} compounds with octahedral and square-pyramidal geometry are nearly equal in number.

An analysis of the ligand structures shows that the most common iron coordination compounds are those containing 2 – 4 nitrogen atoms in the coordination sphere and 2 – 3 oxygen atoms in a polydentate or chelating ligand. Chloride anions are most frequently present as monodentate ligands.

3.3.1. Octahedral iron(II and III) coordination compounds

The main mechanism of cytotoxic activity of octahedral iron coordination compounds, as in the case of ferrocene derivatives, involves the generation of reactive oxygen species. The key contribution of ROS to the cytotoxicity was reported in eight publications (see Refs 70, 71, 74, 83, 84, 86, 90, 98) out of 18 studies, in which attempts were made to elucidate the mechanism of action. The second most common mechanism is associated with hydrolytic DNA damage and cleavage under light irradiation described in five studies (see below).

Structures 101 – 103



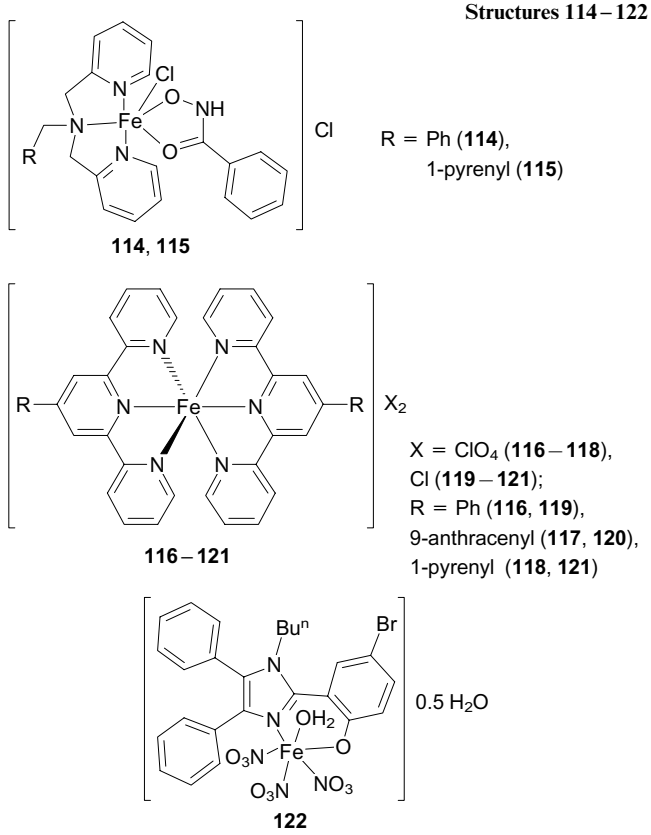
101 **102** **103**

Jana *et al.*[90] studied in detail the mechanisms of cytotoxic activity of octahedral Fe^{II} and Fe^{III} coordination compounds **101** – **103** with ligands of similar chemical nature, such as tris(2-pyridylmethyl)amine, (2-hydroxybenzyl)bis(2-pyridylmethyl)amine and *N*,*N*-bis(4,6-di-*tert*-butyl-2-hydroxybenzyl)-*N*′,*N*′-dimethylethylenediamine. They showed that all these coordination compounds generate ROS. However, the Fe^{II} complexes cause a significant increase in the ROS level in the dark, whereas light irradiation is required for Fe^{III} compounds (in the light, the toxicity of Fe^{III} coordination compounds increases by a factor of 2 – 5[81,86]).

According to the results of the study,[86] iron(III) complexes **104a** – **c**, **105b**,**c** can generate ROS both in the dark and in the light, but the exposure to light leads to a change in their structure. The ligand is decarboxylated to form carbon dioxide (Scheme 4). The ROS level and cytotoxicity are increased by a factor of 2 – 3. Therefore, taking into account that the mechanism of cytotoxicity through photooxidation of DNA was revealed for Fe^{III} coordination compounds, it can be suggested that the photooxidation also depends on the ROS generation and it is a special case of the common mechanism of action, which has some specific features for iron(III) compounds.

Meanwhile, as opposed to ferrocene derivatives, which generate reactive oxygen species in the presence of nitrogenous bases of DNA, octahedral iron coordination compounds bind to DNA only in rare cases and do not require the presence of DNA for the efficient activation of the redox process resulting in ROS generation. The weak electrostatic binding of complexes **106** – **113** (see Table 2) to the major and minor grooves of DNA was observed in the studies.[71,95,103] The binding through partial intercalation of a planar aromatic moiety of ligands of compounds **114** – **121** was also reported.[70,78] The true intercalation was found only for aqua complexes **122**, in which axial ligands (water

Structures 114 – 122

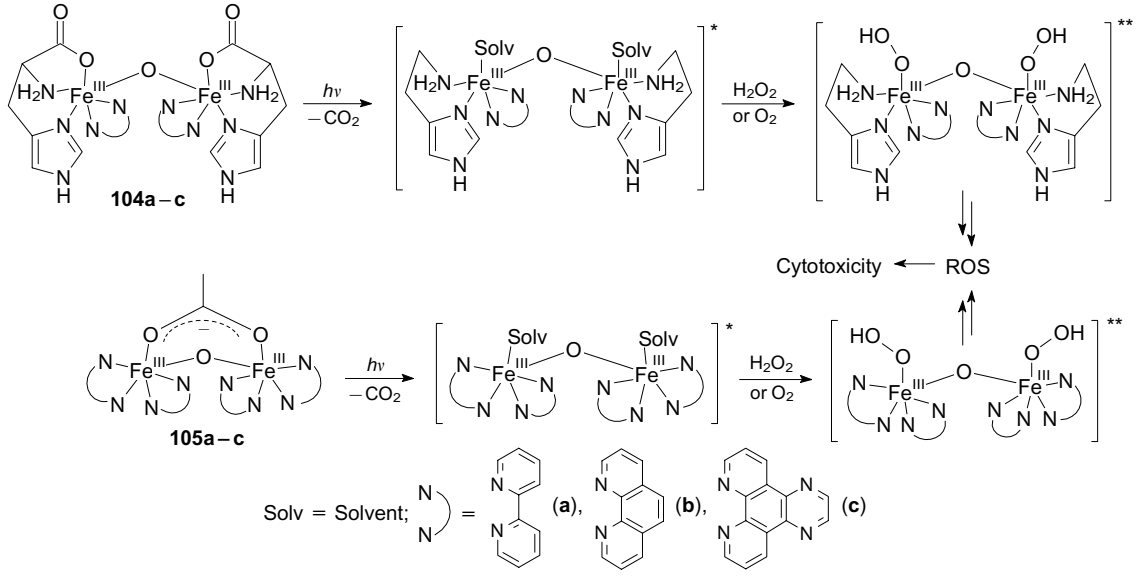


114, **115** R = Ph (**114**), 1-pyrenyl (**115**)

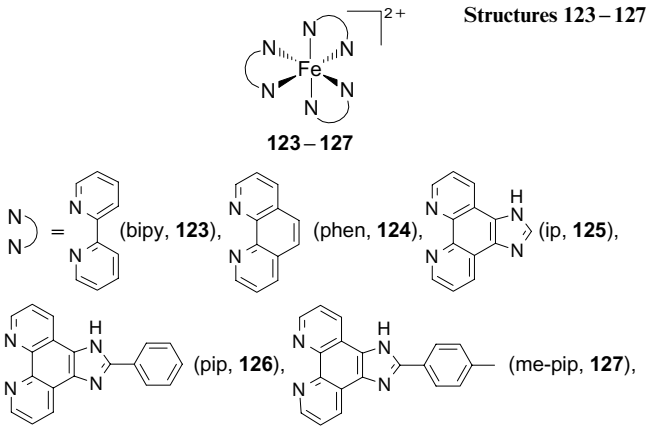
116 – **121** X = ClO_4 (**116** – **118**), Cl (**119** – **121**); R = Ph (**116**, **119**), 9-anthracenyl (**117**, **120**), 1-pyrenyl (**118**, **121**)

122 0.5 H_2O

Scheme 4



Structures 123 – 127



molecules) are easily exchanged with nitrogenous bases of DNA.[99]

There is evidence that the localization of octahedral Fe^{II} complexes in the cell nucleus is determined by lipophilicity of the organic ligand.[79] Coordination compounds **123** – **127** with substituted bipyridines and 1,10-phenanthrolines undergo endocytosis to form the secondary lysosome from the endosome and the primary lysosome of the cell followed by the localization of hydrophilic compound **123** in the nucleus through electrostatic interactions between polar groups and DNA anions, whereas hydrophobic compounds **124** – **127** are localized in the cell membrane and then released into the cytoplasm. The mechanism of cytotoxic activity also depends on the lipophilicity. Thus, hydrophilic complex **123** causes DNA damage and the arrest of the cell cycle at the S phase (p53-dependent), whereas hydrophobic complexes **124** – **127** inhibit the protein kinase B cascade, causing the arrest of the cell cycle at the G0/G1 phase and the induction of apoptosis.

However, most of octahedral iron coordination compounds, regardless of the oxidation state of the central atom, are localized in mitochondria — organoids containing the highest iron ion concentration in the cell. Mitochondrial localization and the mitochondrial pathway of the induction of apoptosis were revealed for a number of iron coordination compounds with organic ligands of different hardness or softness nature.[81, 82, 90, 93, 98, 101]

A nonuniform localization and different variants of the common mechanism of action make it difficult to compare the cytotoxicity for this class of compounds but the compilation of the data shows that the IC_{50} values of octahedral iron coordination compounds are in the range of 0.23 – 90 μM against the HeLa, MCF-7, A375, HepG2, PC-12, RHepG2, A549, HL-7702, LN-229, HaCaT, ECA109, TE-1 and NCI-H460 cell lines. The IC_{50} value is also significantly affected by the structure of the organic ligand. Thus, coordination compounds with aromatic amines and quinolines **89** – **92**, **107** – **112** and **123** – **128** are, on the average, an order of magnitude more toxic compared to other characterized complexes.[72, 79, 83, 95]

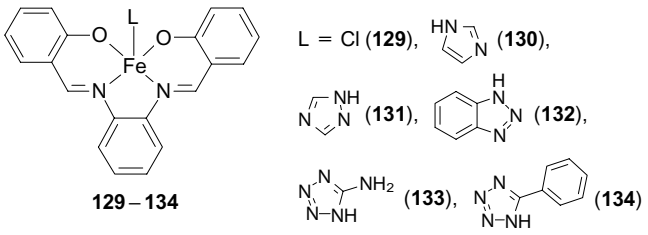
3.3.2. Square-pyramidal iron(III) coordination compounds

Square-pyramidal iron coordination compounds are structurally similar to octahedral complexes and differ from the latter by the absence of one axial ligand and a somewhat lower stability under physiological conditions.[96] It is worth noting that all such cytotoxic complexes described in the literature contain Fe^{III} ions although there are no fundamental limitations on the existence of square-pyramidal Fe^{II} coordination compounds.

Hence, it is reasonable to suggest that the mechanisms of cytotoxicity of square-pyramidal iron complexes should be similar to those of octahedral coordination compounds (see Section 3.3.1). This is consistent with the results of the study,[68] which demonstrated that ROS make a key contribution to the cytotoxicity of iron(III) complex **129** with the salophen ligand exhibiting antiseptic, antipyretic and analgesic activity.

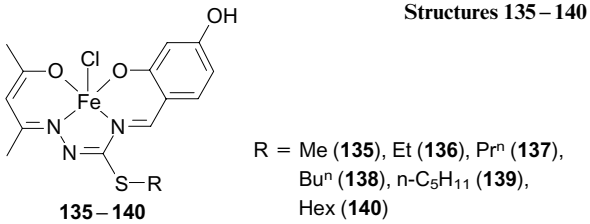
It would be expected that square-pyramidal coordination compounds will have higher DNA intercalating ability due to a more planar structure of the pyramidal coordination compound compared to the octahedral one. However, the experimental data show that square-pyramidal iron(III) complexes **130** – **134** with salophen bind to DNA through electrostatic interactions.[80] According to the results of the study,[80] the introduction of a planar sterically unhindered molecule as an additional monodentate ligand leads to an increase in the binding constant of iron(III) coordination compounds to DNA by approximately two orders of magnitude. Therefore, it can be suggested that the axial ligand rather than complex **134** as a whole intercalates into DNA, while the complex is electrostatically attracted to negatively charged phosphate groups of the DNA molecule.

Structures 129 – 134



An interesting fact is that Fe^{III} coordination compounds **135** – **140** with thiosemicarbazones (see Table 2) do not exhibit cytotoxic activity,[92] as opposed to thiosemicarbazone-containing coordination compounds of other transition metals displaying significant cytotoxicity.[32, 40, 44, 60, 108 – 111]

Structures 135 – 140

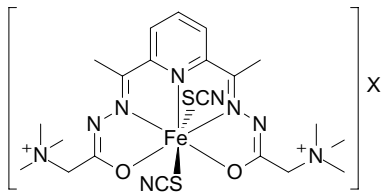


3.3.3. Bipyramidal iron(II) coordination compounds

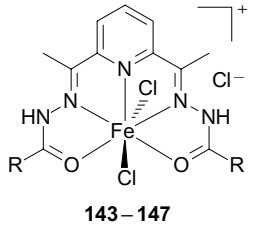
Pentagonal-bipyramidal complexes **141** – **147** belong to another class of iron coordination compounds similar to octahedral complexes with anticancer activity. All coordination compounds with this structure were synthesized based on 2,6-diacetylpyridine bis(hydrazones) as pentadentate ligands.[87, 97]

The IC_{50} values of these complexes measured against the A549 cell line vary from 52 to 190 μM. Therefore, they are, on the average, an order of magnitude less toxic than

Structures 141 – 147



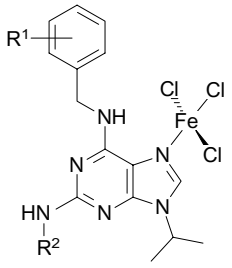
X = SCN (**141**),
Fe(SCN)$_5$ (**142**)



143 – 147

R = (**143**), (**144**), OH (**145**), (**146**), O (**146**)

Structures 148 – 153



148 – 153

R^1 = H (**148**, **151**, **152**),
2-OH, 5-Me (**149**),
3-OH (**150**),
3-OH, 5-Me (**153**);
R^2 = Cl (**148**), OH (**149 – 153**), HO (**152**)

octahedral iron coordination compounds **101 – 128**. This stimulated researchers to study in detail the mechanisms of cytotoxic activity of compounds **143 – 147**. It was found that, as opposed to the octahedral analogues, the ROS generation has no significant importance for the appearance of cytotoxic activity of these complexes.[97] Yao *et al.*[97] demonstrated that the ligands and, to a lesser extent, coordination compounds **143 – 147** inhibit ribonucleotide reductase, which plays a key role in DNA synthesis. The cytotoxicity correlates with the inhibitory concentration of ribonucleotide reductase. Hence, the authors suggested this mechanism of antiproliferative activity as the main one for this subclass of compounds.

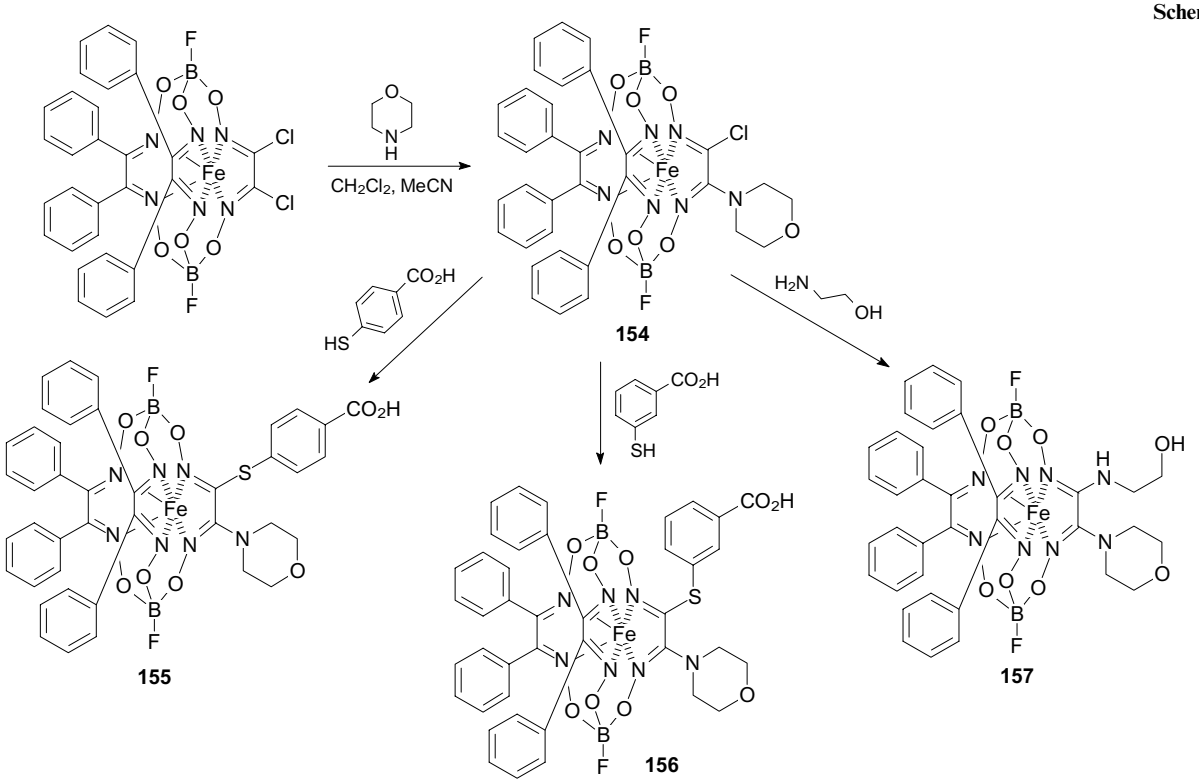
3.3.4. Tetrahedral iron(III) coordination compounds

In the only study,[67] in which tetrahedral iron(III) coordination compounds **148 – 153** based on 6-benzylamino-9-isopropylpurine derivatives were synthesized and characterized, the authors showed that the free organic ligand serves as the active ingredient, although these complexes have IC$_{50}$ values in a micromolar range against the G-361, HOS, K-562 and MCF-7 cell lines. This ligand is released *via* hydrolysis of the coordination compounds in the cell and its cytotoxicity, evaluated under the same conditions, differs from the cytotoxicity of the complexes within the standard error of measurement.

3.3.5. Trigonal-prismatic iron(II) coordination compounds

Four Fe^{II} coordination compounds **154 – 157** with unusual trigonal-prismatic structures (Scheme 5, Fig. 9) were described for the first time by Belov *et al.*[75] as effective inhibitors of DNA and RNA transcription. The mechanism of inhibition of the enzyme T7 RNAP (T7-RNA polymerase) involves the stabilization of the enzyme complex with DNA and RNA by hydrogen bonds and van der Waals interactions. The stabilization of the complex simultaneously with DNA, RNA and the active site of the enzyme leads to the irreversible inhibition of nucleic acid synthesis in the cell. Although *in vitro* experiments in cell lines were not performed, the IC$_{50}$ values for T7 RNAP, varying in the range of 0.5 – 2.5 μM, indicate that these coordination

Scheme 5



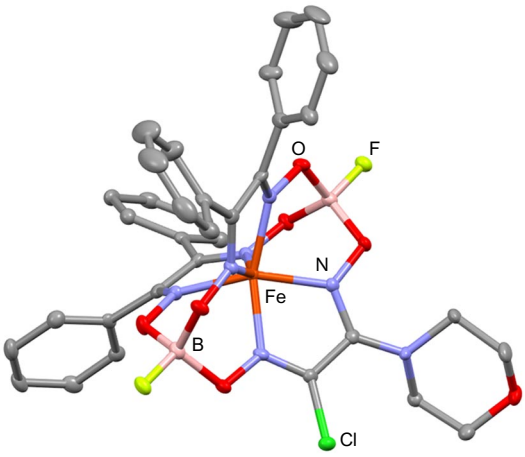


Figure 9. Molecular structure of compound **154**. The Figure was prepared by the authors using the X-ray diffraction data [75] and the data from the Cambridge Crystallographic Data Center (CCDC 976252).

compounds are promising for further evaluation as anticancer agents.

3.4. Prospects of the development of anticancer agents based on iron ions

The above data on the mechanisms of action, stability under physiological conditions and the intracellular distribution of cytotoxic iron complexes suggest that the most stable coordination compounds are based on ferrocene derivatives. They are not decomposed, do not undergo metabolism in the body with the release of a free iron ion, are equally stable as ferrocene and a ferrocenium cation and are stable during numerous oxidation–reduction cycles.

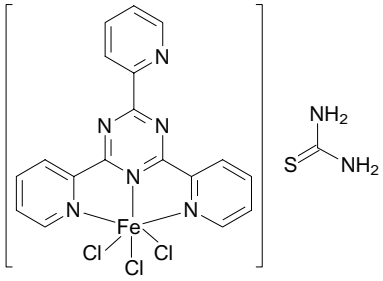
Besides, it is ferrocene derivatives that are localized at the sugar phosphate backbone of DNA through electrostatic attraction and efficiently generate ROS only when involved in a complex with heterocyclic bases of DNA. Therefore, such compounds more efficiently cause oxidative stress and nucleus lesions leading to the induction of apoptosis and ferroptosis. It should also be noted that ferrocene derivatives exhibit certain selectivity against cancer cells and passive targeting to the most vulnerable organelles in the cancer cell; however, their molecular target remains unknown.

Using ferrocifens, it was shown that the introduction of the ferrocenyl moiety into the known therapeutic agent [hydroxytamoxifen (**61**)] can lead to the improvement of its cytotoxic properties and the optimization of the mechanism of action, which provides a route to the development of dual drugs and prodrugs based on ferrocenes.

Hence, it can be suggested that the rational design of ferrocene derivatives taking into account the revealed common structural motifs of the most cytotoxic known sandwich Fe complexes will allow the development of new-generation anticancer agents exhibiting higher selectivity and cytotoxicity compared to the available pharmaceuticals.

Nevertheless, classical iron coordination compounds also have some advantages, such as the localization in cell mitochondria, efficient transport into the cell through transferrin receptors and generation of ROS in the excited (high-spin) state, for example, under light irradiation. Octahedral iron coordination compound **158** with 2,4,6-tris(2-pyridyl)-1,3,5-triazine exhibited the highest cytotoxic activity compared to the related Mn^{II}, Co^{II} and Ni^{II} complexes; its IC_{50} values against the Hep-G2 and MCF-7 HeLa cell lines were found to be 5–8 times lower.[102]

Structure 158



158

Due to these properties, iron coordination compounds, in particular, the most stable octahedral structures, are promising for the development of chemotherapeutic drugs and agents for photodynamic therapy of cancer.

4. Cobalt coordination compounds as cytotoxic agents

Due to the redox, chemical and magnetic properties, cobalt ions can theoretically be used to prepare biologically active coordination compounds with a wide range of therapeutic applications.[112] Besides, cobalt compounds in the most common oxidation states (+2 and +3) are stable under physiological conditions and can serve for the development of anticancer agents.

As in the case of the complexes of other metals considered above, the geometry of the coordination sphere and the oxidation state of the central metal atom (cation) are the key factors responsible for the mechanism of action and the degree of cytotoxic activity of cobalt coordination compounds.

An analysis of the published data demonstrates that the cytotoxic activity of cobalt(II) coordination compounds was evaluated for a rather large number of representatives (43 complexes in 29 studies), whereas only 14 examples (9 studies) were described for cobalt(III) compounds. A comparison of the X-ray diffraction data for these two classes of compounds leads to the conclusion that all cobalt(III) coordination compounds exhibiting biological activity have the same geometry of the ligand environment, namely octahedral, although this geometry is sometimes distorted in the case of polydentate ligands and bulky substituents. Cobalt(II) coordination compounds are characterized by more diverse geometries: octahedral (22 examples in 29 studies, 51%), tetrahedral (9 examples in 29 studies, 21%) and bipyramidal (10 examples in 29 studies, 23%). In rare cases, the square-planar arrangement of the ligands was achieved (2 examples, 5%). Almost all coordination polyhedra are strongly distorted with respect to the ideal bond lengths and bond angles; nevertheless, they can be assigned to particular classes based on the X-ray diffraction data.

A comparison of the ligand structures shows that polydentate and chelating ligands containing two or more nitrogen atoms are most typical of cytotoxic cobalt coordination compounds (Table 3). Different monodentate ligands complete the coordination sphere of cobalt ions to 6 and they are most often in axial positions.

Table 3. Cytotoxic cobalt coordination compounds.

No.	Complex (serial number of the compound)	Coordination sphere	Binding mode	Metal coordination geometry	Mechanism of cytotoxic activity	IC_{50} max (cell line)	Ref.
1	1,8,15,22-(4-EtC(O)$C_6H_4O)_4$-Co^{II} phthalocyanine (**233**)	CoN_4	Tetradentate	Square-planar	Unknown	19.53 μM (L929), 8.85 μM (MCF-7), 12.14 μM (MG63)	113
2	Co^{II}(ma)(phen)Cl (**176**), $Co^{II}(ma)_2(phen)\cdot 5H_2O$ (**177**)	CoN_2O_2Cl, CoN_2O_4	Each ligand is bidentate	Distorted octahedral	Binding to G4-DNA and double-stranded DNA, inhibition of topoisomerase 1	55 – 75 μM (MCF-7), 160 μM (MCF-710A)	114
3	$[Co^{II}(dpamH)_2(5\text{-Me-saloH})]Br$, $[Co^{II}(dpamH)_2(3\text{-OMe-saloH})]Cl$, $[Co^{II}(dpamH)_3]Br_2\cdot H_2O\cdot EtOH$	CoN_4O_2 or CoN_6	All ligands are bidentate	Distorted octahedral	Unknown. Nitro derivatives were found to be more toxic	10.82 – 15.49 μM (HeLa), 50 – 200 μM (Caki-1, HT-29, MTSV-17, MCF-7)	115
4	$[Co^{II}(Cl)L]BF_4\cdot 0.5$ MeOH (L is bis(3,5-dimethylpyrazol-1-ylmethyl)(2-pyridylmethyl)amine)	CoN_4Cl	Tetradentate + chloride anion	Distorted trigonal-bipyramidal	Unknown, Cu and Co complexes with the ligand have similar toxicity	~10 μM (HL-60)	116
5	$[Co^{II}(4,4'\text{-dmb})_3](PF_6)_3$ (**173**)	CoN_6	Each ligand is bidentate	Octahedral	Binding to the major groove of DNA and ROS generation	Not measured	71
6	Co^{II} 2,3,9,10,16,17,23,24-(4-$Pr^nO_2C)_8$-phthalocyanine (**234**)	CoN_4	Tetradentate chelate	Square-planar	Generation of ROS in the presence of ascorbic acid	Not measured	117
7	$[Co^{II}Cl_2(AP)_2]$ (**212**)	CoO_2Cl_2	Monodentate	Distorted tetrahedral	Intercalation into DNA, oxidative DNA cleavage in the presence of H_2O_2	54.69 μM (HeLa), 84.12 μM (MCF-7)	118
8	$[Co^{III}(trien)(phen)](ClO_4)_2Cl$ (**159**), $[Co^{III}(trien)(phen)](NO_3)_3$ (**160**)	CoN_6	Bidentate and tetradentate	Distorted octahedral	Binding to the major groove of DNA and oxidative DNA cleavage leading to the induction of apoptosis	**159**: 96 μM (HepG2); **160**: 813 μM (HepG2)	119
9	$[Co^{III}(HL\cdot Cl)(HL\cdot H_2O)]$ (**161**, **162**) (HL are substituted pyridine-4-carbaldehyde thiosemicarbazones)	$CoN_2O_2S_2$	Tridentate	Distorted octahedral	Intercalation into DNA. DNA cleavage correlates with the strength of intercalation	**161**: 6.01 ± 0.08 μM (MCF-7), 83.24 ± 1.03 μM (HeLa); **162**: 1.00 ± 0.09 μM (MCF-7), 20.28 ± 2.09 μM (HeLa)	108
10	$[Co^{II}LX_2]$ (L is 3,4,12,13- tetraoxo-7,9,16,18-tetraphenyl-1,2,5,6,10,11,14,15-octaazacyclooctadeca-6,9,15,18-tetraene; X = Cl, NO_3)	CoN_4X_2	Tetradentate	Octahedral	Unknown	X = Cl: 3.90 ± 0.7 μM (Hep3B), 7.36 ± 2.0 μM (HeLa), 5.12 ± 2.5 μM (MCF-7), 12.40 ± 0.9 μM (PBMC); X = NO_3: 4.86 ± 0.6 μM (Hep3B); 3.95 ± 0.2 μM (HeLa); 7.54 ± 0.8 μM (MCF-7); 14.08 ± 1.5 μM (PBMC)	120

Table 3 (continued).

No.	Complex (serial number of the compound)	Coordination sphere	Binding mode	Metal coordination geometry	Mechanism of cytotoxic activity	IC_{50} max (cell line)	Ref.
11	$[Co^{III}L_2]Cl$ (HL are R-substituted 2-acetylpyridine thiosemicarbazones: R = H (**163**), Me (**164**), Ph (**165**))	CoN_4S_2	Tridentate	Distorted octahedral	Intercalation into DNA. Antioxidant activity excludes ROS generation. Toxicity does not correlate with the strength of intercalation	**163**: 22.99 ± 0.08 μM (MCF-7), 32.12 ± 1.03 μM (A431); **164**: 7.24 ± 0.09 μM (MCF-7), 16.85 ± 2.09 μM (A431); **165**: 1.99 ± 0.13 μM (MCF-7), 9.30 ± 0.03 μM (A431)	109
12	$[Co^{III}L_2][NHEt_3] \cdot 2\ H_2O$ (H_2L is 2-(2-hydroxybenzylidene-amino)phenol)	CoN_2O_4	Tridentate	Octahedral	Unknown	~0.25 μM (HeLa)	121
13	$[Co^{II}LX_2]$ (**224**, **225**) (X = DMF, H_2O); $[Co^{II}(H_2L)Y_2]$ (**226**, **227**) (Y = N_3, NCS) (HL are 2,6-diacetylpyridine bis(4-substituted benzoylhydr-azones))	CoN_5X_2 CoN_5Y_2	Pentadentate + axial monodentate ligands	Distorted pentagonal-bipyramidal	Intercalation into DNA with the loss of axial ligands, oxidative DNA cleavage in the presence and in the absence of H_2O_2	Not measured	122
14	$Co^{II}(Cltpy)Cl_2$ (**231**), $Co^{II}(Cltpy)(SCN)_2$ (**232**)	CoN_3Cl_2 CoN_5	Tridentate	Distorted trigonal-bipyramidal	Unknown	**231**, **232**: 6.2 – 24 μM (MCF-7), 67 – 145 μM (K562); $(\mathbf{231})_3$: non-toxic (MCF-7), 6.2 μM (K562)	123
15	$Co^{II}L_2$ (**189**) (HL is 5-methyl-4-phenyl-2-(salicylideneamino)triazole)	CoN_4O_2	Tridentate	Distorted octahedral	Ability to inhibit tyrosine kinase is consistent with cytotoxicity values, but the concentrations are different	12.61 μM (HepG2), 14.08 μM (MCF-7)	124
16	$[Co^{II}(HL^1)_2Cl_2]$ (**178**) [a]	CoO_4Cl_2	Bidentate	Distorted octahedral	Selective binding to G4-DNA, the complex was shown to be accumulated in mitochondria and induce mitochondrial dysfunction and activation of apoptosis *via* the mitochondrial pathway	10.2 ± 0.6 μM (SK-OV-3/DDP), 18.3 ± 0.5 μM (Hep-G2), 28.6 ± 0.7 μM (HCT-8), 16.8 ± 0.5 μM (T-24), 35.7 ± 1.1 μM (NCI-H460), 40.2 ± 0.4 μM (BEL-7402), 27.3 ± 0.6 μM (SK-OV-3), > 100 μM (HL-7702)	125

Table 3 (continued).

No.	Complex (serial number of the compound)	Coordination sphere	Binding mode	Metal coordination geometry	Mechanism of cytotoxic activity	IC_{50} max (cell line)	Ref.
	$[Co^{II}(L^2)_2][Co^{III}Cl_4]\cdot 2H_2O$ (**179**)	CoN_6	Tridentate	Distorted octahedral	Selective binding to G4-DNA, the complex was shown to be accumulated in mitochondria and induce mitochondrial dysfunction and activation of apoptosis *via* the mitochondrial pathway. Inhibition of telomerase	1.0 ± 0.8 μM (SK-OV-3/DDP), 4.3 ± 1.1 μM (Hep-G2), 15.3 ± 1.2 μM (HCT-8), 3.1 ± 0.8 μM (T-24), 9.4 ± 0.6 μM (NCI-H460), 9.1 ± 0.9 μM (BEL-7402), 8.2 ± 1.1 μM (SK-OV-3), > 100 μM (HL-7702)	
17	$Co^{II}(HL)Cl$ (H_2L are (2-hydroxybenzyl)-(2-pyridylmethyl)(3-R-2-hydroxy propyl) amines: R = Cl (**228**), ONaph-1 (**229**), ONaph-2 (**230**))	CoN_2O_2Cl	Tridentate	Distorted trigonal-bipyramidal	Induction of apoptosis *via* the mitochondrial pathway, practically non-toxic against normal cells	**228**: 259 ± 2 μM (U937); **229**: 176 ± 2 μM (H460), 32 – 51 μM (THP-1, U937, Molt-4); **230**: 90 ± 2 μM (Colo-205), 147 ± 2 μM (H460), 54 ± 2 μM (THP-1), 36 ± 2 μM (U937), 65 ± 1 μM (Molt-4)	126
18	$[2\text{-mimH}]_2[Co^{II}(pydc)_2]ClO_4\cdot H_2O$	CoN_2O_4	Tridentate	Distorted octahedral	Unknown	~ 100 μM (MCF-7, HL-60)	127
19	$[Co^{II}(L^3)_2]\cdot 2H_2O$ (**166**), $[Co^{III}(HL^4)(L^4)]\cdot H_2O$ (**167**) [b]	CoN_4O_2	Tridentate	Distorted octahedral, octahedral	Intercalation into DNA	19.65 ± 0.56 μM (MCF-7); 12.86 ± 0.89 μM (MCF-7). Non-toxic against MCF-10A normal cells	128
20	$Co^{II}L_2(NCS)_2$ (**186, 187**) (L is benzyl 2-(cycloalkylmethylene)-hydrazinecarboxylate)	CoN_4O_2	Bidentate	Octahedral	Induction of apoptosis	48–54 μM (K-562)	129
21	$[Co^{II}(Caf)_4](PF_6)_2$ (**221**)	CoN_4	Monodentate	Tetrahedral	Phosphatidylinositol 3-kinase (PI3Kγ) was suggested as a new target for anticancer therapy. The Co complex has a moderate affinity	Not measured	130
22	$[Co^{III}(tpa)(cur)](ClO_4)_2$ (**172**)	CoN_4O_2	Tetradentate and bidentate	Octahedral	Co^{III} Complexes exhibit efficient cellular uptake and release curcumin over a period of time in the presence of intracellular reducing agents	Not measured	131
23	$Co^{II}LCl_2$ (**213 – 220**) (L are 3-substituted 2-amino-5-(2-pyridylmethylidene)imidazol-4-ones)	CoN_2Cl_2	Bidentate	Tetrahedral	Unknown, but ROS generation is not involved	47 – 140 μM (MCF-7)	132

Table 3 (continued).

No.	Complex (serial number of the compound)	Coordination sphere	Binding mode	Metal coordination geometry	Mechanism of cytotoxic activity	IC_{50} max (cell line)	Ref.
24	$[Co^{II}(phen)_2Cl_2]$ (**174**), $[Co^{II}(phen)_2L]$ (**175**), (HL is 1*H*-pyrazole-3,5-dicarboxylic acid)	CoN_4Cl_2, CoN_5O	Bidentate	Octahedral	Intercalation into DNA, oxidative DNA cleavage mediated by ROS. Low toxicity against normal cells at the minimum therapeutic dose	< 17.5 μM (MCF-7, HeLa, MIA-PA-CA 2, HepG2, A-498)	112
25	$[Co^{II}(L)_2]ClO_4$ (L is pyridine-2-carbaldehyde (*E*)-semicarbazone)	CoN_4O_2	Tridentate	Octahedral	Unknown; probably, the higher lipophilicity of the complex compared to the metal salt makes an important contribution to cytotoxicity	> 4 μM (AGS)	133
26	$Co^{II}L_2Cl_2$ (**201** – **209**) (L is 1-(4-bromobenzyl)-2-phenyl-1*H*-benzimidazole)	CoN_2Cl_2	Monodentate	Tetrahedral	Unknown	~ 1 – 10 μM (A2780, DU-145). Related Zn complexes are more toxic, variation of the substituents in the ligand has an insignificant effect	53
27	$Co^{II}L_2$ (**188**) (HL is 9-(2-benzoyl-hydrazono)-9*H*-fluorene-1-carboxylic acid)	CoN_2O_4	Tridentate	Distorted octahedral	Induction of apoptosis, weakly damages DNA	44 – 47 μM (A549), 27 – 47 μM (MCF-7)	134
28	$[Co^{II}(dicl)_2L]$ (L = phen (**180**), bipy (**181**), $(Py)_2$ (**182**), dpam (**183**), $(Himi)_2$ (**184**), $(im)_2$ (**185**))	CoN_2O_4	Bidentate + bidentate or monodentate N ligands	Distorted octahedral (for the bidentate nitrogen ligand and pyridine), tetrahedral for methyl-imidazole	Intercalation into DNA and antioxidant activity were established	Not measured	135
29	$[Co^{III}(paqh)_2](ClO_4)_2$, $[Co^{III}(mpkqh)_2](ClO_4)_2$, $[Co^{III}(ppkqh)_2](ClO_4)_2$	CoN_6	Tridentate	Octahedral	Unknown	24 – 52 μM (MCF-7), 46 – 59 μM (HCT-116), 35 – 51 μM (Hep-G2)	136
30	$Co^{II}L_2(H_2O)_4$ (**190**) (HL is theophylline)	CoN_2O_4	Monodentate	Distorted octahedral	High selectivity against the protein p53	Not measured	137
31	$Co^{II}L_2$ (**211**) (HL is *N*-hydroxy-*N*-(*p*-tolyl)-benzamide)	CoO_4	Bidentate	Distorted tetrahedral	Binding to the minor groove of DNA; the binding constants for cobalt are higher compared to those for copper and, consequently, the activity is higher	38.09 μM (MCF-7)	138

Table 3 (continued).

No.	Complex (serial number of the compound)	Coordination sphere	Binding mode	Metal coordination geometry	Mechanism of cytotoxic activity	IC_{50} max (cell line)	Ref.
32	$Co^{II}LX_2$ (X = Cl (**191**), NO_3 (**192**), OAc (**193**); L is 12-chloro-4,5-dihydro-2H-[1,2,5,6]tetraazecino[3,4-*b*]indole-3,6(7*H*,9*H*)-dione)	$CoN_2O_2X_2$	Tetradentate	Distorted octahedral	Cytotoxicity correlates with the inhibition of EGFR tyrosine kinase. Zinc complexes are more toxic (~47 μM)	~100 μM (SCC4)	139
33	$Co^{II}L_2Cl_2$, (HL is 2-acetyl-5-chlorothiophene thiosemicarbazone)	CoS_2Cl_2	Monodentate	Distorted tetrahedral	Unknown, cobalt complexes are less toxic that the related zinc and palladium complexes but are more selective	15 (DLD-1)	110
34	$Co^{II}L$ (**222**), Co^{II}_2L (**223**) (H_2L is the Schiff base of *o*-vanillin and *o*-phenylenediamine)	CoN_2O_2	Tetradentate	Distorted tetrahedral	Unknown. Toxicity of the binuclear complexes is higher than that of the mononuclear nickel complexes and the free ligand	**222**: 60.25 ± 5.50 μM (HCT-116); **223**: 45.50 ± 11.39 μM (HCT-116)	140
35	$Co^{II}(HL^5)$ (**210**) [c]	CoN_2O_2	Tetradentate	Tetrahedral	Causes late apoptosis and necrosis *via* the interaction with the minor groove of DNA	1.91 ± 0.1 μM (K562)	58
36	$[Co^{III}(phen)_2(L^6)](ClO_4)_3$ (**168**), $[Co^{III}(bipy)_2(L^6)](ClO_4)_3$ (**169**), $[Co^{III}(dmb)_2(L^6)](ClO_4)_3$ (**170**) [d]	CoN_6	Bidentate	Octahedral	Intercalation into DNA, DNA photocleavage under UV irradiation (365 nm). All complexes trigger apoptosis. The activity correlates with intercalation into DNA	10–20 μM (SC-OV-3)	141
37	$Co^{III}L_2PF_6$ (**171**) (L is methyl pyrazin-2-yl ketone 4-(4-methoxyphenyl)thiazol-2-ylhydrazone)	CoN_6	Tridentate	Distorted octahedral	Cobalt complex causes the induction of apoptosis, whereas the related iron and nickel complexes cause necrosis. Binding to the minor groove of DNA (the binding of the cobalt complex is stronger compared to the other complexes)	45 μM (U-937)	142

Note. The following abbreviations are used: ma is 3-hydroxy-2-methyl-4-pyrone, dpam is di(2-pyridyl)amine, R-saloH is substituted salicylaldehyde, 4,4′-dmb is 4,4′-dimethyl-2,2′-bipyridine, trien is triethylenetetramine, Cltpy is 4′-chloro-2,2′:6′,2″-terpyridine, Naph is naphthyl, mimH is methylimidazole, pydc is pyridine-2,6-dicarboxylic acid, tpa is tris(2-pyridylmethyl)amine, Hdicl is diclofenac (2-[2-(2,6-dichloroanilino)phenyl]acetic acid), im is imidazole, Py is pyridine, paqh is pyridine-2-carbaldehyde 2-quinolylhydrazone, mpkqh is methyl 2-pyridyl ketone 2-quinolylhydrazone, ppkqh is phenyl 2-pyridyl ketone 2-quinolylhydrazone. [a] HL^1 is 6-hydroxyoxoisoaporphine, HL^2 is 4,6-di(2-pyridyl)benzo[*h*]isoindolo[4,5,6-*de*]quinolin-8(5*H*)-one; [b] L^3 is 2-[2-(6-methyl-5-oxo-2,5-dihydro-1,2,4-triazin-3-yl)hydrazono]propanoic acid, L^4 is 2-[2-(2-amino-6-methyl-5-oxo-2,5-dihydro-1,2,4-triazin-3-yl)hydrazono]propanoic acid; [c] H_3L^5 is 2-hydroxy-1,3-bis{2-[(2-hydroxy-5-nitrophenylmethylene)aminomethyl]phenyloxy}-propane; [d] L^6 is 2-(5-chloro-3a,*H*-isoindol-3-yl)-1*H*-imidazo[4,5-*f*][1,10]phenanthroline.

Chloride anions are the most common monodentate ligands.

4.1. Octahedral cobalt(III) coordination compounds

The mechanism of cytotoxic activity of octahedral Co^{III} coordination compounds is apparently associated with the DNA binding followed by DNA damage leading to the induction of apoptosis *via* a DNA-dependent pathway. In particular, the DNA binding *via* different pathways was demonstrated in six of seven studies, where the mechanism of action of Co^{III} complexes **159** – **171** was described.[108, 109, 119, 128, 141, 142] The changes in the cell morphology characteristic of apoptosis were observed for compounds **159** – **161** and **171** in two (out of seven) studies.[119, 142] The mechanisms of DNA binding are different for different coordination compounds and are determined by the ease of the loss of axial ligands required for the intercalation between nitrogenous base pairs of DNA.

In the cases when all coordination sites are occupied by polydentate ligands (compounds **159** and **171**, Fig. 10) and it makes no sense to speak about the loss of axial ligands with the retention of the complex, the electrostatic binding occurs to the major [119] or minor [142] grooves of DNA. If the axial positions in the coordination sphere are occupied by labile axial moieties of polydentate ligands, which are able to dissociate without the rearrangement of the remainder of the complex (compounds **161** and **162**, Fig. 11),[108] coordination compounds intercalate into DNA (the cytotoxicity correlates with the DNA binding constant). Besides, if the equatorial ligands contain planar conjugated moieties and fused aromatic rings, the intercalation into DNA is additionally facilitated and the binding constants can be as high as $(1.93 - 3.71) \times 10^5$ L mol^{-1}.[141]

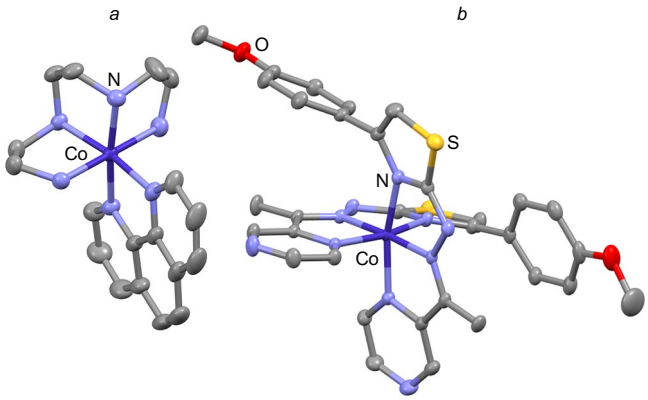
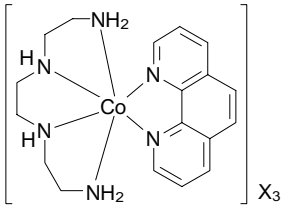


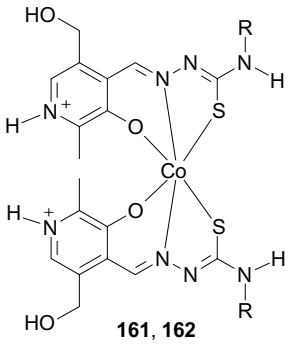
Figure 10. Molecular structures of coordination compounds **159** (*a*) [119] and **171** (*b*),[142] which are incapable of releasing axial ligands and which bind to the major and minor grooves of DNA, respectively. The Figure was prepared by the authors using the X-ray diffraction data [119, 142] and the data from the Cambridge Crystallographic Data Center (CCDC 922741 and 1935712).

Structures 159 – 172



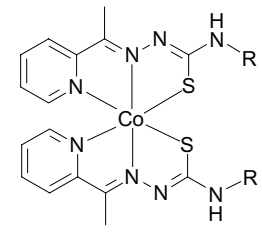
159, **160**

X_3 = $(ClO_4)_2Cl$ (**159**), $(NO_3)_3$ (**160**)



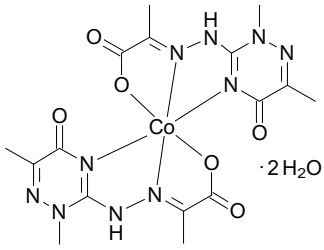
161, **162**

R = H (**161**), Me (**162**)

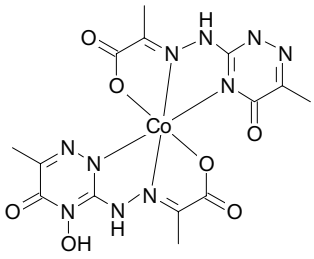


163 – **165**

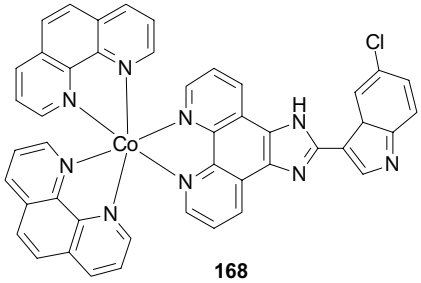
R = H (**163**), Me (**164**), Ph (**165**)



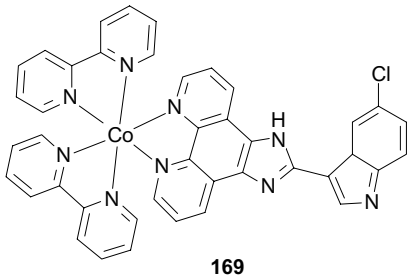
166



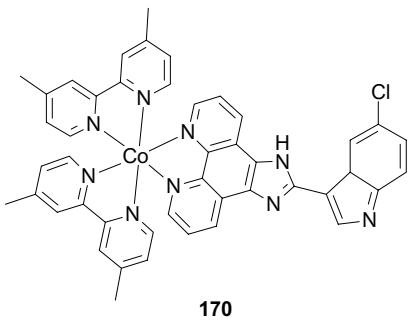
167



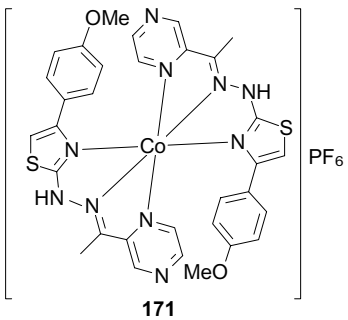
168



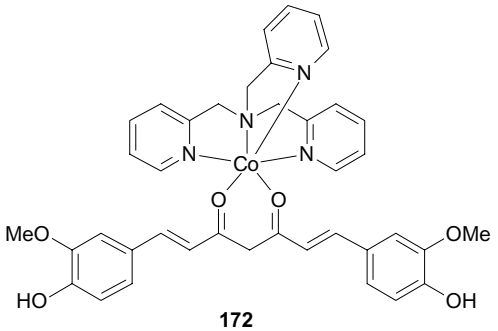
169



170



171



172

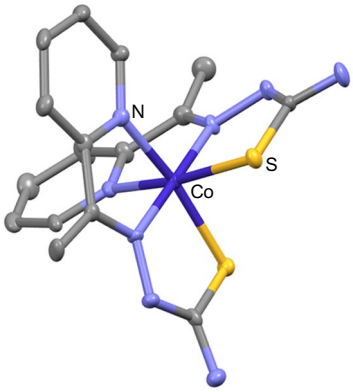


Figure 11. Molecular structure of coordination compound **162** capable of intercalation into DNA due to flexible moieties of the ligands in axial positions.[108] The Figure was prepared by the authors using the X-ray diffraction data[108] and the data from the Cambridge Crystallographic Data Center (CCDC 917524).

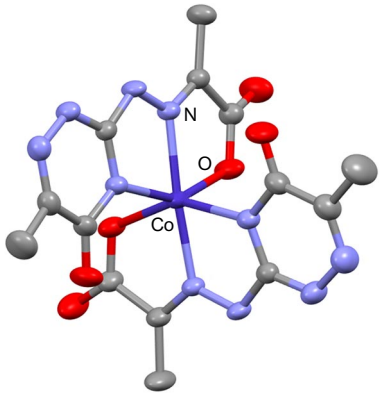


Figure 12. Molecular structure of cobalt(II) coordination compound **166** structurally similar to Co^{III} complex **167**; both complexes have similar mechanisms of cytotoxic activity.[128] The Figure was prepared by the authors using the X-ray diffraction data[128] and the data from the Cambridge Crystallographic Data Center (CCDC 1013116).

Additional evidence that the DNA intercalation occurs after the primary electrostatic binding of the octahedral coordination compound to DNA and the loss of axial ligands is provided by the study of the mechanism of translocation into the cell and the intracellular distribution of cobalt(III) complex **172** with tris(2-pyridylmethyl)amine and curcumin.[131] Investigations by time-resolved inductively coupled plasma mass spectrometry (ICPMS) and fluorescence spectroscopy demonstrated that the Co^{III} coordination compound exhibits efficient cellular uptake followed by the reduction with intracellular reducing agents and the excretion of curcumin (diaxial ligand) in the free form. However, the oxidation state of cobalt ions in these compounds after the cellular uptake was not systematically studied. Only in a few studies, cobalt(III) complexes were demonstrated to have antioxidant and reducing properties after intracellular localization.[109] Taking into account the conclusions drawn in the study,[131] this fact cannot be with certainty extended to all octahedral Co^{III} coordination compounds.

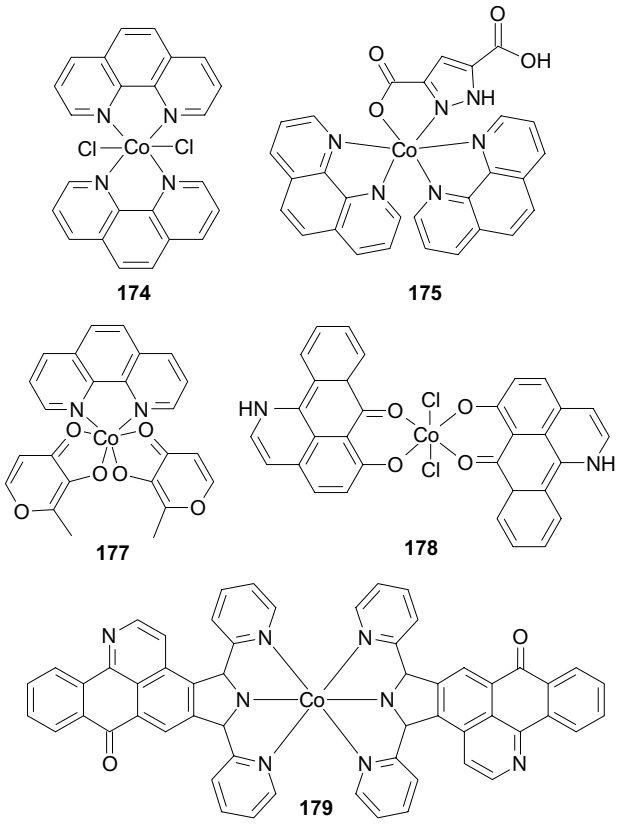
In a number of studies, cobalt complexes **159** – **160** and **168** – **170** was shown to exhibit nuclease activity *via* mechanisms of oxidative DNA cleavage[119] and DNA photocleavage under UV irradiation at a wavelength (λ) of 365 nm,[141] respectively. The possibility of DNA cleavage after the DNA binding is apparently the key factor in the induction of apoptosis *via* a DNA-dependent pathway, which begins after the incubation of cancer cells with cobalt(III) coordination compounds.

However, it cannot be ruled out that the binding and subsequent cleavage of chromosomal DNA of the cell is only one of the possible mechanisms of cytotoxic activity of Co^{III} complexes, because the mechanism of action of these coordination compounds was not comprehensively studied. Besides, the IC_{50} values of compounds **163** – **165** do not correlate with the DNA binding affinity.[109]

4.2. Octahedral cobalt(II) coordination compounds

The general features revealed for the mechanisms of cytotoxic activity of octahedral cobalt(III) coordination compounds are largely true for octahedral Co^{II} complexes. This may be indicative of a key role of the coordination geometry compared to the oxidation state of the central atom. Thus, the most frequently observed mechanism of cytotoxicity found for cobalt(II) coordination compounds **166** (Fig. 12) and **173** – **187**, as well as for Co^{III} complex **167**, involves the DNA binding (6 studies out of 15)[71, 112, 114, 125, 128, 135] and the subsequent induction of apoptosis (3 studies out of 16).[125, 129, 134]

Structures 174, 175, 177 – 179



Similar patterns were revealed in the investigation of the DNA binding mode. The only coordination compound **175** (Fig. 13) in this series, which is incapable of intercalation into DNA and which binds to the minor groove of DNA through electrostatic interactions, contains rigid conformationally fixed ligands, which simultaneously occupy one axial position and one equatorial position, *i.e.*, this compound cannot lose axial ligands.[112]

A new property of octahedral cobalt(II) coordination compounds, which is not described for its oxidized analogues, is the selective binding to DNA quadruplexes, which provides higher selectivity of the cytotoxic effect.[114, 125] According to the results of the study,[114] the binding constants of complexes **176** and **177** to G4-DNA (7.34×10^3 and 6.72×10^4 L mol^{-1}, respectively) are 1.4 and 1.5 times higher than those to double-stranded (ds)

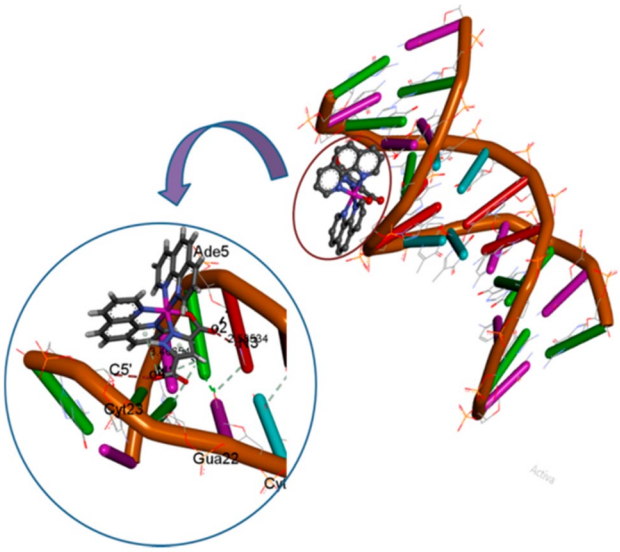


Figure 13. Results of molecular docking demonstrating the binding of compound **175** to the minor groove of DNA.[112] Reproduced with the permission of Elsevier.

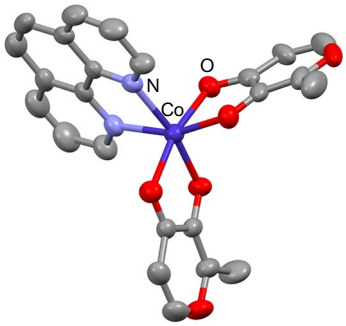
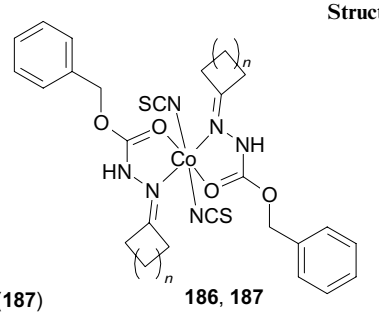


Figure 14. Molecular structure of cobalt(II) coordination compound **177** based on phenanthroline and 2-methyl-4-oxo-4*H*-pyran-3-olate exhibiting selective binding to G4-DNA.[114] The Figure was prepared by the authors using the X-ray diffraction data [114] and the data from the Cambridge Crystallographic Data Center (CCDC 774861).

DNA (5.11×10^3 and 4.32×10^4 L mol^{-1}) (Fig. 14). Coordination compounds **178** and **179** with oxoisoaporphine derivatives are more selective; their $^{G4}DC_{50}$ values (the concentration of the compound required to displace 50% of thiazole orange from the complex with G4-DNA) vary in the range of 0.89–14.01 μM for different quadruplex sequences.[125] Meanwhile, the corresponding parameters for ds-DNA ($^{ds}DC_{50}$) are 43.64 and 97.55 μM, respectively, upon the binding of these compounds to cellular DNA isolated from calf thymus.

Nithya *et al.*[129] studied compounds **186** and **187** and came to a similar conclusion about an important contribution of the DNA intercalation to the overall cytotoxicity of octahedral cobalt coordination compounds.

Structures 186, 187



n = 1 (**186**), 2 (**187**)

186, **187**

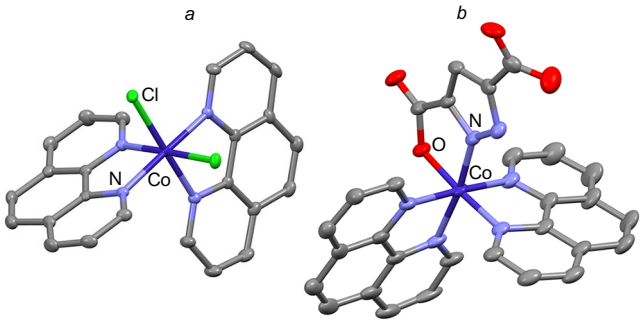
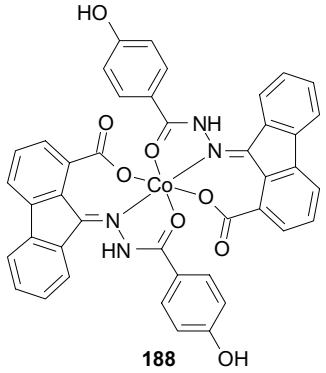


Figure 15. Molecular structures of cobalt(II) coordination compounds **174** (*a*) and **175** (*b*) exhibiting nuclease activity mediated through the generation of reactive oxygen species.[112] The Figure was prepared by the authors using the X-ray diffraction data [112] and the data from the Cambridge Crystallographic Data Center (CCDC 1826438 and 1817080, respectively).

Structure 188



188

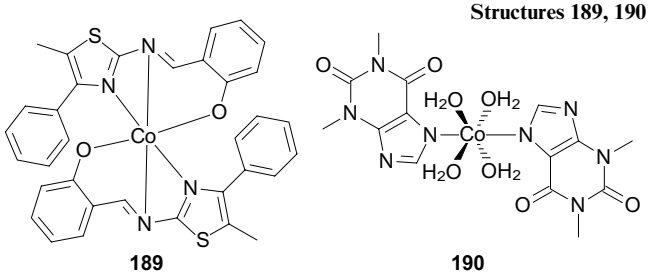
As in the case of octahedral Co^{III} coordination compounds, their Co^{II}-containing analogues **174**, **175** and **188** (Fig. 15) exhibit nuclease activity and DNA cleaving ability through generation of reactive oxygen species,[112, 134] but this activity is weaker compared to that of cobalt(III) complexes.

However, insufficient nuclease activity of octahedral cobalt(II) coordination compounds **178** and **179**, which reduces the contribution of apoptosis *via* a DNA-dependent pathway to the overall cytotoxicity, is compensated by high tendency to accumulation in mitochondria (50% of the Co level in the cells are still localized in the nucleus due to high DNA binding affinity, and the remaining 50% of Co accumulate in mitochondria) and the impairment of mitochondrial function leading to the induction of apoptosis *via* the mitochondrial pathway.[125]

Meanwhile, a rather large number of studies on the mechanism of cytotoxic activity of octahedral cobalt(II) coordination compounds showed that, apart from two main mechanisms of action considered above, other less frequent mechanisms related mainly to the inhibition of different enzymes cannot be ruled out. Thus, it was shown that coordination compounds **178**, **179**, **189** and **190** can inhibit tyrosine kinase,[124] telomerase,[125] PI3Kγ,[137] which are key enzymes of the cell cycle responsible for an unlimited number of possible cancer cell divisions.

In some cases, the inhibition of enzymes of the cell cycle can be considered as the main mechanism of cytotoxic

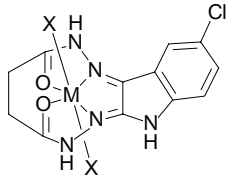
Structures 189, 190



189 **190**

activity. In particular, the analysis of the expression of tyrosine kinases (TRKs) in four cancer cell lines (HepG2, MCF-7, A549, HCT116) revealed a correlation between the TRK expression in the cell line and the cytotoxicity of Co^{II} complex **189** with 2-amino-5-methyl-4-phenylthiazole.[124] This compound does not exhibit cytotoxicity against the A549 and HCT116 cell lines, for which the inhibition of TRK was not observed, and it has IC_{50} values of 9.11 μM against the MCF-7 cell line (19% inhibition of TRK) and 8.16 μM against the HepG2 cell line (33% inhibition of TRK). Similar patterns were found for Co^{II}, Zn^{II} and Ni^{II} coordination compounds (**191** – **200**) with a macrocyclic ligand based on 5-chloroisatin and succinic acid dihydrazide.[139] All these complexes have IC_{50} values of about 90 μM against the SCC4 cell line. Zinc(II) coordination compound **200** was found to be the most toxic (IC_{50} = 41.4 μM) and it has the highest affinity for the active site of EGFR tyrosine kinase.

Structures 191 – 200



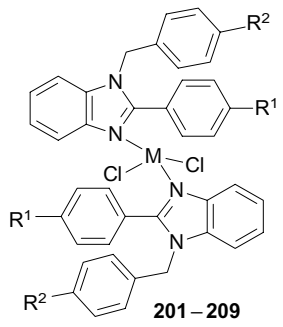
191 – 200

M = Co^{II}: X = Cl (**191**), NO_3 (**192**), OAc (**193**); M = Ni^{II}: X = Cl (**194**), NO_3 (**195**), OAc (**196**); M = Cu^{II}: X = Cl (**197**), NO_3 (**198**), OAc (**199**); M = Zn^{II}, X = Cl (**200**)

4.3. Tetrahedral cobalt(II) coordination compounds

The cytotoxic activity of tetrahedral cobalt(II) coordination compounds is relatively low and, in terms of IC50 values, these compounds are less effective compared not only to octahedral analogues but also to Zn^{II} complexes.[53, 110] In particular, 9 pairs of coordination compounds **201** – **209** were studied, and only in the pair of analogues **205** based on substituted benzimidazoles, the cobalt(II) complex exhibited cytotoxicity comparable with that of related zinc(II) complexes.[53] For tetrahedral Co^{II} coordination compounds, it is more difficult to distinguish the main mechanism of

Structures 201 – 209



201 – 209

R^1 = H: R^2 = Cl (**201**), Br (**202**), Me (**203**), Ph (**204**), styryl (**205**); R^1 = Cl: R^2 = Cl (**206**), Me (**207**), H (**208**, **209**); R^1 = R^2 = H (**208**); M = Co, Zn

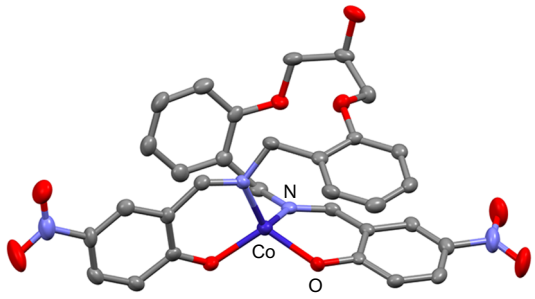
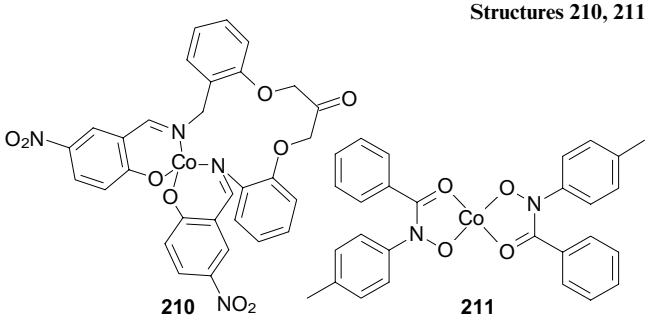


Figure 16. Molecular structure of complex **210**.[58] The Figure was prepared by the authors using the X-ray diffraction data [58] and the data from the Cambridge Crystallographic Data Center (CCDC 1828805).

cytotoxic activity, because detailed *in vitro* biological evaluations of their anticancer activity are quite few in the literature. However, in most of the studies on the mechanism of cytotoxic activity reviewed here, it was stated that tetrahedral cobalt(II) complexes bind to DNA.

According to the results of the study,[58] tetrahedral coordination compound **210** (Fig. 16), unlike octahedral Co^{II} complexes, causes late apoptosis and necrosis of the cells *via* a DNA-dependent pathway after the binding to the minor groove of DNA. Thakur *et al.*[138] also demonstrated that the binding constant of tetrahedral cobalt complex **211** with bis(*N*-*p*-tolyl)hydroxamic acid to the minor groove of DNA is 74% higher compared to related copper compounds, and its value correlates with the cytotoxicity of the compounds against the MCF-7 cell line: IC_{50} (μM) = 38.09 for Co^{II} *versus* 89.52 for Cu^{II}.

Structures 210, 211

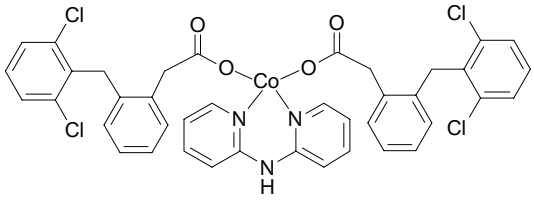


210 **211**

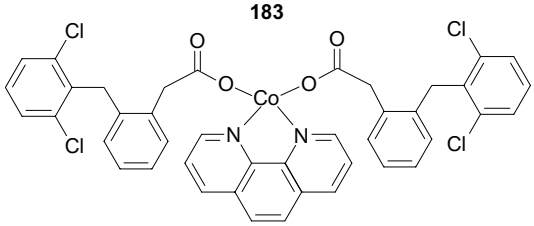
It was shown [118, 135] that tetrahedral cobalt(II) coordination compounds **180** – **185** and **212** have DNA intercalating ability. In this case, the higher binding constants of Co^{II} coordination compounds were 66% higher than those of the copper complex with the same ligands (3.71×10^4 *versus* 2.45×10^4 L mol^{-1}); however, a direct correlation between the DNA binding affinity and the cytotoxicity was not found for complex **212**.[118] Moreover, the binding constants of tetrahedral complexes **183** and **185**, which were measured from the displacement of ethidium bromide from the complex with DNA, were lower compared to the octahedral analogues as was demonstrated by the analysis of the strength of the interaction between DNA and cobalt(II) coordination compounds **180** – **185** with different geometries and different ligand environment *via* an intercalation pathway.[135]

Another important feature of the intracellular behaviour of Co^{II} coordination compounds having a tetrahedral

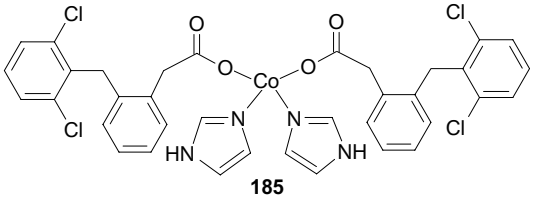
Structures 183 – 185, 203, 213 – 220



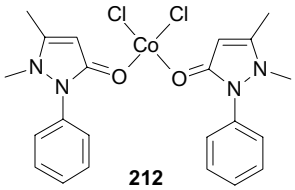
183



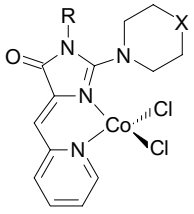
184



185



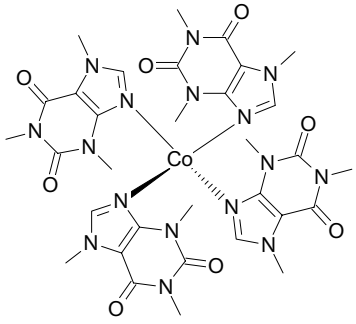
212



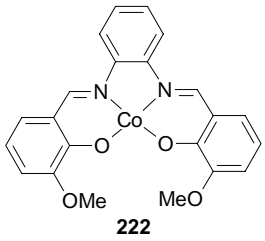
X = O: R = Ph (**213**), Me (**214**), All (**215**), $(CH_2)_2N_3$ (**216**);
X = CH_2: R = Ph (**217**), Me (**218**), All (**219**), $(CH_2)_2N_3$ (**220**)

213 – 220

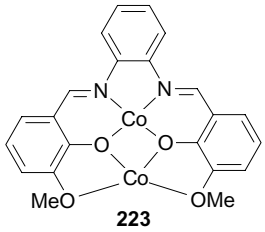
Structures 221 – 223



221



222



223

ligand environment is that many representatives (*e.g.*, compounds **213** – **220**) not only do not generate ROS [132] but also exhibit significant antioxidant activity. Perontsis *et al.*[135] demonstrated that cobalt complexes **183** and **185** are effective scavengers of three most abundant types of free radicals: DPPH [2,2-diphenyl-1-(2,4,6-trinitrophenyl)hydrazin-1-yl], ABTS [2,2′-azinobis(3-ethylbenzothiazoline-6-sulfonic acid)] and the hydroxyl radical.

However, unlike octahedral cobalt(II) coordination compounds, tetrahedral complexes, most likely, do not exhibit cytotoxic activity against cells through the inhibition of enzymes of the cell cycle. In particular, it was shown [130] that the complex $[Co^{II}(Caf)_4]$ (**221**) has the lowest calculated binding energy to the active site of phosphatidylinositol 3-kinase (PI3K) compared to the related cadmium, zinc, nickel and copper complexes and even the free ligand. This is indirectly evidenced by the pronounced additive effect found for dinuclear cobalt(II) coordination compounds **222** and **223**.[140] A twofold increase in the cytotoxicity in the presence of the second Co^{II} ion in the coordination compound indicates that the mechanism of cytotoxic activity is metal-dependent and is not determined by the structural features of the molecule.

4.4. Bipyramidal cobalt(II) coordination compounds

The mechanisms of cytotoxic activity of bipyramidal Co(II) coordination compounds are poorly studied, which makes it difficult to reveal general patterns and decreases the reliability of general conclusions. Besides, in some publications, the authors did not try to discover new targets and elucidate the mechanisms of action of these complexes. Some researchers only measured the average IC_{50} values for a series of compounds [116] or compared their behaviour with that of structurally similar octahedral Co^{III} and Cu complexes.[122, 126]

It was reported in the literature that pentagonal-bipyramidal cobalt(II) coordination compounds **224** – **227** with equatorial pentadentate ligands, substituted 2,6-diacetylpyridine bis(benzoylhydrazones) (Fig. 17), demonstrate the behaviour similar to that of octahedral complexes with labile axial ligands. In the presence of a DNA molecule, these compounds lose both axial monodentate ligands (regardless of their nature: DMF, H_2O, N_3^-, NCS^-) and bind to DNA by intercalation with the binding constants of $(1-3)\times10^5$ L mol^{-1}. The binding constant depends primarily on the structure of the equatorial pentadentate ligand and remains almost unchanged with a variation of

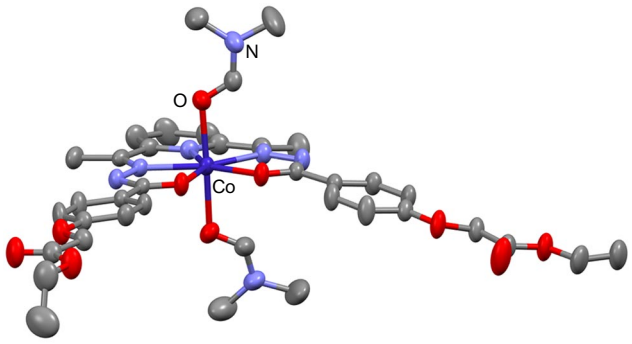
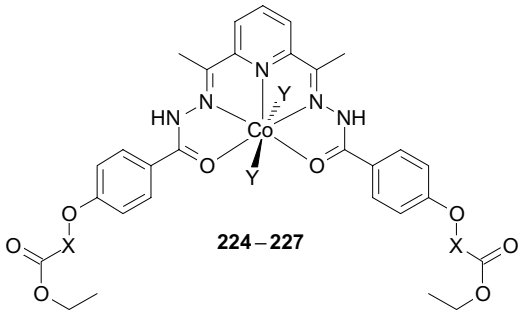


Figure 17. Molecular structure of complex **224**.[122] The Figure was prepared by the authors using the X-ray diffraction data [122] and the data from the Cambridge Crystallographic Data Center (CCDC 1034434).

Structures 224 – 227



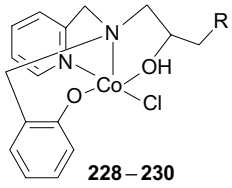
X = CH_2: Y = DMF (**224**), H_2O (**225**);
X = $(CH_2)_3$: Y = N_3 (**226**), SCN **227**)

the ligands in axial positions.[122] The authors compared the evaluated constants with the data for known octahedral cobalt(III) coordination compounds and concluded that the binding constants to DNA are similar within experimental error.

The second main mechanism of cytotoxic activity characteristic of octahedral cobalt(II) coordination compounds involves the induction of apoptosis *via* the mitochondrial pathway, which is also typical of bipyramidal coordination compounds. In particular, Morcelli *et al.*[126] studied Co^{II} coordination compounds **228** – **230** with (2-hydroxybenzyl)-*N*-(2-pyridylmethyl)(2-hydroxy)propylamine (Fig. 18), having trigonal-bipyramidal structures and containing no labile axial ligands, which facilitate the intercalation into DNA, and showed that these compounds exhibit cytotoxicity, being localized in mitochondria of the U937 cell line and leading to the induction of apoptosis *via* the mitochondrial pathway.

Compounds with terpyridine ligands take a special place among complexes of biogenic metals with proven cytotoxic activity. These ligands allow the synthesis of coordination compounds with square-pyramidal geometry, which often exhibit cytotoxic activity through unique mechanisms.[55]

Structures 228 – 230



R = Cl (**228**), 1-NaphO (**229**),
2-NaphO (**230**)

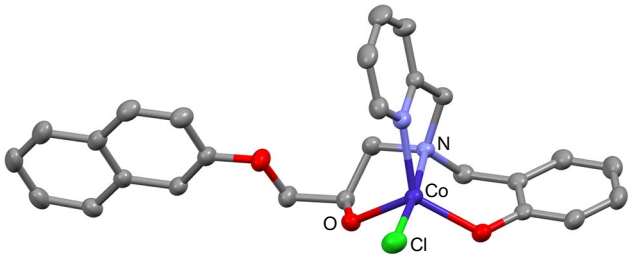
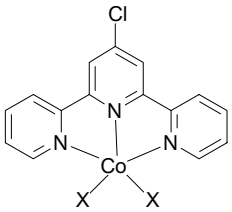


Figure 18. Molecular structure of complex **230**.[126] The Figure was prepared by the authors using the X-ray diffraction data [126] and the data from the Cambridge Crystallographic Data Center (CCDC 1422463).

Structures 231, 232



X = Cl, SCN

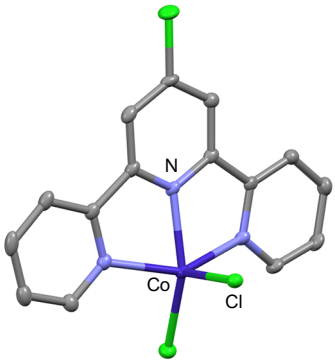


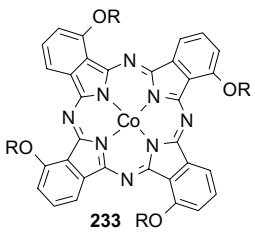
Figure 19. Molecular structure of complex **231**.[123] The Figure was prepared by the authors using the X-ray diffraction data [123] and the data from the Cambridge Crystallographic Data Center (CCDC 1021667).

Related cobalt(II) compounds are also known; however, it was shown that the complexes Co^{II}(4-Cltpy)Cl_2 (**231**) and Co^{II}(4-Cltpy)$(SCN)_2$ (**232**) with 4-chloro-2,2′:6′,2″-terpyridine (Fig. 19) have a trigonal-bipyramidal environment of the cobalt ion.[123] The mechanism of their cytotoxicity was not considered, but the IC_{50} values (6.2 ± 2.7 and 24.1 ± 2.9 μM against the MCF-7 cell line for compounds **231** and **232**, respectively) are significantly smaller than the corresponding value of the related Cu^{II} terpyridine complex ($IC_{50} = 55.2 \pm 5.1$ μM) and are close to the average IC_{50} values of other bipyramidal cobalt(II) coordination compounds considered in this Section.[116]

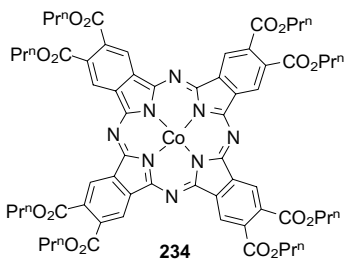
4.5. Square-planar cobalt(II) coordination compounds

The square-planar coordination geometry is observed very rarely for Co^{II} complexes. Compounds with this geometry are available only through the synthesis of phthalocyanine derivatives of cobalt. In two studies [113, 117] of square-planar cobalt coordination compounds as anticancer agents, attempts were made to determine their molecular target and elucidate the mechanism of their action. However, the sets of compounds were too small to extrapolate the results to all square-planar cobalt coordination compounds.

Structures 233, 234



OR =



Medvedev and Leshchenko [117] suggested that the main mechanism of action of cobalt phthalocyanine complexes **233** and **234** involves the generation of reactive oxygen species in the presence of intracellular reducing agents, *e.g.*, ascorbic acid. It was shown that Co phthalocyanines **233** and **234** at concentrations of 3 – 5 μM cause the hydrolysis of high-molecular-weight DNA by 30 and 50%, respectively. In this study, the antiproliferative activity of the cobalt phthalocyanine complex was not evaluated, but IC_{50} of related Co^{II} coordination compounds **234** with the phenoxy-substituted phthalocyanine ligand against a number of cell lines were found to be 19.53 (L929), 8.85 (MCF-7) and 12.14 μM (MG63), *i.e.*, these values are in the same range as IC_{50} of other cobalt(II) coordination compounds.

4.6. Prospects of the development of anticancer agents based on cobalt ions

The published data show that coordination compounds based on Co^{II} and Co^{III} ions can be considered as promising anticancer agents due to high affinity of cobalt for different N-, O-, S-donor ligands and the diversity of available coordination geometries.

Some cobalt complexes have IC_{50} values against cancer cell lines comparable with the cytotoxicity of cisplatin and other therapeutic pharmaceuticals and are often characterized by higher selectivity against cancer cells compared to cisplatin.

In particular, octahedral Co^{II} coordination compounds demonstrate high selectivity towards G4-DNA. This is an important property because, in the case of the proper design of compounds, it can provide excellent selectivity against cancer cells, which is not typical of the coordination compounds of other biogenic metals considered in this review.

Meanwhile, attempts to change or finely tune the mechanism of cytotoxic activity of cobalt coordination compounds by changing the oxidation state of the central atom were not successful. The mechanisms of action of Co^{II} and Co^{III} complexes are almost identical with the only difference that cobalt(III) ions are more susceptible to redox reactions leading to the generation of reactive oxygen species in the cell due to relatively lower stability of this ion under physiological conditions. The key advantage of Co^{II} coordination compounds is the selectivity towards G4-DNA, which is not typical of Co^{III} coordination compounds.

Besides, the selection of cobalt(III) as a complex-forming ion imposes severe restrictions on the geometry of the resulting coordination compounds, which significantly reduces the range of available mechanisms of cytotoxic activity, while do not lead to a significant increase in stability or IC_{50} values compared to Co^{II} coordination compounds more abundant in the literature.

So to sum up, it can be expected that effective new-generation anticancer agents will be developed based on the most common octahedral cobalt(II) coordination compounds, which are easy to synthesize, are characterized in more detail and are selective towards G4-DNA. These agents will be selective against cancer tissues, exhibit cytotoxic activity with diverse mechanisms, have activity comparable with that of platinum-based drugs used in clinical practice and possess higher selectivity compared to the available drugs.

5. Copper coordination compounds as cytotoxic agents

The redox potentials of the copper(I) and copper(II) ions allow coordination compounds based on this metal in both oxidation states to exist in solution at physiological pH values. The redox potential (E^0) of the Cu^{2+}/Cu^{+} pair varies from +0.44 to +0.39 V,[143] due to which the $Cu^{II}-Cu^{I}$ transition can occur in the presence of different intracellular reducing agents. An interesting distinguishing features of copper compounds is that, according to the hard and soft acid and base (HSAB) theory, Cu^{+} ions are considered as soft Lewis acids, whereas Cu^{2+} ions are of intermediate hardness. In total, these three factors provide a possibility to design physiologically active coordination compounds based on copper in different oxidation states and with different geometries, which can undergo the $Cu^{II}-Cu^{I}$ redox transition directly in the cell.

An analysis of the published data (Table 4) shows that copper(II) complexes (39 examples in 31 studies) and copper(I) complexes (a few examples in 5 studies) were tested for anticancer activity. This imbalance towards Cu^{II} coordination compounds is attributed to their higher stability in solution, storage stability and the simplicity of the synthesis. However, even a relatively smaller series of monovalent copper complexes includes three types of coordination geometry: tetrahedral (4 examples), trigonal-pyramidal (1 example) and triangular (1 example). Only one of these types is observed for copper(II) coordination compounds. Hence, some conclusions can be drawn about the dominant mechanism of their cytotoxic activity.

The coordination geometry of Cu^{II} complexes is far more diverse: square-pyramidal (19 examples), square-planar (9 examples), octahedral (6 examples), tetrahedral (3 examples) and trigonal-bipyramidal (2 examples). Square-pyramidal coordination compounds, which are most stable in solution, are most well-characterized.

5.1. Square-pyramidal copper(II) coordination compounds

The studies performed in the past decade focused to a large extent on the mechanism of cytotoxic activity of square-pyramidal copper(II) coordination compounds (21 publications, 50% of the analyzed studies). This coordination geometry is optimal for the Cu^{II} ion and is represented by a wide range of structural types, from commonly observed CuN_5, CuN_3Hal_2 and CuN_3O_2 (including successive replacements of up to three nitrogen atoms in the coordination sphere by oxygens to form CuN_4O and so on up to CuN_2O_3) to rather rare CuN_2SHalO and CuN_2Hal_2O.

A comparison of the results of different publications demonstrates that the main mechanism of cytotoxic activity of square-pyramidal copper(II) coordination compounds involves the generation of reactive oxygen species. This mechanism was found in 12 studies [144, 145, 147, 149, 150, 155, 166, 167, 173, 178 – 180] out of 21 publications on this issue. This mechanism leads to DNA damage, mitochondrial dysfunction and the induction of apoptosis *via* the DNA-dependent or mitochondrial pathway; the morphological changes in cells characteristic of apoptosis are described in 11 studies.[146, 147, 149, 150, 153, 155, 158, 159, 178 – 180]

It was shown that the generation of reactive oxygen species by square-pyramidal copper(II) coordination compounds can be performed in all possible ways: under irradiation with light of appropriate intensity at a wave-

Table 4. Cytotoxic copper coordination compounds.

No.	Complex (serial number of the compound)	Coordination sphere	Binding mode	Metal coordination geometry	Mechanism of cytotoxic activity	IC_{50} max (cell line)	Ref.
1	$[Cu^{II}(4\text{-Ph-tpy})L](ClO_4)_2$ (L = phen, dpq, dppz)	CuN_5	Tridentat + bidentate	Distorted square-pyramidal	Intercalation into DNA facilitated by the planar ligand, ROS generation and DNA damage upon light irradiation	3.7 ± 0.8 μM (HeLa) in the light, 12.4 ± 0.9 μM (HeLa) in the dark	144
2	$LCu^{II}X_2$ (X = Cl, Br, $H_2O + 0.5\,SO_4$), $[LCu^{II}X]^+Y^-$ (X = OAc, H_2O; Y = OAc, NO_3, ClO_4)	CuN_3X_2, CuN_3X	Tridentate + monodentate	Square-pyramidal, square-planar	Generation of ROS and oxidative DNA cleavage. Pyramidal coordination compounds are more cytotoxic than the compounds with square geometry	$LCu^{II}Cl_2$: 156 ± 0.35 μM (Caco-2)	145
3	$[Cu^{II}LX](ClO_4)$ (HL is 2-[(2-dimethylamino-ethyl)methylideneamino)phenol: X = bipy (**235**), phen (**236a**), dpq (**236b**), dppz (**237a**), dmdppz (**237b**))	CuN_4O	Tridentate + bidentate	Distorted square-pyramidal	Binding to DNA, DNA cleavage (in the absence of reducing agents and irradiation) leading to the induction of apoptosis. The binding affinity of the complexes with planar aromatic ligands is much higher, these complexes more efficiently cleave DNA and are most toxic	**235**: 20.0 ± 0.10 μM; **236a**: 2.00 ± 0.05 μM; **236b**: 1.58 ± 0.01 μM; **237a**: 0.46 ± 0.02 μM; **237b**: 0.65 ± 0.01 μM (all against MCF-7)	146
4	$Cu^{II}LCl_2$ (L = dthp, dmtp, dtp)	CuN_3Cl_2	Tridentate + 2 monodentate ligands	Distorted square-pyramidal	Intercalation into DNA, ROS generation in the presence of sodium ascorbate and oxidative DNA cleavage leading to the induction of apoptosis. The thiazole-containing ligand is the most planar one, and its complex is the most active and effective intercalating agent	125–189 μM (HeLa), 139–272 μM (Hep-G2), 93–147 μM (BEL-7402)	147
5	$Cu^{I}(L^1)(PPh_3)Cl$ (**329**) [a]	CuN_2PCl	Bidentate + 2 monodentate ligands	Tetrahedral	Intercalation into DNA, weak hydrolytic cleavage and very strong antioxidant activity	3.04 μM (HeLa), 4.34 μM (MCF-7)	148
6	$[Cu^{II}(pmdt)(diimine)](ClO_4)_2$ (diimine = bipy (**238**), phen (**239**), dmp (**240**), dpq (**241**))	CuN_5	Tridentate + bidentate	Distorted square-pyramidal	**238**: weak binding to the groove of DNA; **239**, **241**: intercalation of the planar ligand; **240**: strong binding to the minor groove of DNA. Cleavage of DNA, ROS generation in the immediate vicinity of DNA followed by the induction of apoptosis	1.5–12 μM (MCF-7); complex **240** is the most toxic, complex **238** is the least toxic	149
7	$Cu^{II}(4\text{-R-tpy})Cl_2$ (R = 3-$MeOC_6H_4$, 4-$MeOC_6H_4$, 3,5-$(MeO)_2C_6H_3$)	CuN_3Cl_2	Tridentate + 2 monodentate ligands	Distorted square-pyramidal	Intercalation of the terpyridine ligand into DNA, ROS generation in the presence of glutathione leading to oxidative DNA cleavage and apoptosis. The cytotoxicity correlates with the concentration of H_2O_2 generated in the cells; the intercalation promotes localization; hence, the complex with the strongest DNA binding ability induces the lowest ROS generation (shielded from glutathione and oxygen) and is less toxic	2.72–8.98 μM (HeLa, HepG2, BEL-7402)	150

Table 4 (continued).

No.	Complex (serial number of the compound)	Coordination sphere	Binding mode	Metal coordination geometry	Mechanism of cytotoxic activity	IC_{50} max (cell line)	Ref.
8	$[Cu^{II}LCl](ClO_4)$, $[CuLBr_2]$ (L is (2-pyridylmethyl)-(quinolin-8-yl)amine)	CuN_3X_2 (X = Cl, Br)	Tridentate + 2 monodentate ligands	Distorted square-pyramidal	Intercalation into DNA followed by oxidative DNA cleavage	1.72 – 1.85 μM (HeLa), 0.46 μM (MCF-7), 0.43 – 0.990 μM (A549)	151
9	$[Cu^{II}(bipy)(pic)_2]$ (**292**)	CuN_2O_4	Tetradentate + bidentate	Distorted octahedral	Binding to the minor groove of DNA is stronger compared to the square-pyramidal complexes and the complex with the same ligands but with square-pyramidal geometry. The toxicity correlates with intercalation	4.5 ± 0.3 μM (HepG2), 8.4 ± 0.5 μM (SMMC-7721), 10.2 ± 1.1 μM (A549)	152
10	$[Cu^{II}L(phen)]$ (HL are 4-X-2-[(2-hydroxy-benzylidene)amino]benzoic acids): X = F (**261**), Cl (**262**))	CuN_3O_2	Tridentate + bidentate	Distorted square-pyramidal	Inhibition of the proteasome (particularly, chymotrypsin-like activity) leads to the induction of apoptosis. The toxicity is fully consistent with the proteasome inhibition in terms of the concentration, the complex that does not inhibit the proteasome is non-toxic	~7 μM (MDA-MB-231)	153
11	$[Cu^{II}LX_4]$ (**249 – 256**) (L is aminoalkylaminoneo-cryptolepine; X = Cl, Br, H_2O, OAc)	CuN_2O_2Br, CuN_2O_3Cl, CuN_2O_4	Bidentate + monodentate	Square-pyramidal or octahedral	Unknown, the square-pyramidal complex has the highest toxicity	< 0.58 μM (HT-29)	154
12	$[Cu^{II}LX]$ (L is 2-[(2-hydroxybenzylidene)-amino]acetic acid: X = epoxyphen (**289**), phen (**290**), amphen (**291**))	CuN_3O_2, CuN_3O_3	Tridentate + bidentate	Distorted octahedral, square-pyramidal	All complexes intercalate into DNA, the pyramidal complex has a stronger DNA intercalating ability compared to the octahedral complex; the charged ligand has an additional binding affinity for DNA. Oxidative DNA damage and the induction of apoptosis were found. The complex with a moderate binding affinity and a moderate ability to induce ROS generation and DNA damage has selectivity against cancer cells, because it is tolerated by normal cells, whereas it is not tolerated by cancer cells due to a sum of factors	3 – 12 μM (HeLa, A549, HCT 116, MDA-MB231)	155
13	$[Cu^{II}L(OAc)_2]$ (**282 – 285**) (L are amino-substituted 2-pyridylimidazo[1,2-*a*]pyridines)	CuN_2X_2 (X = Cl, O)	Bidentate + monodentate ligands	Distorted square	Localization in the nucleus and DNA damage leading to the induction of apoptosis, paraptosis and necrosis. Copper complexes are much more toxic than zinc c ompounds	0.6 – 3 μM (MCF-7, HT-29, HL-60, K562, MDA-MB231)	39
14	$[Cu^{II}LCl_2]$ (L are 1-R-2-(2-pyridyl)benz-imidazoles: R = Me, $PhCH_2$, 4-$FC_6H_4CH_2$ (**286**), $C_6F_5CH_2$ (**287**))	CuN_2Cl_2	Bidentate + monodentate ligands	Distorted square	Weak binding to DNA, ROS generation, the complex that most actively generates ROS has the highest cytotoxicity	5.5 – 12 μM (A549)	156

Table 4 (continued).

No.	Complex (serial number of the compound)	Coordination sphere	Binding mode	Metal coordination geometry	Mechanism of cytotoxic activity	IC_{50} max (cell line)	Ref.
15	$[Cu^{II}L_2]$ (**326**) (HL is the Schiff base of 3,5-di-*tert*-butyl-2-hydroxybenzaldehyde and dehydroabietylamine)	CuN_2O_2	Bidentate	Distorted tetrahedral	Unknown; probably, the release of the free ligand, which is more toxic than the complex	8.07 ± 0.12 μM (MCF-7), 12.22 ± 0.44 μM (A549), 3.02 ± 0.02 μM (HUVEC)	157
16	$[Cu^{II}LX]$ (**263**), $[Cu^{II}L(MeOH)X]$ (**264 – 267**) (L are *N*-substituted 2-pyridylcarbaldehyde thiosemicarbazones; X = Cl, Br, NO_3)	CuN_2SX, CuN_2SOX	Tridentate + monodentate ligands	Distorted square, square-pyramidal	Induction of apoptosis through the activation of the protein p53, inhibition of telomerase and the impairment of mitochondrial function. The square complexes only inhibit p53 and telomerase, the square-pyramidal complexes additionally decrease the c-myc and hTERT level and, consequently, they are an order of magnitude more toxic	1.3 – 1.8 μM (Hep-G2), 1.3 – 1.5 μM (NCI-H460), 1.3 – 1.9 μM (SK-OV-3)	158
17	$[Cu^{II}L(B)]$ (**268 – 270**) (HL are salicylaldehyde 3-chloropyridazin-6-ylhydrazones, B = bipy, phen)	CuN_4O	Tridentate + bidentate	Square-pyramidal	Induction of apoptosis. Inhibition of FGFRs (fibroblast growth factor receptors); the higher the binding constant according to the molecular docking, the higher the toxicity	6.26 – 20.57 μM (MDA-MB-231), 7.80 – 17.48 μM (L6)	159
18	$[Cu^{II}$ (bpdmpz)Cl$]ClO_4$ (**257**), $[Cu^{II}$(bdmpzp)Cl]X (X = ClO_4 (**258a**), PF_6 (**258b**)), $[Cu^{II}$(tdmpza)Cl$]ClO_4$ (**259**), $[Cu^{II}$ (bedmpzp)Cl$]PF_6$ (**260**)	CuN_4Cl	Tetradentate	Distorted trigonal-bipyramidal (**257**), distorted square-pyramidal (**258**, **259**)	A series of complexes with continuous geometric distortions from square-pyramidal to trigonal-bipyramidal. The toxicity changes in parallel with the distortion. The square-pyramidal complex is not damaged upon the interaction with cytochrome C, cysteine and glutathione, whereas the bipyramidal complex is completely decomposed by these compounds	**257**: > 50 μM (A2780), 33.1 μM (A2780R), > 50 μM (HOS), > 50 μM (Caco2); **258**, **259**: 1.4 μM (A2780), 8.3 μM (A2780R), 4.7 μM (HOS), 10.8 μM (Caco2)	160
19	$[Cu^{II}L_2]$ (HL is the Schiff base of 4-morpholinoaniline and 3-R-salicylaldehyde (R = H, Bu^t))	CuN_2O_2	Bidentate	Distorted square-planar	Binding to the minor groove of DNA	32 – 34 μM (MCF-7)	161
20	$[Cu^{II}L_4X]X$ (L is 2-amino-5-dehydroabiethyl-1,3,4-thiadiazole; X = Cl (**327**), Br (**328**))	CuN_4X	Monodentate	Distorted trigonal-bipyramidal	Induction of apoptosis *via* the mitochondrial pathway and ROS generation. The unique property is the binding to the cell surface death receptor	**328**: 3 – 16 μM; **329**: 4 – 14 μM (HepG2, MCF-7, HeLa, A431)	162

Table 4 (continued).

No.	Complex (serial number of the compound)	Coordination sphere	Binding mode	Metal coordination geometry	Mechanism of cytotoxic activity	IC_{50} max (cell line)	Ref.
21	$[Cu^{II}LX_2]$ [L is *N*-(1,10-phenanthrolin-5-yl)-pelargonamide; X = NO_3 (**274**), acetylsalicylate (**275**)	CuN_2O_2	Bidentate + monodentate ligands	Distorted square	DNA followed by its cleavage through hydrolysis; the complexes suppress ROS generation; the introduction of aspirin into the complex leads to its mitochondrial localization and induction of apoptosis *via* the mitochondrial pathway	1.1 – 1.8 μM (HeLa, SKOV-3)	163
22	$[Cu^{II}L_2(phen)]$ [b] (HL are tolfenamic, mefenamic and flufenamic acids)	CuN_2O_4	Bidentate	Distorted octahedral	Intercalation of the phenanthroline moiety into DNA, efficient DNA cleavage both mediated by ROS generation and *via* a hydrolytic pathway. Reversible $Cu^{II} - Cu^{I}$ redox conversion promotes DNA cleavage	Not measured	164
23	$[Cu^{II}LCl]Cl$ (**271 – 273**) (HL are N-substituted 5-(1-methyl-1*H*-imidazol-3-io)-salicylaldehyde chloride thiosemicarbazones)	CuNOSCl	Tridentate + monodentate ligand	Distorted square	In an aqueous environment, the coordinated chloride anion is exchanged with a water molecule, but the geometry of the complexes remains unchanged. Induction of apoptosis	28 – 57 μM (MCF-7)	165
24	$[Cu^{II}LBr_2](H_2O)(DMF)_2]$ (**242**) (L is 2-[5-(3-pyridyl)-4-(4-pyridyl)-4*H*-1,2,4-triazol-3-yl]pyridine)	CuN_3Br_2	Tridentate + monodentate ligands	Distorted square-pyramidal	Generation of ROS, induction of apoptosis	80 – 90 μM (MG-63, U2SO, Saos-2)	166
25	$[Cu^{II}L(tpy)Cl] \cdot H_2O$ (HL = nar (**293a,b**)); [c] $[CuL(bipy)(NO_3)] \cdot 1.5\,H_2O$ (HL = que (**294**))	CuN_3O_2Cl, CuN_3O_2	Tridentate + bidentate	Octahedral, square-pyramidal	The octahedral coordination compound has the highest toxicity and induces apoptosis *via* a caspase-dependent pathway, both compounds generate ROS and damage mitochondria	**293**: < 0.8 μM (MCF-7), 18.2 μM (MDA-MB-231); **294**: 22.8 μM (MCF-7), 43.5 μM (MDA-MB-231)	167
26	$[Cu^{I}(phen)(PR_3)Br]$ (R = Ph (**330**), Cy (**331**), 4-FC_6H_4 (**333**)), $[Cu^{I}(phen)(PR_3)_2]Br$ (R = 4-$MeOC_6H_4$ (**332**))	CuN_2PBr, CuN_2P_2	Bidentate + monodentate ligands	Trigonal-pyramidal, distorted tetrahedral	The tetrahedral complex is much more toxic than the pyramidal complex, it has higher lipophilicity and higher DNA intercalation ability, shows good binding energies for androgen receptors cells in PC-3 cells according to the docking scores	**330 – 332**: 25 – 91 μM (MCF-7), 33 – 56 μM (PC-3); **333**: 35 μM (MCF-7), 18 μM (PC-3)	168
27	$[L_2Cu^{I}Cl]$ (**334 – 337**) (L are substituted *N*-phenyl-*N*′-(methoxycarbonyl)thioureas))	CuS_2Cl	Monodentate	Triangular	Very strong DNA fragmentation, the mechanism is unknown	12 – 17 μM (2008), 16 – 20 μM (C13), 14 – 23 μM (IGROV-1), 40 – 47 μM (WRL-68)	169

Table 4 (continued).

No.	Complex (serial number of the compound)	Coordination sphere	Binding mode	Metal coordination geometry	Mechanism of cytotoxic activity	IC_{50} max (cell line)	Ref.
28	$[Cu^{II}(L^2)(pdc)]_2$ (**245**), $[Cu(L^3)_2]_2$ (**246**) [d]	CuN_2O_3	Bidentate	Square-pyramidal, square-pyramidal, which is transformed into square geometry in an aqueous solution	Intercalation into DNA, complex **245** retains the dimeric structure, whereas **246** is transformed in a solution into two mononuclear square-planar complexes and has lower DNA intercalation efficiency	**245**: 24 ± 6.24 μM (MCF-7); **246**: activity is absent	170
29	CuLCl (**338**) (L is (−)-camphor thiosemicarbazone)	CuS_2Cl	Monodentate	Triangular-planar	Unknown	9.8 ± 0.5 μM (MCF-7)	171
30	$[Cu(dmp)L_2]$ (**247**), $[Cu(phen)(H_2O)L_2]$ (**248**) (HL is 4,5-dichloroisothiazole-3-carboxylic acid)	CuN_3O_2, CuN_3O_3	Bidentate	Square-pyramidal, octahedral	Binding to DNA (the square-pyramidal complex has a higher binding affinity compared to the octahedral complex; the binding constants correlate with the cytotoxicity), inhibition of cytochrome P450	**247**: 0.97 ± 0.03 μM (Hep-G2), 1.8 ± 0.3 μM (MCF-7); **248**: 3.06 ± 0.07 μM (Hep-G2), 4.2 ± 0.2 μM (Hep-G2)	172
31	$[Cu^{II}LCl]$ (**276 – 281**) (HL are N-substituted 2,3-dihydroxy- and 2-hydroxy-3-methoxybenzaldehyde thiosemicarbazones)	CuNOSCl	Tridentate + monodentate ligand	Square-planar	Mitochondrial localization and induction of apoptosis *via* the mitochondrial pathway without ROS generation. It is suggested that the complex inhibits PDI	0.02 – 0.04 μM (LoVo-OXP, LoVo).Very high toxicity but low selectivity (index ∼0.1 – 0.3)	111
32	$[Cu^{II}(sac)_2(bzimpy)]\cdot 3\,DMF$ (**244a**), $[Ni(bzimpy)_2](sac)_2\cdot H_2O\cdot Pr^iOH$ (**244b**)	CuN_4O	Tridentate + monodentate ligands	Square-pyramidal	Binding to the major groove of DNA due to steric hindrance of the ligands in the complex. Generation of ROS, DNA double-strand breaks and mitochondrial dysfunction lead to the induction of apoptosis simultaneously *via* two pathways, which accounts for high toxicity	**Cu**: 1.68 ± 0.05 μM (A549), 23.56 ± 0.45 μM (HT-29), 2.96 ± 0.06 μM (MCF-7), 14.30±0.13 μM (MCF-7 – 10A); **Ni**: 1.86 ± 0.09 μM (A549), 41.47 ± 8.07 μM (HT-29), 6.10 ± 1.33 μM (MCF-7), 66.5 ± 4.98 μM (MCF-7 – 10A)	173
33	$Cu^{II}(trop)_2$ (**288**)	CuO_4	Bidentate	Square-planar	Induces apoptosis and exhibits efficient cellular uptake not only by the MCF7 and MDA-MB-231 cells but also by MCF-7 spheroids, being 26 times more effective than cisplatin against 3D models	5.2 ± 1.8 μM (MCF-7), 4.0 ± 0.2 μM (MDA-MB-231); SI = 2.5 – 2.9. Under the same conditions, SI of cisplatin is ∼1	174
34	Cu^{II}(2-pbmq)(MeOH)Br_2, $[Cu^{II}$ (2-pbmq)$(PPh_3)Br]_2$	CuN_2Br_2O $CuNPBr_2$	Bidentate, monodentate	Distorted square-pyramidal, tetrahedral	The pyramidal coordination compound exhibits higher DNA intercalation affinity compared to the tetrahedral complex and displays stronger DNA cleavage activity *in vitro*. However, the tetrahedral complex displays more efficient cellular uptake and is accumulated in the nucleus and mitochondria rather than in the cytoplasm leading to the efficient development of apoptosis *via* the mitochondrial pathway	Pyramidal: 23.4 – 25.99 μM (SMMC7721, BGC823, TFK-1); tetrahedral: 3.18 – 3.76 μM (SMMC7721, BGC823, TFK-1)	175

Table 4 (continued).

No.	Complex (serial number of the compound)	Coordination sphere	Binding mode	Metal coordination geometry	Mechanism of cytotoxic activity	IC_{50} max (cell line)	Ref.
35	$[Cu^{II}L_2]$ (**295 – 303**) (HL is *N*-Ar-*N′*-(tetrahydrophthalimido)-substituted thioureas)	CuN_2S_2	Bidentate	Distorted tetrahedral; the geometry is retained in solution	Induction of apoptosis in cancer cells and 70% weaker apoptosis in normal cells. Putative inhibition of interleukin-6 release	11 – 62 μM (PC-3), SI-1 – 7 (HaCaT)	176
36	L_2Cu_2Cl (L are 1-aryl-5-(2-pyridylmethylidene)-2-thioxo-imidazolin-4 -ones)	CuN_2SCl	Tridentate	Distorted square-pyramidal. Bidentate	Induce early apoptosis, exhibit efficient cellular uptake, do not generate ROS and are not reduced in the cell	1.4 – 9.6 μM (MCF-7)	177
37	$LCuCl_2$ (**304 – 325**) (L is 1-aryl-2-methylthio-4-(2-pyridiyl-methylidene)-1*H*-imidazol-5(4*H*)-ones)	CuN_2Cl_2	Bidentate	Bidentate	Efficiency was shown using MTT assays not only in 2D but also in 3D cell cultures,[e] hydrolytically cleave DNA, do not generate ROS	1.8 – 12 μM (MCF-7)	177
38	LCu_2Cl_n (n = 2 – 4, (L is 1,2-bis[1-aryl-4-(2-pyridyl-methylidene)-5-oxo-1*H*-imidazol-1-yl-methylthio]ethane)	CuN_2Cl_n	Bidentate	Distorted tetrahedral	Binding to DNA, ROS generation and the involvement in intramolecular redox reactions	0.6 – 19 μM (MCF-7)	177
39	$[Cu^{II}(Trp)(Hnor)_2(DMSO)]NO_3$	CuN_3OS	Bidentate + monodentate ligands	Square-pyramidal	Generation of ROS, induction of apoptosis in cancer cells *via* the mitochondrial pathway. Glutathione consumption, which is indicative of the redox transformation involving copper and intracellular reducing agents	10 ± 1.3 μM (MCF-7), 27 ± 1.1 μM (Hep-G2), > 100 μM (Hek-293)	178
40	$[Cu(Gluc)(HPB)(H_2O)](Gluc)$, $[Cu(Gluc)(HPBC)(H_2O)](Gluc)$	CuN_2O_3	Bidentate	Square-pyramidal	Binding to DNA, ROS generation, induction of apoptosis in cancer cells *via* the mitochondrial pathway	13.3 ± 1.4 μM (A549), 4.6 ± 0.1 μM (A549)	179
41	$[Cu_2(L^4)Cl_4]_2$, $[Cu(L^5)Cl_2]_2 \cdot 4H_2O$ [f]	CuN_3Cl_2	Tridentate + 2 monodentate ligands	Distorted square-pyramidal	Generation of ROS (singlet oxygen and OH*); oxidative DNA cleavage leading to the induction of apoptosis	13.4 ± 0.7 μM (Hep-G2), 10.6 ± 1.9 μM (HeLa), 27.4 ± 0.1 μM (HUVEC)	180

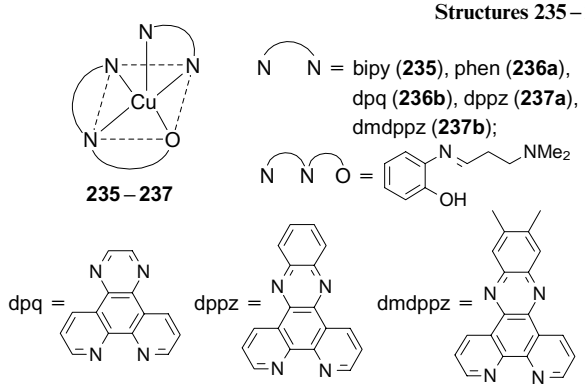
Note. The following abbreviations are used: tpy is terpyridine, dpq is dipyridyl[3,2-*f*:2′,3′-*h*]quinoxaline, dppz is dipyridyl[3,2-*a*:2′,3′-*c*]phenazine, dmdppz is 11,12-dimethylpyridyl[3,2-*a*:2′,3′-*c*]phenazine, dthp is 2,6-di(thiazol-2-yl)pyridine, dmtp is 2,6-di(5-methyl-4*H*-1,2,4-triazol-3-yl)pyridine, dtp is 2,6-di(4*H*-1,2,4-triazol-3-yl)pyridine, pmdt is *N*,*N*,*N′*,*N″*,*N″*-pentamethyldiethylenetriamine, dmp is 5,6-dimethyl-1,10-phenanthroline, pic is picrate, FGFR is fibroblast growth factor receptor, bpdmpzp is (3,5-dimethyl-1*H*-pyrazol-1-ylmethyl)bis(2-pyridylmethyl)amine, bdmpzp is bis(3,5-dimethyl-1*H*-pyrazol-1-ylmethyl)(2-pyridylmethyl)amine, tdmpza is tris(3,5-dimethyl-1*H*-pyrazol-1-ylmethyl)amine, bedmpz is bis[2-(3,5-dimethyl-1*H*-pyrazol-1-yl)ethyl](2-pyridylmethyl)amine, que is quercetin, nar is naringenin, pdc is pyridine-2,5-dicarboxylate, PDI is disulfide isomerase, sac is saccharin (*o*-sulfobenzimide), bzimpy is 2,6-bis(benzimidazol-2-yl)pyridine, tropH is tropolone (2-hydroxycyclohepta-2,4,6-trien-1-one), pbmq is [2-(pyrazin-2-yl)-1*H*-benzo[*d*]imidazol-1-ylmethyl]quinoline, Hnor is norharman (β-carboline), Gluc is D-gluconic acid, HPB is 2-(2-pyridyl)benzimidazole, HPBC is 5-chloro-2-(2-pyridyl)benzimidazole. [a] L^1 is 1,5-dimethyl-2-phenyl-4-(2-pyridylmethylideneamino)-1,2-dihydropyrazol-3-one; [b] mefenamic acid is 2-(2,3-dimethylphenylamino)benzoic acid, tolfenamic acid is 2-(3-chloro-2-methylphenylamino)benzoic acid, flufenamic acid is 2-(3-(trifluoromethyl)phenylamino)benzoic acid; [c] compounds **293a**,**b** differ in the configuration of the tpy ligand (see Section 5.3), [d] HL^2 is the Schiff base of 2-(*N′*,*N′*-dimethylpiperazino)ethylamine and salicylaldehyde; HL^3 is Schiff base of 2-(diisopropylamino)ethylamine and salicylaldehyde; [e] 3D-MTT assay is the evaluation of cytotoxicity in cell spheroids, which more accurately mimic solid tumours compared to the conventional MTT assay; [f] L^4 is 4,4′-oxybis[*N*,*N*-bis(2-pyridylmethyl)aniline]; L^5 is 4-methyl-*N*,*N*-bis(2-pyridylmethyl)aniline.

length of 458 nm (photoexcitation of the ligand),[144] in the presence of intracellular reducing agents, such as sodium ascorbate[139] and glutathione,[150, 155, 178] and using the starting complexes.[146, 173] For some coordination compounds, the ROS generation is not just the main but the only mechanism of cytotoxicity, and the IC_{50} value fully correlates with the concentration of H_2O_2 that is produced in the cell in the presence of the complex.[150]

The intracellular localization is an important factor, which relates the effective cytotoxicity of the coordination compound to its ability to generate ROS in the cell. Reactive oxygen species can exert a significant cytotoxic effect leading to the damage of classical biological targets (DNA and mitochondria), thereby causing the induction of apoptosis *via* the DNA-dependent or mitochondrial pathway. Some research groups demonstrated that the localization in the cell and the efficient DNA damage by reactive oxygen species are completely determined by the ligand environment of the square-pyramidal copper complex,[146, 150, 155] and the degree of interaction with DNA directly affects the toxicity.[151, 172] In particular, it was shown[146] that complexes **235**–**237** (Fig. 20) containing planar aromatic bidentate ligands are localized on DNA through intercalation of the ligand between nitrogenous base pairs, and structurally labile 2,2′-bipyridine, which has weak intercalating ability, gives a less toxic complex compared to planar and fully conjugated dipyridophenazine. However, the introduction of two methyl groups into dipyridophenazine, which significantly hinder the intercalation of the latter into DNA, leads to a decrease in the cytotoxicity: IC_{50} increases from 0.46 to 0.65 μM against the MCF-7 cell line.

Ganeshpandian *et al.*[149] reached similar conclusions. They showed that not only the strength of intercalation but also the mechanism of DNA binding can be changed by varying the nature of the bidentate ligand with the retention of the tridentate pmdt ligand in the copper(II) coordination environment using the following series: 2,2′-bipyridine, phenanthroline, 5,6-dimethylphenanthroline, dipyridyl[3,2-*d*:2′,3′-*f*]quinoxaline (compounds **238**–**241**, respectively, Fig. 21). The interaction of 2,2′-bipyridine-containing complex **238** with DNA is insufficiently strong for the localization of the complex and the ROS-mediated DNA damage and it does not lead to significant toxicity ($IC_{50} \approx 12$ μM). Coordination compounds based on phenanthroline (**239**) and dipyridyl[3,2-*d*:2′,3′-*f*]quinoxaline (**241**) intercalate into DNA, which leads to a decrease in IC_{50} to 2.6–2.5 μM. Meanwhile, complex **240** with 5,6-dimethylphenanthroline, which is incapable of intercalation due to the presence of two methyl groups, efficiently binds to the major groove of DNA, thereby causing a decrease in IC_{50} to 1.5 μM. This is attributed to the fact that the complex, which is efficiently

Structures 235–237



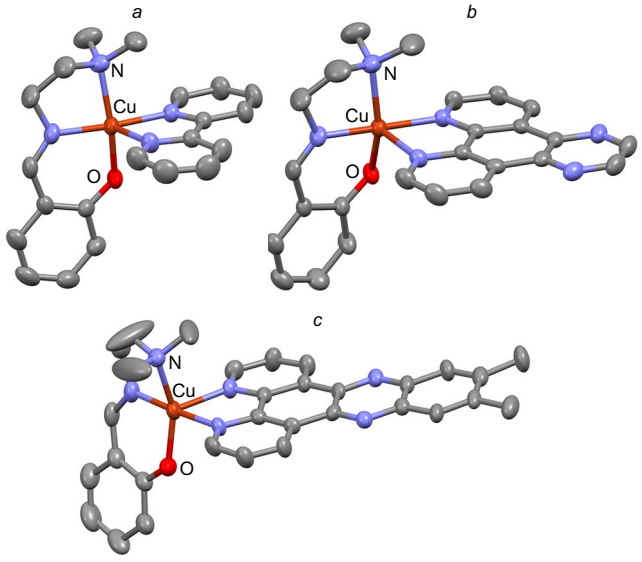
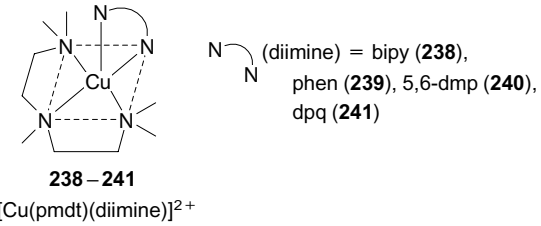


Figure 20. Molecular structures of copper coordination compounds **235** (*a*), **236b** (*b*) and **237b** (*c*) capable of intercalation into DNA exclusively due to the presence of the planar aromatic ligand responsible for the DNA binding affinity.[146] The Figure was prepared by the authors using the X-ray diffraction data.[146]

Structures 238–241



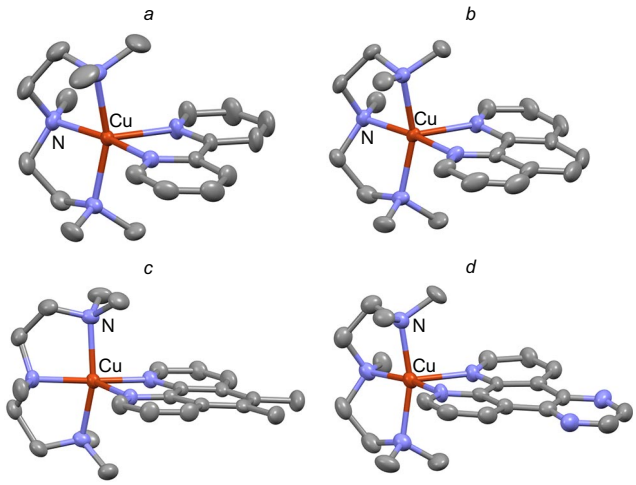


Figure 21. Molecular structures of coordination compounds **238**–**241** (*a*–*d*, respectively), which differ in the structure of the conjugated aromatic ligand that influences the DNA binding affinity and the binding mode.[149] The Figure was prepared by the authors using the X-ray diffraction data[149] and the data from the Cambridge Crystallographic Data Center (CCDC 841674, 841675, 841676 and 841677).

bound to the major groove of DNA, is simultaneously localized in the vicinity of the biological target and is open to free diffusion of water molecules and intracellular reducing agents, leading to the most efficient ROS generation in the immediate vicinity of DNA.

Similar characteristic patterns also account for the fact that the dinuclear copper(II) coordination compound $[Cu^{II}LBr_2](H_2O)(DMF)_2$ (**242**) and the nickel(II) coordination compound $[NiL_2(H_2O)_2](NO_3)_2$ (**243**), where L is 2-[5-(3-pyridyl)-4-(4-pyridyl)-4*H*-1,2,4-triazol-3-yl]pyridine, containing two copper or nickel ions in the square-pyramidal environment, cannot interact with the major and minor grooves of DNA. These compounds do not exhibit cumulative toxicity and are even inferior to mononuclear Cu^{II} and Ni^{II} complexes (**244a**,**b**),[173] which are, on the average, characterized by much lower toxicity.[166]

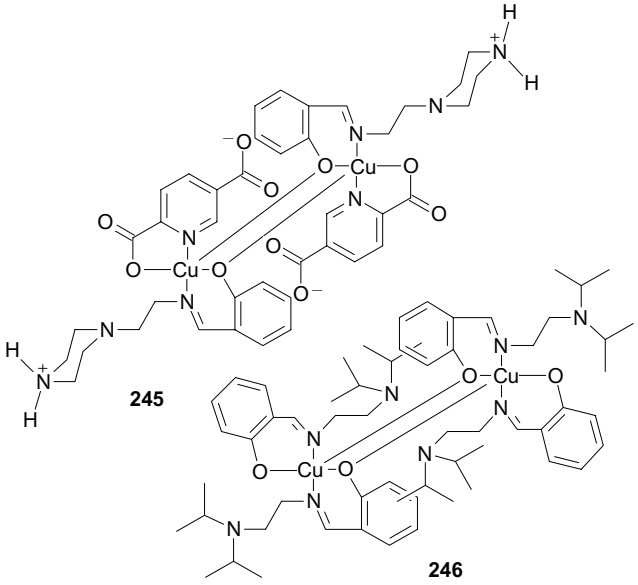
A comparison of square-pyramidal dinuclear Cu^{II} complexes **245** and **246** (Fig. 22), which retain the capability of intercalation,[170] and mononuclear square-planar copper(II) coordination compound **242**, which also binds to DNA by intercalation, shows that the former complexes are more toxic, but their toxicity is an order of magnitude lower compared to mononuclear square-pyramidal complexes **235**–**241** described above (IC ≈ 20 μM against the MCF-7 cell line).

In a few studies, copper(II) coordination compounds bearing structurally similar ligands and having different geometries were compared, and it was shown that square-pyramidal Cu^{II} complexes more efficiently intercalate into DNA compared to tetrahedral[175] and octahedral complexes.[167, 172] In particular, it was demonstrated[172] that square-pyramidal compound **247** with the 4,5-dichloroisothiazole-3-carboxylate ligand binds to DNA 4.6 times stronger than octahedral complex **248** ($K_b = 6.4 \times 10^4$ *versus* 1.4×10^4 L mol^{-1}), and the binding constant generally correlates with the cytotoxicity (Fig. 23).

In some cases, when the ROS generation by coordination compounds localized on DNA is the main mechanism of action for complexes with different geometries, it is consistent with IC_{50}. Examples are compounds **249**–**256** based on aminoalkylamino derivatives of neocryptolepine (5-methyl-5*H*-indolo[2,3-*b*]quinoline). Thus, the IC_{50} value is not higher than 0.58 μM for square-pyramidal complexes **249**, **250**, **253** and **254** and is as low as 8.77 μM for octahedral complexes **251**, **252**, **255** and **256** with these ligands.[154]

However, in many cases the generation of ROS by octahedral and tetrahedral copper(II) complexes localized on DNA is not the main mechanism of cytotoxicity. Due to this fact, the IC_{50} values of these compounds can be lower than those of compounds showing a more efficient intercalation or do not correlate at all with the intercalation strength.

Structures 245, 246



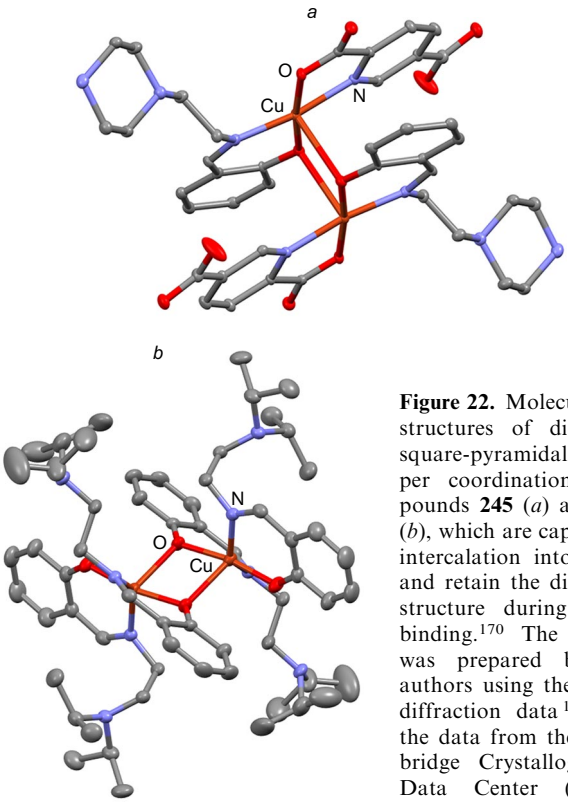
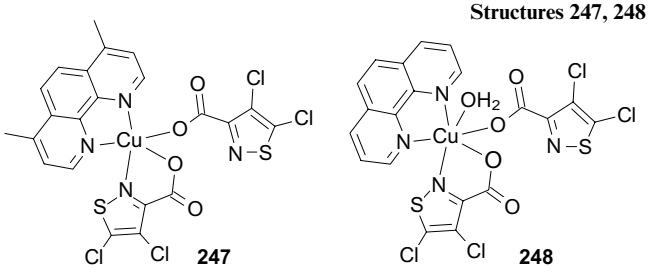


Figure 22. Molecular structures of dinuclear square-pyramidal copper coordination compounds **245** (*a*) and **246** (*b*), which are capable of intercalation into DNA and retain the dinuclear structure during DNA binding.[170] The Figure was prepared by the authors using the X-ray diffraction data[170] and the data from the Cambridge Crystallographic Data Center (CCDC 1839877 and 1019784).

Structures 247, 248



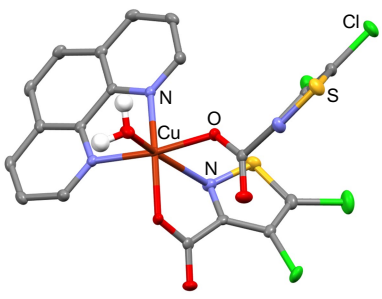
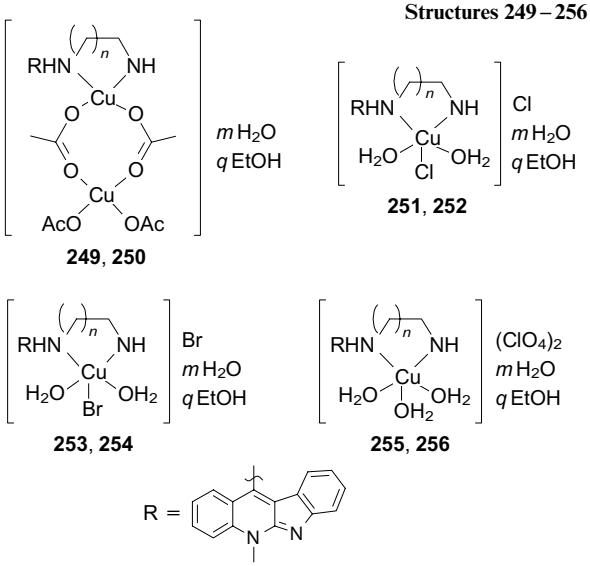


Figure 23. Molecular structure of compound **248**.[172] The Figure was prepared by the authors using the X-ray diffraction data[172] and the data from the Cambridge Crystallographic Data Center (CCDC 1974136).

Structures 249 – 256



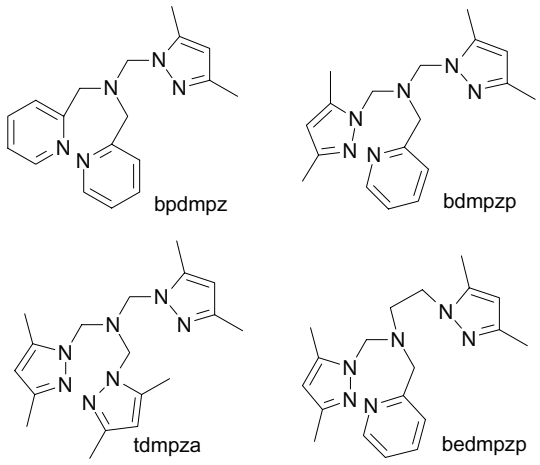
249, **250** **251**, **252** **253**, **254** **255**, **256**

R =

Compound	*n*	*m*	*q*	Compound	*n*	*m*	*q*
249	2	0.75	0.75	**253**	1	3.25	–
250	3	3	–	**254**	2	3	0.5
252	2	6	–	**255**	1	2.75	–
251	1	3	0.5	**256**	2	7.5	0.5

The second very important factor, which directly affects the efficiency of the cytotoxic effect through the ROS generation in the vicinity of DNA, is the stability of coordination compounds in the presence of intracellular reducing agents (*e.g.*, glutathione) and oxidizing agents (cytochrome C) along with the ability to undergo a cyclic redox transition generating more than one H_2O_2 molecule per Cu^{II} complex. Massoud *et al.*[160] synthesized the coordination compounds $[Cu^{II}(bpdmpz)Cl]ClO_4$ (**257**), $[Cu^{II}(bdmpzp)Cl]X$, where $X = ClO_4$ (**258a**), PF_6 (**258b**), $[Cu^{II}(tdmpza)Cl]ClO_4$ (**259**) and $[Cu^{II}(bedmpzp)Cl]PF_6$ (**260**) with organic ligands bearing pyridyl- and(or) pyrazolylalkyl substituents (Fig. 24). This series of compounds was characterized by a gradual change in the geometry of the complex from ideal square-pyramidal ($\tau = 0.08$)‡ to ideal trigonal-bipyramidal ($\tau = 0.88$) through intermediate geometries ($\tau = 0.14 – 0.29$).

Ligand structures



‡ τ is the trigonality index, which allows the assignment of the structure of the five-coordinate complex to square-pyramidal, trigonal-bipyramidal or intermediate forms.

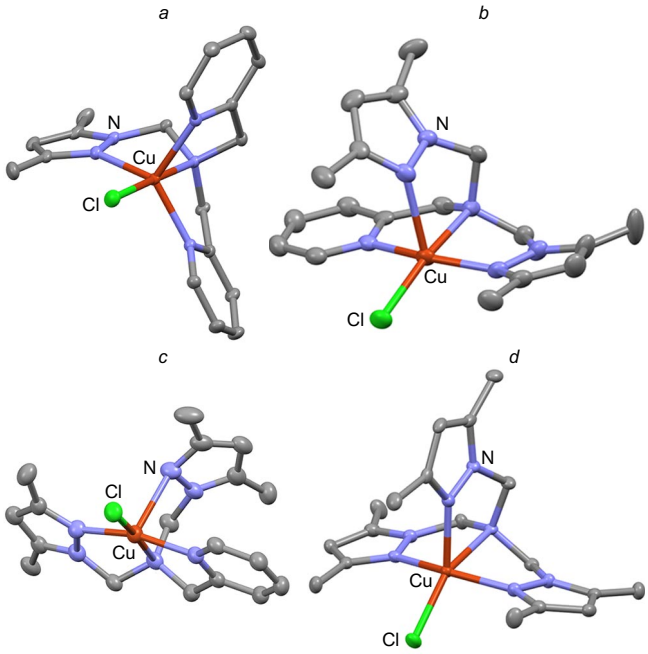
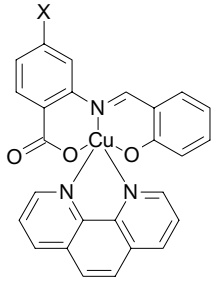


Figure 24. Molecular structures of coordination compounds **257 – 260** (*a – d*, respectively) with a continuous change in the geometry from ideal square-pyramidal to ideal trigonal-bipyramidal through intermediate forms.[160] The Figure was prepared by the authors using the X-ray diffraction data [160] and the data from the Cambridge Crystallographic Data Center (CCDC 1558493, 1558494, 1558495 and 1558496).

It was shown that the cytotoxicity (IC_{50}) of the complexes gradually decreases with a change in the distortion of the geometry from square-pyramidal towards trigonal-bipyramidal (from 1.4 to > 50 μM against the A2780 cell line, from 8.3 to 33.1 μM against the A2780R cell line, *etc.*). It was also found that in the presence of L-cysteine and glutathione, square-pyramidal complex **260** is stable despite its involvement in redox cycles (the mass spectrum of a solution recorded after 24 h showed unchanged peaks of the coordination compound, glutathione and L-cysteine in the oxidized and reduced forms). By contrast, trigonal-bipyramidal complex **257** was completely decomposed (the mass spectrum of the spectrum showed only signals of copper adducts along with the oxidized forms of glutathione and L-cysteine).

However, it should be taken into account that, apart from the main mechanism of cytotoxic activity, other mechanisms, which are less typical of the class of square-pyramidal copper(II) coordination compounds but which

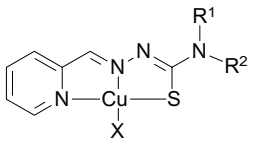
Structures 261, 262



X = F (**261**), Cl (**262**)

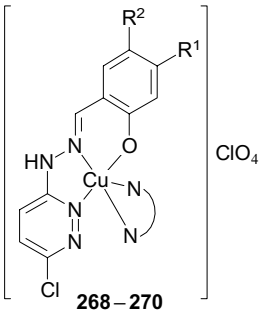
261, **262**

Structures 263 – 270



263 – 270

R^1R^2N = MeNH (**263**), PhNH (**264**), piperidino (**265**), Et_2N (**266**), pyrrolidino (**267**); X = Cl (**263**), NO_3 (**264**), Br (**265**), Cl + MeOH (**266**), Br + MeOH (**267**)



268 – 270

R^1 = NEt_2, R^2 = H: N N = bipy (**268**), phen (**269**); R^1 = H, R^2 = Br, N N = bipy (**270**)

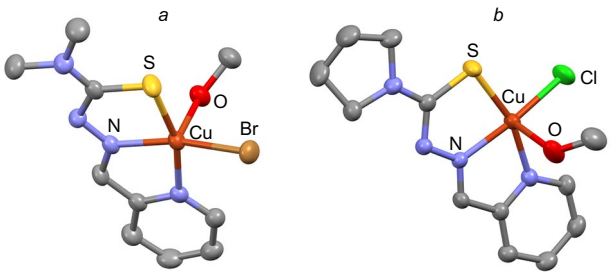


Figure 25. Molecular structures of compounds **266** (*a*) and **267** (*b*).[158] The Figure was prepared by the authors using the X-ray diffraction data[158] and the data from the Cambridge Crystallographic Data Center (CCDC 1829669 and 1829671).

were found for individual representatives, can contribute to the overall toxicity. Thus, it was demonstrated that coordination compound **261** based on 2-[(2-hydroxybenzylidene)amino]-4-fluorobenzoic acid and phenanthroline can inhibit proteasomal chymotrypsin-like activity (unlike 4-chloro-containing analogue **262**),[153] leading to the induction of apoptosis; the IC_{50} value of the proteasome is equal within experimental error to the cytotoxicity IC_{50} value.

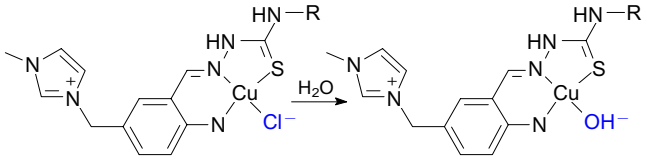
A series of coordination compounds **263 – 270** with square-pyramidal geometry (Fig. 25) also can inhibit telomerase and trigger apoptosis through the activation of the protein p53, which leads to a decrease in the expression of cmyc and hTERT,[158] or through the inhibition of overexpressed fibroblast growth factor receptors (FGFRs) in the cancer cell line MDA-MB-231.[159]

5.2. Square-planar copper(II) coordination compounds

The structural motifs most commonly observed for square-planar copper(II) complexes are CuN_2O_2 (or CuN_2Hal_2) and CuNOSCl. Besides, more rarely observed structures, from CuN_3Hal to CuO_4, are also described in the literature. Bidentate organic ligands are more favourable than tridentate ligands, which are characteristic of square-pyramidal complexes, for the formation of coordination compounds with this geometry.

Stability of square-planar compounds in aqueous solutions at physiological pH values is relatively lower than that of square-pyramidal compounds. In particular, the exchange of monodentate ligands in compounds **271 – 273** with hydroxide anions was described; however, it does not

Scheme 6



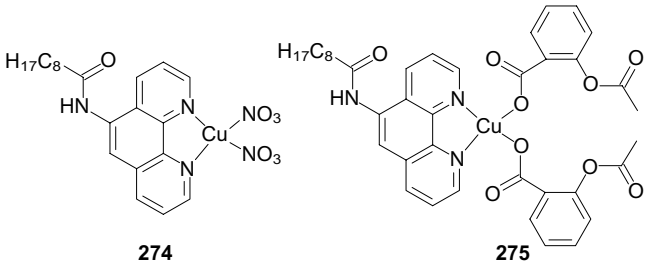
271 – 273

R = H (**271**), Me (**272**), Ph (**273**)

lead to a change in the geometry of the coordination sphere[165] (Scheme 6).

In most of the publications on the mechanisms of cytotoxic activity of square-planar Cu^{II} coordination compounds, the authors suggested that the main mechanism involves the induction of apoptosis *via* the mitochondrial pathway, for example, for coordination compounds **274** and **275**, or (more rarely) *via* a DNA-dependent pathway. Morphological changes in the cells characteristic of apoptosis are described in 5 of 9 publications (see the studies[39, 111, 163, 165, 174]).

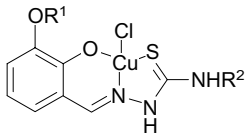
Structures 274, 275



274 **275**

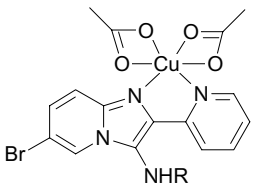
Some research groups reported that square-planar copper coordination compounds **276 – 281** selectively accumulate in mitochondria and cause mitochondrial dysfunction without generation of reactive oxygen species.[111, 163] Even square-planar coordination compounds **282 – 285**, which cause the induction of apoptosis *via* a DNA-dependent pathway, often damage DNA *via* hydrolysis without generation of ROS.[39, 163] As mentioned in the previous Section, even if the ROS generation contributes to the overall cytotoxicity of square-planar copper(II) coordination compounds, the H_2O_2 level in the cell is much lower than in the case of square-pyramidal complexes with related ligands.[145] Besides, the former compounds have much lower DNA

Structures 276 – 285



276 – 281

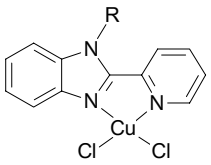
R^1 = Me: R^2 = H (**276**), Ph (**277**), Et (**278**); R^1 = OH: R^2 = H (**279**), Ph (**280**), Et (**281**)



282 – 285

R = Cy (**282**), Bn (**283**), CH_2CO_2Et (**284**), 1-Ad (**285**)

Structures 286, 287



R = 4-$FC_6H_4CH_2$ (**286**),
$C_6F_5CH_2$ (**287**)

286, **287**

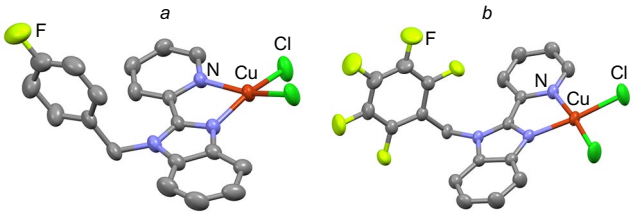


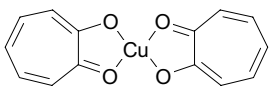
Figure 26. Molecular structures of fluorine-containing square-planar copper(II) coordination compounds **286** (*a*) and **287** (*b*).[156] The Figure was prepared by the authors using the X-ray diffraction data[156] and the data from the Cambridge Crystallographic Data Center (CCDC 1496890 and 1496892).

intercalating efficiency compared to the latter compounds.[156, 170]

Only in one study,[156] it was shown that the ROS generation is the main mechanism of action of square-planar coordination compounds **286** and **287** (Fig. 26). It was noted that these complexes weakly bind to DNA, which is typical of square-planar copper(II) coordination compounds, and, consequently, have low toxicity (IC_{50} = 5.5–12 μM against the A549 cell line)[156] comparable to that of square-pyramidal complexes, which also have weak DNA binding affinity.[155]

The distinguishing features of square-planar Cu^{II} coordination compound **288** with tropolone (2-hydroxycyclohepta-2,4,6-trien-1-one) are high selectivity against cancer cells (the selectivity index $SI_{MCF\text{-}7} = IC_{50}(L929)/IC_{50}(MCF\text{-}7) = 1.9$, $SI_{MDA\text{-}MB\text{-}231} = 2.5$) and the absence of multicellular resistance (a decrease in toxicity against multicellular aggregates compared to individual cells).[174] In particular, the evaluation of cytotoxicity using 2D and 3D models showed that tropolone-based coordination compounds are not only efficiently taken up by cancer cells but also accumulate in MCF-7 spheroids, being 26 times more toxic than cisplatin under similar conditions. Actually, $IC_{50}(3D) = 4.9$ μM is equal within experimental error to $IC_{50}(2D) = 5.2 \pm 1.8$ μM, which is indicative of highly efficient transport of the coordination compound into multicellular spheroids.[174]

Structure 288



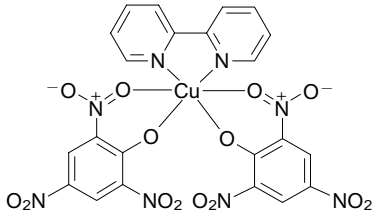
288

5.3. Octahedral copper(II) coordination compounds

Less common octahedral Cu^{II} coordination compounds can exhibit cytotoxic activity through different mechanisms, and it impossible to select the dominant mechanism because of a small number of representatives. Octahedral coordination compounds are characterized by intercalation into DNA through a planar bidentate aromatic ligand;[164] however, the DNA cleavage occurs both *via* the oxidative pathway, typical of square-pyramidal coordination compounds, and *via* the hydrolytic pathway characteristic of square-planar copper(II) compounds. Meanwhile, in some studies it was shown that the DNA binding constants for intercalating octahedral complexes are an order of magnitude lower than the corresponding values for square-pyramidal coordination compounds with related ligands: $\sim 3 \times 10^5$ L mol^{-1} for octahedral compound **289** *versus* $\sim 2 \times 10^6$ L mol^{-1} for square-pyramidal compounds (**290**, **291**).[155] Besides, the toxicity of these compounds against a wide range of cell lines varies in the range of 2.21–8.77 μM for octahedral mono- and dinuclear complexes *versus* 0.58 μM for the square-pyramidal compound (**249**).[154]

On the other hand, as shown with an example of coordination compound **292** (Fig. 27),[152] octahedral complexes can efficiently bind to the minor groove of DNA, resulting in the localization optimal for DNA damage by

Structures 292



292

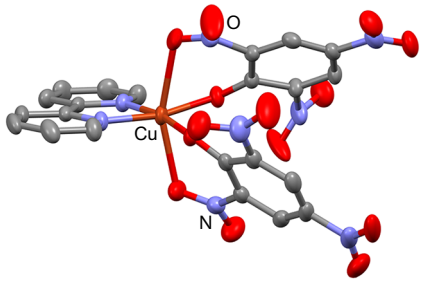
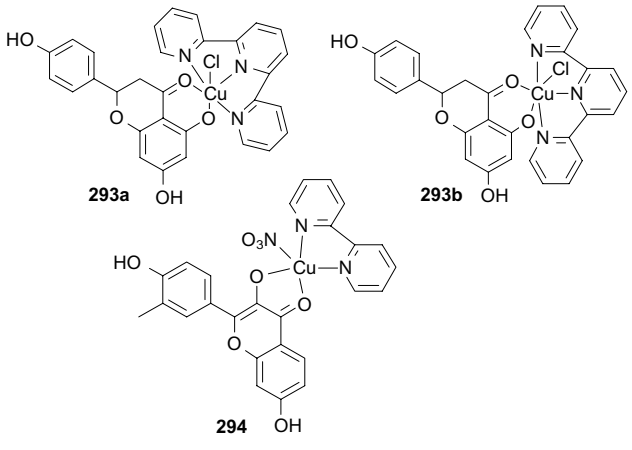


Figure 27. Molecular structure of copper(II) coordination compound **292** based on 2,2′-bipyridine and picrate anions.[152] The Figure was prepared by the authors using the X-ray diffraction data[152] and the data from the Cambridge Crystallographic Data Center (CCDC 876984).

Structures 293, 294



reactive oxygen species (like the localization of Cu^{II} complex **240** with square-pyramidal geometry, which is the most toxic compound in the series of Cu^{II} analogues, in the major groove of DNA [149]). In this pair of coordination compounds **240** and **292**, like in the case of square-pyramidal complexes **238** – **241**, the DNA binding affinity is responsible for the DNA binding mode and directly correlates with the cytotoxicity.

Among more rare mechanisms, determined for cytotoxic activity of octahedral copper coordination compounds, only the induction of apoptosis *via* a caspase-dependent pathway is worthy of note.[167] The presence of the additional pathway of the induction of apoptosis, which was not revealed for square-pyramidal and square-planar analogues, allows isomeric octahedral Cu^{II} complexes **293a**,**b** to exhibit $IC_{50} < 0.8$ μM against the MCF-7 cell line, while square-pyramidal complex **294** with the same ligands has lower toxicity ($IC_{50} = 22.8$ μM).

5.4. Tetrahedral copper(II) coordination compounds

Scarce studies on tetrahedral Cu^{II} complexes with anticancer activity make it impossible to ultimately suggest the mechanism of their cytotoxic activity. Based on the morphological changes in the PC3 and SW480 cell lines, it was found that after 72 h, tetrahedral copper(II) coordination compounds **295** – **303** can cause the induction of apoptosis at concentrations of 11 – 62 and 4 – 88 μM, respectively, with $SI_{HaCat} = 3 - 20$ (the selectivity index against the normal cells HaCat).[176] The factor responsible for selectivity was not elucidated.

The stability of the tetrahedral complexes in solution also remains an open question. Thus, in two of three studies,[157, 176, 177] it was shown that coordination compounds **295** – **303** and **304** – **325** (Fig. 28 *a*) are stable in solution. The absorption and EPR spectra of these compounds do not significantly change with time.[176, 177] Meanwhile, Zhao *et al.*[157] suggested that the main mechanism of cytotoxic activity involves the release of a cytotoxic ligand through the hydrolysis of dehydroabietylamine-based complex **326** (Fig. 28 *b*) (the decomposition of the complex in solution) in the cell.

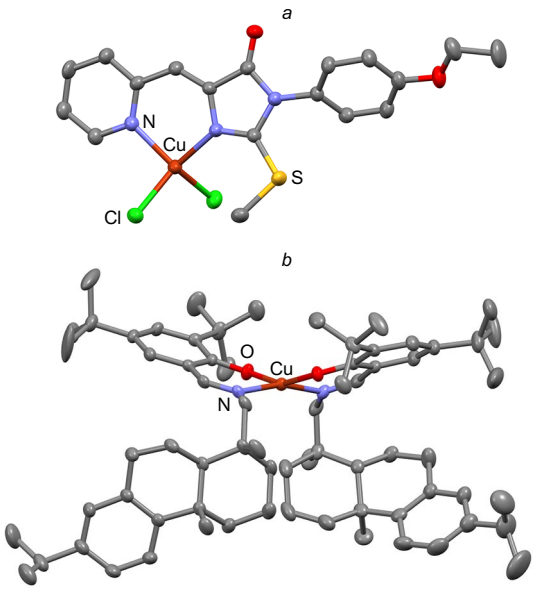
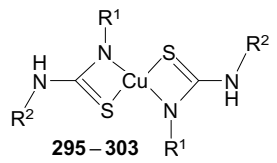
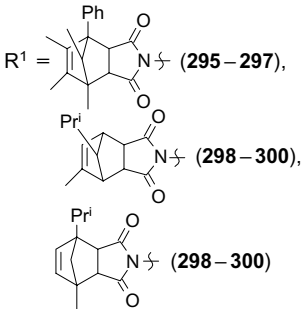


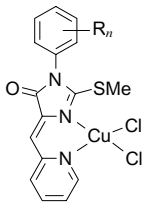
Figure 28. Molecular structures of tetrahedral coordination compounds with methylthioimidazol-4-one (**314**)[177] and dehydroabietylamine (**326**)[157] ligands. The Figure was prepared by the authors using the X-ray diffraction data[157, 177] and the data from the Cambridge Crystallographic Data Center (CCDC 1886553 and 1478435).

Structures 295 – 326

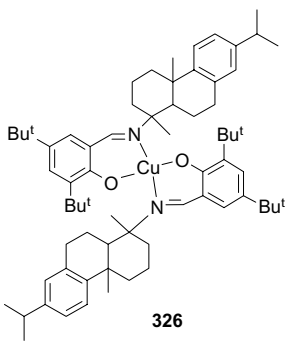




R^2 = 2-Br- (**295**, **298**, **301**),
3-Br- (**296**, **299**, **302**),
4-BrC_6H_4 (**297**, **300**, **303**)



304 – 325



326

R_n = 2-F (**304**), 3-F (**305**), 4-F (**306**),
2-Br (**307**), 3-Br (**308**), 4-Br (**309**),
2-Cl (**310**), 3-Cl (**311**), 4-Cl (**312**),
4-OMe (**313**), 4-OEt (**314**),
4-But (**315**), 4-SMe (**316**),
3,4-$(OMe)_2$ (**317**), 4-Me (**318**), 2-But (**319**), 2-Br,4-F (**320**),
2-Me,3-Cl (**321**), 2,4,6-Me_3 (**322**), 2-OMe,4-Cl,5-Me (**323**),
2,5-F_2 (**324**), 3,5-F_2 (**325**)

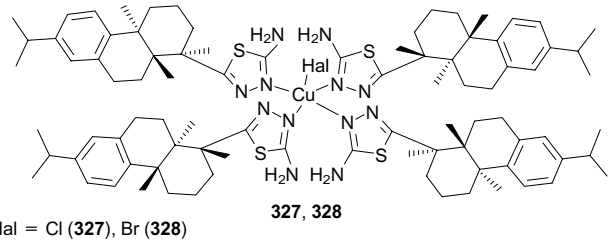
5.5. Trigonal-bipyramidal copper(II) coordination compounds

Copper(II) coordination compounds with trigonal-bipyramidal structures exhibiting cytotoxic activity are poorly characterized in the literature. A few examples of these complexes both with a tetradentate ligand and with five monodentate ligands are known. Hence, it is difficult to analyze the optimal structural motifs giving rise to trigonal-bipyramidal compounds.

A small number of coordination compounds with this structure available in the literature is attributed to their low stability in aqueous solutions, particularly in the presence of intracellular reducing agents, such as glutathione and L-cysteine, which cause the complete decomposition of the trigonal-bipyramidal complexes.[160]

In the only study,[162] in which the mechanism of cytotoxic activity of trigonal-bipyramidal coordination compounds **327** and **328** was investigated (Fig. 29), it was shown that these compounds induce apoptosis *via* the mitochondrial pathway, cause mitochondrial dysfunction and generate ROS. Low stability of these compounds in the presence of intracellular reducing agents is additionally evidenced by the fact that the compounds with the highest cytotoxicity bind to cell surface death receptors on the cell membrane in the MCF-7 cell line.[162] Therefore, the most toxic trigonal-bipyramidal complexes are

Structures 327, 328



327, **328**

Hal = Cl (**327**), Br (**328**)

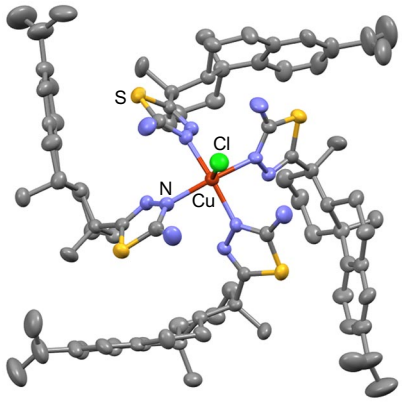


Figure 29. Molecular structure of compound **327**.[162] The Figure was prepared by the authors using the X-ray diffraction data[162] and the data from the Cambridge Crystallographic Data Center (CCDC 1887431).

those, which are not decomposed in the presence of intracellular reducing agents exhibiting cytotoxic activity without cellular uptake.

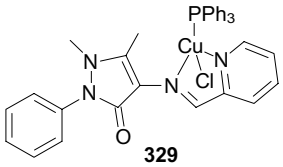
5.6. Tetrahedral copper(I) coordination compounds

As was mentioned in the introductory part of Section 5, Cu^{I} ions, according to the HSAB theory, are softer than Cu^{II} ions. This has a significant effect on the favourable ligand environment of this metal. In the majority of coordination compounds considered above, copper(II) ions are surrounded by ligands with electron-donating nitrogen, oxygen and, more rarely, sulfur atoms (*i.e.*, ligands of intermediate or high hardness), whereas the coordination sphere of the copper(I) ion usually involves one or several molecules of triphenylphosphine or its substituted analogue (soft ligands).[148, 168] According to the results of the study,[181] the presence of phosphine ligands is a key factor responsible for high biological activity of the complex.

In the cited studies, DNA was found to be the main molecular target for tetrahedral Cu^{I} coordination compounds. Attempts were made [148, 168] to elucidate the mechanism of cytotoxic activity of complexes **329** – **332**. It was demonstrated that these compounds can intercalate into DNA with constants of about 2.45×10^5 (Ref. 148) and 12.6×10^4 L mol^{-1}.[168] It was mentioned that the tetrahedral coordination compounds, *e.g.*, complex **329** (Fig. 30), do not tend to cleave DNA, but cause insignificant DNA damage through a hydrolytic mechanism and exhibit antioxidant activity, excluding the ROS generation.[148]

Besides, it was found that tetrahedral Cu^{I} coordination compounds **330** – **332** (Fig. 31) based on triphenylphosphine and phenanthroline can bind to androgen receptors overexpressed on the surface of prostate and breast cancer cells, in particular PC-3 and MCF-7 (according to the molecular docking results).[168]

Structure 329



329

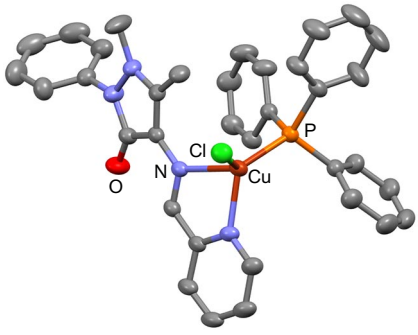
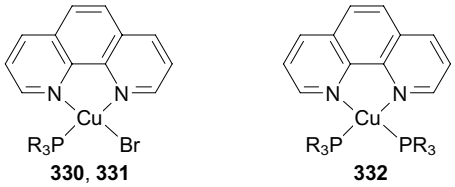


Figure 30. Molecular structure of tetrahedral copper(I) coordination compound **329**.[148] The Figure was prepared by the authors using the X-ray diffraction data[148] and the data from the Cambridge Crystallographic Data Center (CCDC 885697).

5.7. Triangular and trigonal-pyramidal copper(I) coordination compounds

Copper(I) complexes with trigonal-pyramidal and triangular geometry of the coordination sphere formed by four and three ligands, respectively, have received little study. It was

Structures 330 – 332



330, **331** **332**

R = Ph (**330**), Cy (**331**), 4-MeOC$_6$H$_4$ (**332**)

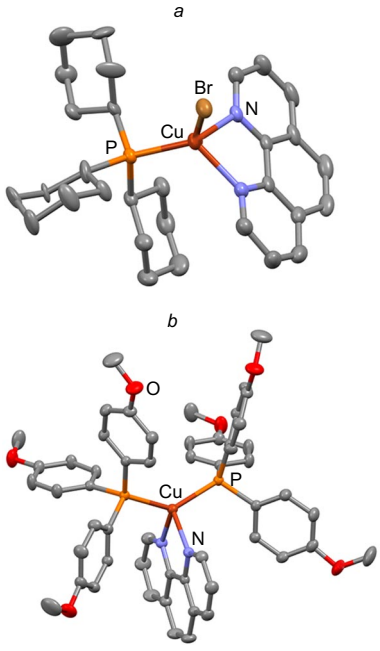
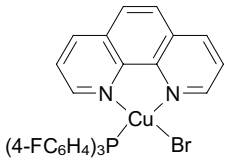


Figure 31. Molecular structures of tetrahedral copper(I) coordination compounds **331** (*a*) and **332** (*b*) capable of binding to DNA and androgen receptors in PC-3 cells.[168] The Figure was prepared by the authors using the X-ray diffraction data[168] and the data from the Cambridge Crystallographic Data Center (CCDC 1837855 and 1837856).

Structure 333



333

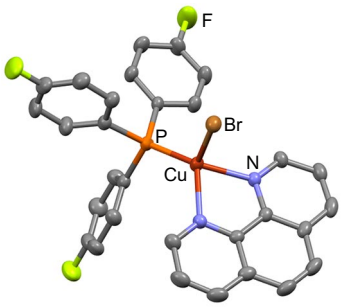
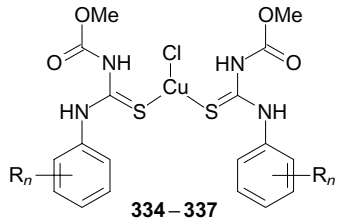


Figure 32. Copper(I) coordination compound **333** with trigonal-pyramidal geometry.[168] The Figure was prepared by the authors using the X-ray diffraction data[168] and the data from the Cambridge Crystallographic Data Center (CCDC 1837854).

demonstrated[168] that trigonal-pyramidal copper(I) compound **333** (Fig. 32) is less toxic compared to the tetrahedral analogues (IC_{50} = 81–91 μM *versus* 35 μM against the MCF-7 cell line) and more weakly binds to androgen receptors as a target for tetrahedral Cu^{I} coordination compounds. The mechanism of DNA binding was determined as the intercalation, but the binding affinity is low with constants in the range of $(6.7–20) \times 10^4$ L mol^{-1}.[168]

Planar-triangular copper(I) coordination compounds **334**–**337** with ligands of the thiocarbamine series (Fig. 33) were characterized in the studies.[169, 171] Systematic investigations of the putative mechanisms of their cytotoxicity were not performed and molecular targets were not identified as yet. Pandey *et al.*[169] found only very strong DNA fragmentation caused by complexes **335**–**337** with multiple double-strand breaks and evaluated the selectivity against cancer cells; SI = IC_{50}(WRL-68)/IC_{50}(2008, C-13, IGROV-1) = 3.6–1.89.

Structures 334–337



334–337

R_n = 2-OMe (**334**),
4-OMe (**335**),
2-Cl, 4-NO_2 (**336**),
2-OMe, 4-NO_2 (**337**)

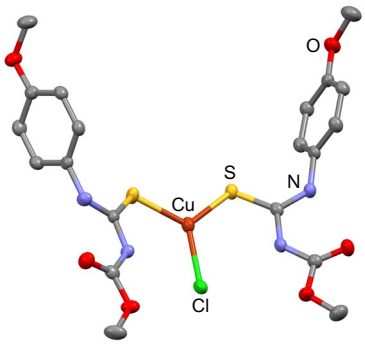


Figure 33. Molecular structure of trigonal-planar compound **335**.[169] The Figure was prepared by the authors using the X-ray diffraction data[169] and the data from the Cambridge Crystallographic Data Center (CCDC 945662).

Kokina *et al.*[171] demonstrated that triangular copper coordination compound **338** with (−)-camphor thiosemicarbazone is promising for the search for new anticancer agents. This complex has the highest toxicity in the series of coordination compounds of this ligand with different metals (Zn, Pd) having different coordination geometry (tetrahedral, square-planar). However, putative biological targets and mechanisms of cytotoxic activity were not revealed.

5.8. Prospects of the development of anticancer agents based on copper ions

Copper coordination compounds have different geometries and are stable in aqueous solutions at physiological pH values in metal oxidation states +2 and +1, several types of coordination geometry being stable for both oxidation states. As opposed to cytotoxic cobalt complexes, in which the change in the oxidation state of complex-forming metal imposes severe restrictions on the geometry of the complex, the properties of copper coordination compounds are more diverse.

Besides, it was shown that copper coordination compounds can be stabilized in different oxidation states with similar geometry by varying the electronic properties of the organic ligand (by introduction of donors or acceptors into the structure). Thus, the introduction of electron-withdrawing moieties into the ligand stabilizes Cu^{I} complexes, whereas electron-donating substituents stabilize Cu^{II} compounds. This allows the fine tuning of the structure and cytotoxic activity of coordination compounds and makes it possible to change the contributions of different mechanisms of cytotoxic activity to the overall cytotoxicity.[111, 165, 177]

Copper ions play an important role in different intracellular processes, mainly in redox processes. Hence, cancer cells with an increased metabolism have a higher demand for copper compared with normal cells, which additionally facilitates the transport of cytotoxic copper coordination compounds to malignant sites.[146, 147, 150] The selective permeability of cancer cell membranes to copper compounds was supposed.[148]

Mechanisms of cytotoxic activity available for copper complexes involve the oxidative DNA damage,[145, 151, 155] the hydrolytic DNA damage, the intercalation[148, 150, 151] and the binding to the minor[152] and major[149, 173] grooves of DNA leading to changes in the gene expression levels and chromatin dysfunction, the generation of reactive oxygen species,[145] the impairment of mitochondrial function and the electron transport chain,[158, 162, 163, 167] the inhibition of different enzymes (*e.g.*, telomerase[158, 177]) and the activation of proteasomes,[153] caspases[167] and the regulator protein p53,[158] leading to the induction of apoptosis *via* the DNA-dependent[146, 147, 149, 155] or mitochondrial[111, 163, 175, 178] pathway. Besides, more rare mechanisms were found for individual coordination compounds. The above data show that copper complexes are the most promising candidates for the preparation of new-generation anticancer agents finely tuned to particular cancer cell lines in terms of properties, high selectivity and low toxicity against normal tissues.

6. Conclusion

The data summarized and integrated in this review make it possible to reveal the coordination geometry – mechanism of cytotoxic activity – IC_{50} relationships for coordination compounds of transition metals most abundant in the human body (zinc, iron, cobalt and copper). In each Section, putative mechanisms of cytotoxic activity, characteristic of the corresponding complex-forming metal in a particular oxidation state, are analyzed and conclusions are made about the most promising structural motifs for each class of compounds described in the literature.

As mentioned above, the main factors responsible for the cytotoxicity and the mechanism of action of metal coordination compounds are the geometry of the coordination sphere, the oxidation state of the metal in the complex and its redox potential. On the whole, the former two factors make it possible to divide all coordination compounds into classes according to the common biological targets, similar mechanisms of action and close ranges of IC_{50} values.

For each type of the coordination geometry, the overall cytotoxicity of the complex is associated with a number of mechanisms, the contributions of which are specified by certain weighting coefficients. Thus, the main mechanism for tetrahedral coordination compounds can be a minor mechanism for its square analogue and *vice versa*. However, in many cases, only one mechanisms makes the major contribution to cytotoxicity, the mechanisms being different for complexes of each structural type. In some cases, in which the coordination sphere is gradually distorted, transforming the geometry of the coordination compound from one type to another, continuous changes in the contributions of different mechanisms to the overall toxicity can be revealed.

Hence, the fine tuning not only of the cytotoxicity but also of the mechanism of action of coordination compounds can be performed by changing the structure, geometry and electronic properties of the organic ligand. Using a large set of examples considered in this review, it was shown that the variation of the ligand structure or the replacement of the ligand by its closest homologue can significantly change not only the cytotoxicity of the coordination compound but also the mechanism of DNA binding and, in some cases, make another mechanism of cytotoxic activity the main one.

Hence, it can be concluded that all cytotoxic coordination compounds of biogenic metals considered in the review offer a possibility of searching for and optimizing new-generation agents for cancer therapy. Each biogenic metal has a number advantages, such as the efficient cellular uptake through transferrins (for iron) or the protein Ctr1 (for copper), high selectivity against cancer cells demonstrated for ferrocene derivatives and selectivity towards G4-DNA characteristic of square-planar zinc compounds and octahedral cobalt(II) compounds. Iron and copper coordination compounds can be considered as the most promising ones. They have the largest diversity of structural motifs and types of coordination geometry and the widest range of available mechanisms of cytotoxic activity.

This review was written with the financial support of the Russian Foundation for Basic Research (Project No. 20-13-50013).

7. List of acronyms and abbreviations

Cell lines:

518A2 — melanoma cell line;
A2780 — human ovarian cancer cell line;
A375 — malignant melanoma cell line;
A431 — epidermoid carcinoma cell line;
A431Pt — Pt-resistant epidermoid carcinoma cell line;
A498 — human kidney carcinoma cell line;
A549 — human lung adenocarcinoma cell line;
AGS — human gastric adenocarcinoma cell line;
BCC — basal cell carcinoma cell line;
BEL-7402 — human papillomavirus-related endocervical adenocarcinoma;
BGC823 — human papillomavirus-related endocervical adenocarcinoma;
BL-2 — Burkitt lymphoma;
C13, CaSki — human papillomavirus-related cervical squamous cell carcinoma;
Caco-2 — human colon adenocarcinoma;
Caki-2 — human papillary renal cell carcinoma;
CEM/ADR5000 — childhood T-cell acute lymphoblastic leukemia cell line;
CO-115 — human colon adenocarcinoma;
Colo-205 — human colon adenocarcinoma;
DLD-1 — human colon adenocarcinoma;
DU-145 — human prostate carcinoma;
Eca-109 — human esophageal squamous cell carcinoma;
G-361 — human melanoma;
NCI-H460 — human large cell lung carcinoma;
HaCaT — spontaneously immortalized normal human cell line;
HCT116 — human colon adenocarcinoma;
HCT-8 — human colon adenocarcinoma;
Hek-293 — transformed human fetal cell line;
HeLa — human papillomavirus-related endocervical adenocarcinoma;
Hep-2 — human papillomavirus-related endocervical adenocarcinoma;
Hep3B — childhood hepatocellular carcinoma;
Hep-G2 — human hepatocellular carcinoma;
HL-60 — human adult acute myeloid leukemia;
HL-7702 — human papillomavirus-related endocervical adenocarcinoma;
HOS — human osteosarcoma;
HT-29 — human colon adenocarcinoma;
HUVEC — normal human cell line;
IGROV-1 — human ovarian endometrioid adenocarcinoma;
IM-9 — transformed normal human cell line;
Jurkat — childhood T-cell acute lymphoblastic leukemia;
K562 — human chronic myelogenous leukemia;
KbV1/Vbl — human papillomavirus-related endocervical adenocarcinoma;
L6 — transformed normal rat myoblast cell line;
L929/A — spontaneously immortalized normal mouse cell line;

LH32 — normal human hepatocytes;
LN-229 — human glioblastoma;
LoVo — human colon adenocarcinoma;
LS-174 — human colon adenocarcinoma;
MCF-7 — human invasive ductal breast carcinoma;
MCF-10A — spontaneously immortalized human cell line;
MDA-MB-231 — human breast adenocarcinoma;
MDA-MB-453 — human breast adenocarcinoma;
MelHo — human melanoma;
MG-63 — human osteosarcoma;
MIA-PA-CA-2 — human pancreatic ductal adenocarcinoma;
MKN-45 — human gastric adenocarcinoma;
Molt-4 — adult T-cell acute lymphoblastic leukemia;
MRC-5 — normal human biotechnology cell line;
MTSV1-7 — normal human mammary luminal epithelial cells;
Nalm-6 — adult B-cell acute lymphoblastic leukemia;
NCI-H322M — minimally invasive human lung adenocarcinoma;
NCI-H460 — human large cell lung carcinoma;
NCTC — spontaneously immortalized mouse cell line;
PBMC — induced pluripotent human stem cells;
PC-3 — human prostate carcinoma;
PC-12 — human lung papillary adenocarcinoma;
Saos-2 — human osteosarcoma;
SCC-4 — human tongue squamous cell carcinoma;
SCC-9 — human tongue squamous cell carcinoma;
SCC-25 — human tongue squamous cell carcinoma;
SK-OV-3 — ovarian serous cystadenocarcinoma;
SMMC-7721 — human papillomavirus-related endocervical adenocarcinoma;
T24 — bladder carcinoma;
TE1 — esophageal squamous cell carcinoma;
TFK-1 — cholangiocarcinoma;
U87MG — human glioblastoma;
U937 — adult acute monocytic leukemia.

Other abbreviations:

ABTS — 2,2′-azinobis(3-ethylbenzothiazoline-6-sulfonic acid);
AcTsc — 3-acetylcoumarin thiosemicarbazone;
Ad — adamantyl;
amphen — 5-amino-1,10-phenanthroline;
andpa — (anthracen-9-yl)bis(2-pyridylmethyl)amine;
AP — antipyrine;
Azil — azilsartan;
bapen — *N*,*N*′-bis(3-aminopropyl)ethylenediamine;
m-BDA — 4,4-difluoro-1,3,5,7-tetramethyl-8-[3-bis(2-pyridylmethyl)aminobenzyl]-4-bora-3a,4a-diaza-*s*-indacene;
bdmpzp — bis(3,5-dimethyl-1*H*-pyrazol-1-ylmethyl)(2-pyridylmethyl)amine;
bedmpz — bis[2-(3,5-dimethyl-1*H*-pyrazol-1-yl)ethyl](2-pyridylmethyl)amine;
BHA — benzhydroxamate;
bipy — 2,2′-bipyridine;
Boc — *tert*-butoxycarbonyl;
bpdmpzp — (3,5-dimethyl-1*H*-pyrazol-1-ylmethyl)bis(2-pyridylmethyl)amine;
BrQ — 7-bromoquinolin-8-ol;
bzimpy — 2,6-bis(benzimidazol-2-yl)pyridine;
Caf — caffeine;
chtsc — cyclohexanone thiosemicarbazone;
Cp — cyclopentadienyl;
CQ — 5-chloro-7-iodoquinolin-8-ol;
Clphen — 5-chloro-1,10-phenanthroline;
Cltpy — 4′-chloro-2,2′:6′,2″-terpyridine;
cur — curcumin (bis(4-hydroxy-3-methoxyphenyl)-1,6-diene-3,5-dione);
Cy — cyclohexyl;
cyclam — 1,4,8,11-tetraazacyclotetradecane;
Cyclen — 1,4,7,10-tetraazacyclododecane;
dBrQ — protonated 5,7-dibromoquinolin-8-ol;
DC_{50} — half-maximal concentration of the compound required to displace 50% of the intercalator from the complex with DNA;
dClQ — 5,7-dichloroquinolin-8-ol;
dmb — 4,4′-dimethyl-2,2′-bipyridine;
dmdppz — 11,12-dimethylpyridyl[3,2-*a*:2′,3′-*c*]phenazine;
dmp — 5,6-dimethyl-1,10-phenanthroline;
dmtp — 2,6-di(5-methyl-4*H*-1,2,4-triazol-3-yl)pyridine;
dpam — 2,2′-dipyridylamine;
dppe — 1,2-bis(diphenylphosphino)ethane;
DPPH — 2,2-diphenyl-1-(2,4,6-trinitrophenyl)hydrazin-1-yl;
dppt — 3-(2-pyridyl)-5,6-diphenyl-1,2,4-triazine;
dppz — dipyridyl[3,2-*a*:2′,3′-*c*]phenazine;
dpq — dipyridyl[3,2-*f*:2′,3′-*h*]quinoxaline;
dthp — 2,6-di(thiazol-2-yl)pyridine;
dtp — 2,6-di(4*H*-1,2,4-triazol-3-yl)pyridine;
epoxyphen — 5,6-epoxy-5,6-dihydro-1,10-phenanthroline;
FGFR — fibroblast growth factor receptors;
Glu — glutamate;
Gluc — D-gluconic acid;
GSH — glutathione;
HAcPipPheF — 2-acetylpyridine N^4-1-(4-fluorophenyl)-piperazinothiosemicarbazone;
H_2Bd — α-benzyl dioxime;
Hdicl — diclofenac (2-[2-(2,6-dichloroanilino)phenyl]-acetic acid;
Hex — *n*-hexyl;
Hfen — fenamic acid (2-phenylaminobenzoic acid);
H_2Gm(morph) — morpholinoglyoxime;
His — histidine;
Hnor — norharman (β-carboline);
HO-1 — haem oxygenase-1;
HPB — 2-(2-pyridyl)benzimidazole;
HPBC — 5-chloro-2-(2-pyridyl)benzimidazole;
HpysR — Schiff base of pyridine-2-carboxaldehyde and S-substituted dithiocarbazate (R = Me, Bn);
IC_{50} — half-maximal inhibitory concentration;
im — imidazole;
ip — imidazo[4,5-*f*][1,10]phenanthroline;
K_b — binding constant;
me-pip — 2-(4-methylphenyl)-1*H*-imidazo[4,5-*f*][1,10]-phenanthroline;
mimH — methylimidazole;
MOPS — 3-morpholinopropylsulfonic acid;
morph — morpholino;
mpkqh — methyl 2-pyridyl ketone 2-quinolylhydrazone;
Naph — naphthyl;
nar — naringenin;

Pamp — pyridine-2-carboxylic acid *N′*-phenyl-*N′*-(2-pyridyl)hydrazide;
paqh — pyridine-2-carbaldehyde 2-quinolylhydrazone;
pbmq — [2-(pyrazin-2-yl)-1*H*-benzo[*d*]imidazol-1-ylmethyl]quinoline;
pdc — pyridine-2,5-dicarboxylate;
PDI — disulfide isomerase;
phdpa — benzylbis(2-pyridylmethyl)amine;
phen — 1,10-phenanthroline;
pic — picrate;
pip — 2-phenylimidazo[4,5-*f*][1,10]phenanthroline;
pmdt — *N*,*N*,*N′*,*N″*,*N″*-pentamethyldiethylenetriamine;
PP — protoporphyrin IX;
ppkqh — phenyl 2-pyridyl ketone 2-quinolylhydrazone;
Py — pyridine;
pydc — pyridine-2,6-dicarboxylic acid;
pydpa — (2-pyrenylmethyl)bis(2-pyridylmethyl)amine;
que — quercetin;
R-DT — R-substituted dithiocarbamate;
ROS — reactive oxygen species;
sac — saccharin (*o*-sulfobenzimide);
Sal — salicylate;
salophen — *N,N′*-bis(salicylidene)-1,2-phenylenediamine;
SI — selectivity index;
tdmpza — tris(3,5-dimethyl-1*H*-pyrazol-1-ylmethyl)-amine;
Tf — trifluoromethanesulfonyl (triflyl);
tmen — *N*,*N*,*N′*,*N′*- tetramethylethylenediamine;
tpa — tris(2-pyridylmethyl)amine;
tpy — 2,2′ :6′,2′-terpyridine;
TRK — tyrosine kinases;
tropH — tropolone (2-hydroxycyclohepta-2,4,6-trien-1-one);
Trp — tryptophan;
TTA — 4,4,4-trifluoro-1-(2-furyl)butane-1,3-dione.

References

1. J.Sun, Q.Wei, Y.Zhou, J.Wang, Q.Liu, H.Xu. *BMC Syst. Biol.*, **11**, 87 (2017)
2. B.Rosenberg. In *Cisplatin*: *Current Status and New Developments*. (Eds A.N.Prestayko, S.T.Crooke, S.K.Carter). (New-York: Academic Press, 1980). P. 9
3. J.C.Dabrowiak. *Metals in Medicine*. (*Inorganic Chemistry: A Textbook Series*). (2nd Edn). (New York: Wiley, 2017)
4. R.P.Miller, R.K.Tadagavadi, G.Ramesh, W.B.Reeves. *Toxins (Basel)*, **2**, 2490 (2010)
5. S.R.McWhinney, R.M.Goldberg, H.L.McLeod. *Mol. Cancer Ther.*, **8**, 10 (2009)
6. B.L.Vallee, D.S.Auld. *Biochemistry*, **32**, 6493 (1993)
7. G.K.Walkup, S.C.Burdette, S.J.Lippard, R.Y.Tsien. *J. Am. Chem. Soc.*, **122**, 5644 (2000)
8. Q.Zhou, T.W.Hambley, B.J.Kennedy, P.A.Lay, P.Turner, B.Warwick, J.R.Biffin, H.L.Regtop. *Inorg. Chem.*, **39**, 3742 (2000)
9. A.Tarushi, K.Lafazanis, J.Kljun, I.Turel, A.A.Pantazaki, G.Psomas, D.P.Kessissoglou. *J. Inorg. Biochem.*, **121**, 53 (2013)
10. A.Tarushi, C.Kakoulidou, C.P.Raptopoulou, V.Psycharis, D.P.Kessissoglou, I.Zoi, A.N.Papadopoulos, G.Psomas. *J. Inorg. Biochem.*, **170**, 85 (2017)
11. R.Crichton. *Iron Metabolism: From Molecular Mechanisms to Clinical Consequences*. (3rd Edn). (New York: Wiley, 2009)
12. S.Inoue, S.Kawanishi. *Cancer Res.*, **47**, 6522 (1987)
13. M.Dizdaroglu, G.Rao, B.Halliwell, E.Gajewski. *Arch. Biochem. Biophys.*, **285**, 317 (1991)
14. M.Dizdaroglu, P.Jaruga. *Free Radical Res.*, **46**, 382 (2012)
15. C.R.Munteanu, K.Suntharalingam. *Dalton Trans.*, **44**, 13796 (2015)
16. P.Chellan, P.J.Sadler. *Philos. Trans. R. Soc. A*, **373**, 20140182 (2015)
17. G.Crisponi, V.M.Nurchi, D.Fanni, C.Gerosa, S.Nemolato, G.Fa. *Coord. Chem. Rev.*, **254**, 876 (2010)
18. M.Reina, L.F.Hernández-Ayala, M.E.Bravo-Gómez, V.Gómez, L.Ruiz-Azuara. *Inorg. Chim. Acta*, **517**, 120201 (2020)
19. P.Štarha, J.Vančo, Z.Trávníček. *Coord. Chem. Rev.*, **380**, 103 (2019)
20. G.Facchetti, I.Rimoldi. *Bioorg. Med. Chem. Lett.*, **29**, 1257 (2019)
21. M.Crespo. *J. Organomet. Chem.*, **879**, 15 (2019)
22. P.Štarha, Z.Trávníček. *Coord. Chem. Rev.*, **395**, 130 (2019)
23. A.S.Kritchenkov, Ya.M.Stanishevskii, Yu.A.Skorik. *Khim.-Farm. Zh.*, **53** (1), 8 (2019)
24. D.A.Arantseva, E.L.Vodovozova. *Russ. J. Bioorgan. Chem.*, **44**, 619 (2018)
25. D.Korman, L.Ostrovskaya, V.Kuz'min. *Voprosy Onkologii*, **64**, 697 (2018)
26. O.A.Zalevskaya, Y.A.Gur'eva, A.V.Kutchin. *Russ. Chem. Rev.*, **88**, 979 (2019)
27. D.V.Andreeva, A.S.Tikhomirov, A.E.Shchekotikhin. *Russ. Chem. Rev.*, **90**, 1 (2021)
28. T.P.Stanojkovic, D.Kovala-Demertzi, A.Primikyri, I.Garcia-Santos, A.Castineiras, Z.Juranic, M.A.Demertzis. *J. Inorg. Biochem.*, **104**, 467 (2010)
29. E.M.Nagy, S.Sitran, M.Montopoli, M.Favaro, L.Marchiò, L.Caparrotta, D.Fregona. *J. Inorg. Biochem.*, **117**, 131 (2012)
30. J.Fang, K.Greish, H.Qin, L.Liao, H.Nakamura, M.Takeya, H.Maeda. *Eur. J. Pharm. Biopharm.*, **81**, 540 (2012)
31. S.Wang, J.E.Avery, B.N.Hannafon, S.E.Lind, W.Q.Ding. *Biochem. Pharmacol.*, **85**, 1611 (2013)
32. D.Palanimuthu, A.G.Samuelson. *Inorg. Chim. Acta*, **408**, 152 (2013)
33. S.Ghammamy, S.Sedaghat. *Russ. J. Gen. Chem.*, **83**, 722 (2013)
34. S.Bhattacharyya, A.Sarkar, S.K.Dey, A.Mukherjee. *J. Inorg. Biochem.*, **140**, 131 (2014)
35. A.H.Mirza, M.H.S.A.Hamid, S.Aripin, M.R.Karim, M.Arifuzzaman, M.A.Ali, P.V.Bernhardt. *Polyhedron*, **74**, 16 (2014)
36. M.Anjomshoa, S.J.Fatemi, M.Torkzadeh-Mahani, H.Hadadzadeh. *Spectrochim. Acta, Part A*, **127**, 511 (2014)

37. N.S.Rukk, L.G.Kuzmina, D.V.Albov, R.S.Shamsiev, S.N.Mudretsova, G.A.Davydova, V.M.Retivov, P.A.Volkov, V.V.Kravchenko, G.N.Apryshko, A.N.Streletskii, A.Y.Skryabina, E.A.Mironova, V.V.Zamalyutin. *Polyhedron*, **102**, 152 (2015)
38. I.S.Tarabukin, Ya.I.Pylina, I.O.Velegzhaninov, O.M.Startseva, D.M.Shadrin, D.V.Belykh. *Butlerov. Soobshch.*, **43** (7), 18 (2015)
39. J.Dam, Z.Ismail, T.Kurebwa, N.Gangat, L.Harmse, H.M.Marques, A.Lemmerer, M.L.Bode, C.B.de Koning. *Eur. J. Med. Chem.*, **126**, 353 (2017)
40. R.Vikneswaran, N.E.Eltayeb, S.Ramesh, R.Yahya. *Polyhedron*, **105**, 89 (2016)
41. A.Adhikari, N.Kumari, M.Adhikari, N.Kumar, A.K.Tiwari, A.Shukla, A.K.Mishra, A.Datta. *Bioorg. Med. Chem.*, **25**, 3483 (2017)
42. A.Banerjee, K.Banerjee, A.Sinha, S.Das, S.Majumder, S.Majumdar, S.K.Choudhuri. *Environ. Toxicol. Pharmacol.*, **56**, 383 (2017)
43. R.Eshaghi Malekshah, M.Salehi, M.Kubicki, A.Khaleghian. *J. Mol. Struct.*, **1150**, 155 (2017)
44. K.N.A.Rahman, J.Haribabu, C.Balachandran, N.S.P.Bhuvanesh, R.Karvembu, A.Sreekanth. *Polyhedron*, **135**, 26 (2017)
45. I.S.Golubeva, A.E.Barmashov, A.A.Rudakova, M.A.Baryshnikova, N.S.Rukk, A.Y.Skryabina, G.N.Apryshko. *Russ. J. Biother.*, **16**, 75 (2017)
46. S.Asadizadeh, M.Amirnasr, F.Fadaei Tirani, A.Mansouri, K.Schenk. *Inorg. Chim. Acta*, **483**, 310 (2018)
47. R.Bonsignore, F.Russo, A.Terenzi, A.Spinello, A.Lauria, G.Gennaro, A.M.Almerico, B.K.Keppler, G.Barone. *J. Inorg. Biochem.*, **178**, 106 (2018)
48. R.Smolková, V.Zeleák, R.Gyepes, D.Sabolová, N.Imrichová, D.Hudecová, L.Smolko. *Polyhedron*, **141**, 230 (2018)
49. N.Muhammad, M.Ikram, A.Wadood, S.Rehman, S.Shujah, Erum, M.Ghufran, S.Rahim, M.Shah, C.Schulzke. *Spectrochim. Acta, Part A*, **190**, 368 (2018)
50. V.R.Martínez, M.V.Aguirre, J.S.Todaro, O.E.Piro, G.A.Echeverría, E.G.Ferrer, P.A.M.Williams. *Toxicol. Vitr.*, **48**, 205 (2018)
51. M.Azam, S.M.Wabaidur, M.J.Alam, A.Trzesowska-Kruszynska, R.Kruszynski, M.Alam, S.I.Al-Resayes, S.Dwivedi, M.R.Khan, M.S.Islam, N.T.M.lbaqami. *Inorg. Chim. Acta*, **487**, 97 (2019)
52. N.S.Rukk, L.G.Kuzmina, R.S.Shamsiev, G.A.Davydova, E.A.Mironova, A.M.Ermakov, G.A.Buzanov, A.Y.Skryabina, A.N.Streletskii, G.A.Vorob'eva, V.M.Retivov, P.A.Volkov, S.K.Belus, E.I.Kozhukhova, V.N.Krasnoperova. *Inorg. Chim. Acta*, **487**, 184 (2019)
53. Ü.Yilmaz, S.Tekin, N.Buğday, K.Yavuz, H.Küçükbay, S.Sandal. *Inorg. Chim. Acta*, **495**, 118977 (2019)
54. C.P.Matos, Y.Addis, P.Nunes, S.Barroso, I.Alho, M.Martins, A.P.A.Matos, F.Marques, I.Cavaco, J.Costa Pessoa, I.Correia. *J. Inorg. Biochem.*, **198**, 110727 (2019)
55. L.Huang, R.Liu, J.Li, X.Liang, Q.Lan, X.Shi, L.Pan, H.Chen, Z.Ma. *J. Inorg. Biochem.*, **201**, 110790 (2019)
56. N.S.Rukk, L.G.Kuz'mina, G.A.Davydova, G.A.Buzanov, V.M.Retivov, S.K.Belus, E.I.Kozhukhova, A.E.Barmashov, A.A.Khrulev, M.A.Simonova, V.N.Krasnoperova. *Mendeleev Commun.*, **29**, 640 (2019)
57. N.Balakrishnan, J.Haribabu, D.Anantha Krishnan, S.Swaminathan, D.Mahendiran, N.S.P.Bhuvanesh, R.Karvembu. *Polyhedron*, **170**, 188 (2019)
58. L.Saghatforoush, K.Moeini, S.A.Hosseini-Yazdi, Z.Mardani, A.Bakhtiari, A.Hajabbas-Farshchi, S.Honarvar, M.S.M.Abdelbaky. *Polyhedron*, **170**, 312 (2019)
59. V.Kuchárová, J.Kuchár, A.Lüköová, R.Jendželovský, M.Majerník, P.Fedoročko, M.Vilková, I.D.Radojević, L.R.Čomić, I.Potočňák. *Polyhedron*, **170**, 447 (2019)
60. Saswati, M.Mohanty, A.Banerjee, S.Biswal, A.Horn, G.Schenk, K.Brzezinski, E.Sinn, H.Reuter, R.Dinda. *J. Inorg. Biochem.*, **203**, 110908 (2020)
61. Mehr-un-Nisa, M.Sirajuddin, S.Ali, M.N.Tahir, M.Iqbal. *Polyhedron*, **177**, 114273 (2020)
62. N.S.Rukk, L.G.Kuzmina, G.A.Davydova, G.A.Buzanov, S.K.Belus, E.I.Kozhukhova, V.M.Retivov, T.V.Ivanova, V.N.Krasnoperova, B.M.Bolotin . *Russ. Chem. Bull.*, **69**, 1394 (2020)
63. W.A.Wani, U.Baig, S.Shreaz, R.A.Shiekh, P.F.Iqbal, E.Jameel, A.Ahmad, S.H.Mohd-Setapar, M.Mushtaque, L.Ting Hun. *New J. Chem.*, **40**, 1063 (2016)
64. M.Arredondo, M.T.Núñez. *Mol. Aspects Med.*, **26**, 313 (2005)
65. M.E.Wall, S.C.Gallagher, J.Trewhella. *Annu. Rev. Phys. Chem.*, **51**, 355 (2000)
66. J.Li, F.Cao, H.L.Yin, Z.J.Huang, Z.T.Lin, N.Mao, B.Sun, G.Wang. *Cell Death Dis.*, **11**, 88 (2020)
67. Z.Trávníček, I.Popa, M.Čajan, R.Zbořil, V.Kryštof, J.Mikulík. *J. Inorg. Biochem.*, **104**, 405 (2010)
68. S.Y.Lee, A.Hille, I.Kitanovic, P.Jesse, G.Henze, S.Wölfl, R.Gust, A.Prokop. *Leuk. Res.*, **35**, 387 (2011)
69. K.Kowalski, A.Koceva-Chyła, A.Pieniazek, J.Bernasińska, J.Skiba, A.J.Rybarczyk-Pirek, Z.Jóźwiak. *J. Organomet. Chem.*, **700**, 58 (2012)
70. U.Basu, I.Khan, D.Koley, S.Saha, P.Kondaiah, A.R.Chakravarty. *J. Inorg. Biochem.*, **116**, 77 (2012)
71. A.Panja. *Polyhedron*, **43**, 22 (2012)
72. A.C.Gonçalves, T.S.Morais, M.P.Robalo, F.Marques, F.Avecilla, C.P.Matos, I.Santos, A.I.Tomaz, M.H.Garcia. *J. Inorg. Biochem.*, **129**, 1 (2013)
73. I.K.Sviridova, N.S.Sergeeva. **62**, *Russ. Chem. Bull.*, 2056 (2013)
74. K.Ghosh, N.Tyagi, P.Kumar, U.P.Singh. *Inorg. Chim. Acta*, **412**, 20 (2014)
75. A.S.Belov, A.V.Vologzhanina, V.V.Novikov, V.V.Negrutska, I.Y.Dubey, Z.A.Mikhailova, E.G.Lebed, Y.Z.Voloshin. *Inorg. Chim. Acta*, **421**, 300 (2014)
76. C.Spoerlein-Guettler, K.Mahal, R.Schobert, B.Biersack. *J. Inorg. Biochem.*, **138**, 64 (2014)
77. A.Valente, A.M.Santos, L.Côrte-Real, M.P.Robalo, V.Moreno, M.Font-Bardia, T.Calvet, J.Lorenzo, M.H.Garcia. *J. Organomet. Chem.*, **756**, 52 (2014)
78. A.Garai, U.Basu, I.Khan, I.Pant, A.Hussain, P.Kondaiah, A.R.Chakravarty. *Polyhedron*, **73**, 124 (2014)

79. J.Chen, Z.Luo, Z.Zhao, L.Xie, W.Zheng, T.Chen. *Biomaterials*, **71**, 168 (2015)
80. J.Vančo, Z.Šindelář, Z.Dvořák, Z.Trávníček. *J. Inorg. Biochem.*, **142**, 92 (2015)
81. A.Garai, I.Pant, P.Kondaiah, A.R.Chakravarty. *Polyhedron*, **102**, 668 (2015)
82. M.Y.Kong, L.Wang, Q.Y.Chen, X.L.Xu, W.L.Lu. *Spectrochim. Acta, Part A*, **151**, 790 (2015)
83. Y.Gou, J.Wang, S.Chen, Z.Zhang, Y.Zhang, W.Zhang, F.Yang. *Eur. J. Med. Chem.*, **123**, 354 (2016)
84. T.Sarkar, R.J.Butcher, S.Banerjee, S.Mukherjee, A.Hussain. *Inorg. Chim. Acta*, **439**, 8 (2016)
85. E.Kinski, P.Marzenell, W.Hofer, H.Hagen, J.A.Raskatov, K.X.Knaup, E.M.Zolnhofer, K.Meyer, A.Mokhir. *J. Inorg. Biochem.*, **160**, 218 (2016)
86. S.B.Chanu, S.Banerjee, M.Roy. *Eur. J. Med. Chem.*, **125**, 816 (2017)
87. K.Anđelković, M.R.Milenković, A.Pevec, I.Turel, I.Z.Matić, M.Vujčić, D.Sladić, D.Radanović, G.Brađan, S.Belošević, B.Čobeljić. *J. Inorg. Biochem.*, **174**, 137 (2017)
88. F.Asghar, A.Badshah, S.Fatima, S.Zubair, I.S.Butler, M.N.Tahir. *J. Organomet. Chem.*, **843**, 48 (2017)
89. A.Pilon, P.Gírio, G.Nogueira, F.Avecilla, H.Adams, J.Lorenzo, M.H.Garcia, A.Valente. *J. Organomet. Chem.*, **852**, 34 (2017)
90. A.Jana, B.K.Verma, A.Garai, P.Kondaiah, A.R.Chakravarty. *Inorg. Chim. Acta*, **493**, 127 (2019)
91. S.Daum, S.Babiy, H.Konovalova, W.Hofer, A.Shtemenko, N.Shtemenko, C.Janko, C.Alexiou, A.Mokhir. *J. Inorg. Biochem.*, **178**, 9 (2018)
92. B.Kaya, O.Şahin, M.Bener, B.Ülküseven. *J. Mol. Struct.*, **1167**, 16 (2018)
93. J.Ye, J.Ma, C.Liu, J.Huang, L.Wang, X.Zhong. *Biochem. Pharmacol.*, **166**, 93 (2019)
94. E.Hillard, A.Vessières, L.Thouin, G.Jaouen, C.Amatore. *Angew. Chem., Int. Ed.*, **45**, 285 (2005)
95. C.P.Matos, Z.Adiguzel, Y.Yildizhan, B.Cevatemre, T.B.Onder, O.Cevik, P.Nunes, L.P.Ferreira, M.D.Carvalho, D.L.Campos, F.R.Pavan, J.C.Pessoa, M.H.Garcia, A.I.Tomaz, I.Correia, C.Acilan. *Eur. J. Med. Chem.*, **176**, 492 (2019)
96. S.El Deeb, B.N.Ma, D.Baecker, R.Gust. *Inorg. Chim. Acta*, **487**, 76 (2019)
97. Q.Yao, J.Qi, Y.Zheng, K.Qian, L.Wei, M.Maimaitiyiming, Z.Cheng, Y.Wang. *J. Inorg. Biochem.*, **193**, 1 (2019)
98. L.P.Chan, Y.P.Tseng, H.Y.Ding, S.M.Pan, F.Y.Chiang, L.F.Wang, T.H.Chou, P.J.Lien, C.Liu, P.L.Kuo, C.H.Liang. *Phytomedicine*, **63**, 153005 (2019)
99. L.H.Abdel-Rahman, A.A.Abdelhamid, A.M.Abu-Dief, M.R.Shehata, M.A.Bakheet. *J. Mol. Struct.*, **1200**, 127034 (2020)
100. H.Skoupilova, M.Bartosik, L.Sommerova, J.Pinkas, T.Vaculovic, V.Kanicky, J.Karban, R.Hrstka. *Eur. J. Pharmacol.*, **867**, 172825 (2020)
101. E.A.Saad, H.A.Kiwan, M.M.Hassanien, H.E.Al-Adl. *J. Drug Deliv. Sci. Technol.*, **57**, 101671 (2020)
102. A.A.Hassoon, R.G.Harrison, N.Nawar, S.J.Smith, M.M.Mostafa. *J. Mol. Struct.*, **1203**, 127240 (2020)
103. A.M.Abu-Dief, L.H.Abdel-Rahman, A.A.Abdelhamid, A.A.Marzouk, M.R.Shehata, M.A.Bakheet, O.A.Almaghrabi, A.Nafady. *Spectrochim. Acta, Part A*, **228**, 117700 (2020)
104. P.Köpf-Maier, H.Köpf, E.W.Neuse. *Angew. Chem., Int. Ed. Engl.*, **23**, 456 (1984)
105. L.A.Ostrovskaya, I.K.Sviridova, N.S.Sergeeva, A.A.Simenel, L.V.Snegur. *Russ. Chem. Bull.*, **63**, 2405 (2014)
106. P.Köpf-Maier, H.Köpf, E.W.Neuse. *J. Cancer Res. Clin. Oncol.*, **108**, 336 (1984)
107. P.Köpf-Maier, H.Köpf. *Bioinorg. Chem. Struct. Bond.*, **70**, 103 (1988)
108. R.Manikandan, P.Vijayan, P.Anitha, G.Prakash, P.Viswanathamurthi, R.J.Butcher, K.Velmurugan, R.Nandhakumar. *Inorg. Chim. Acta*, **421**, 80 (2014)
109. R.Manikandan, P.Viswanathamurthi, K.Velmurugan, R.Nandhakumar, T.Hashimoto, A.Endo. *J. Photochem. Photobiol. B*, **130**, 205 (2014)
110. B.Şen, H.K.Kalhan, V.Demir, E.E.Güler, H.A.Kayali, E.Subaşı. *Mater. Sci. Eng. C*, **98**, 550 (2019)
111. M.Carcelli, M.Tegoni, J.Bartoli, C.Marzano, G.Pelosi, M.Salvalaio, D.Rogolino, V.Gandin. *Eur. J. Med. Chem.*, **194**, 112266 (2020)
112. H.Y.Khan, M.O.Ansari, G.G.H.A.Shadab, S.Tabassum, F.Arjmand. *Bioorg. Chem.*, **88**, 102963 (2019)
113. C.Hepokur, A.Günsel, M.N.Yarasir, A.T.Bilgiçli, B.Tüzün, G.Tüzün, I.Yaylim. *RSC Adv.*, **7**, 56296 (2017)
114. L.F.Chin, S.M.Kong, H.L.Seng, K.S.Khoo, R.Vikneswaran, S.G.Teoh, M.Ahmad, S.B.A.Khoo, M.J.Maah, C.H.Ng. *J. Inorg. Biochem.*, **105**, 339 (2011)
115. M.Lalia-Kantouri, M.Gdaniec, T.Choli-Papadopoulou, A.Badounas, C.D.Papadopoulos, A.Czapik, G.D.Geromichalos, D.Sahpazidou, F.Tsitouroudi. *J. Inorg. Biochem.*, **117**, 25 (2012)
116. S.B.Kumar, Z.Mahendrasinh, S.Ankita, R.Mohammedayaz, P.Pragna, E.Suresh. *Polyhedron*, **36**, 15 (2012)
117. A.I.Medvedev, V.V.Leshenko. *Tsitologiya*, **54**, 417 (2012)
118. S.Sathiyaraj, K.Sampath, G.Raja, R.J.Butcher, S.K.Gupta, C.Jayabalakrishnan. *Inorg. Chim. Acta*, **406**, 44 (2013)
119. H.Gopinathan, N.Komathi, M.N.Arumugham. *Inorg. Chim. Acta*, **416**, 93 (2014)
120. A.Kareem, H.Zafar, A.Sherwani, O.Mohammad, T.A.Khan. *J. Mol. Struct.*, **1075**, 17 (2014)
121. P.Ghosh, A.R.Chowdhury, S.K.Saha, M.Ghosh, M.Pal, N.C.Murmu, P.Banerjee. *Inorg. Chim. Acta*, **429**, 99 (2015)
122. C.Gökçe, N.Dilek, R.Gup. *Inorg. Chim. Acta*, **432**, 213 (2015)
123. G.Zhang, J.Tan, Y.Z.Zhang, C.Ta, S.Sanchez, S.Y.Cheng, J.A.Golen, A.L.Rheingold. *Inorg. Chim. Acta*, **435**, 147 (2015)
124. M.M.Abd-Elzaher, A.A.Labib, H.A.Mousa, S.A.Moustafa, M.M.Ali, A.A.El-Rashedy. *Beni-Suef Univ. J. Basic Appl. Sci.*, **5**, 85 (2016)
125. Q.P.Qin, J.L.Qin, T.Meng, W.H.Lin, C.H.Zhang, Z.Z.Wei, J.N.Chen, Y.C.Liu, H.Liang, Z.F.Chen. *Eur. J. Med. Chem.*, **124**, 380 (2016)

126. S.R.Morcelli, É.S.Bull, W.S.Terra, R.O.Moreira, F.V.Borges, M.M.Kanashiro, A.J.Bortoluzzi, L.L.F.Maciel, J.C.de A.Almeida, A.H.Júnior, C.Fernandes. *J. Inorg. Biochem.*, **161**, 73 (2016)
127. S.Abdolmaleki, M.Ghadermazi, M.Ashengroph, A.Saffari, S.M.Sabzkohi. *Inorg. Chim. Acta*, **480**, 70 (2018)
128. S.Parveen, G.Velmurugan, E.Sinn, P.Venuvanalingam, S.Govindarajan. *J. Photochem. Photobiol. B*, **189**, 152 (2018)
129. P.Nithya, R.Rajamanikandan, J.Simpson, M.Ilanchelian, S.Govindarajan. *Polyhedron*, **145**, 200 (2018)
130. H.EL Hamdani, M.EL Amane. *J. Mol. Struct.*, **1184**, 262 (2019)
131. Q.X.Sun, X.Wei, S.Q.Zhang, M.L.Chen, T.Yang, J.H.Wang. *Anal. Chim. Acta*, **1066**, 13 (2019)
132. O.O.Krasnovskaya, Y.V.Fedorov, V.M.Gerasimov, D.A.Skvortsov, A.A.Moiseeva, A.V.Mironov, E.K.Beloglazkina, N.V.Zyk, A.G.Majouga. *Arab. J. Chem.*, **12**, 835 (2019)
133. R.Fekri, M.Salehi, A.Asadi, M.Kubicki. *Inorg. Chim. Acta*, **484**, 245 (2019)
134. M.Kumbar, S.A.Patil, S.S.Toragalmath, S.S.Jawoor, A.Shettar. *Inorg. Chim. Acta*, **500**, 119210 (2020)
135. S.Perontsis, A.Dimitriou, P.Fotiadou, A.G.Hatzidimitriou, A.N.Papadopoulos, G.Psomas. *J. Inorg. Biochem.*, **196**, 110688 (2019)
136. A.D.M.Mohamad, M.J.A.Abualreish, A.M.Abu-Dief. *J. Mol. Liq.*, **290**, 111162 (2019)
137. H.EL Hamdani, M.EL Amane, C.Duhayon. *J. Mol. Struct.*, **1190**, 125 (2019)
138. Y.Thakur, R.Agrawal, M.Tripathi, M.K.Siddiqi, E.Mohapatra, R.H.Khan, R.Pande. *J. Mol. Struct.*, **1197**, 691 (2019)
139. S.Ali, V.Singh, P.Jain, V.Tripathi. *J. Saudi Chem. Soc.*, **23**, 52 (2019)
140. H.Bahron, S.S.Khaidir, A.M.Tajuddin, K.Ramasamy, B.M.Yamin. *Polyhedron*, **161**, 84 (2019)
141. C.Ravi, R.K.Vuradi, S.Avudoddi, M.Ramchander, S.Satyanarayana. *Russ. J. Bioorg. Chem.*, **45**, 273 (2019)
142. P.Bera, A.Aher, P.Brandao, S.K.Manna, G.Mondal, A.Jana, A.Santra, H.Jana, P.Bera. *Polyhedron*, **182**, 114503 (2020)
143. D.X.West, A.E.Liberta, S.B.Padhye, R.C.Chikate, P.B.Sonawane, A.S.Kumbhar, R.G.Yerande. *Coord. Chem. Rev.*, **123**, 49 (1993)
144. S.Roy, S.Saha, R.Majumdar, R.R.Dighe, A.R.Chakravarty. *Polyhedron*, **29**, 2787 (2010)
145. M.M.Ibrahim, A.M.M.Ramadan, G.A.M.Mersal, S.A.El-Shazly. *J. Mol. Struct.*, **998**, 1 (2011)
146. P.Jaividhya, R.Dhivya, M.A.Akbarsha, M.Palaniandavar. *J. Inorg. Biochem.*, **114**, 94 (2012)
147. G.Y.Li, K.J.Du, J.Q.Wang, J.W.Liang, J.F.Kou, X.J.Hou, L.N.Ji, H.Chao. *J. Inorg. Biochem.*, **119**, 43 (2013)
148. S.Sathiyaraj, K.Sampath, R.J.Butcher, R.Pallepogu, C.Jayabalakrishnan. *Eur. J. Med. Chem.*, **64**, 81 (2013)
149. M.Ganeshpandian, R.Loganathan, S.Ramakrishnan, A.Riyasdeen, M.A.Akbarsha, M.Palaniandavar. *Polyhedron*, **52**, 924 (2013)
150. J.W.Liang, Y.Wang, K.J.Du, G.Y.Li, R.L.Guan, L.N.Ji, H.Chao. *J. Inorg. Biochem.*, **141**, 17 (2014)
151. J.Lu, Q.Sun, J.L.Li, L.Jiang, W.Gu, X.Liu, J.L.Tian, S.P.Yan. *J. Inorg. Biochem.*, **137**, 46 (2014)
152. K.Zheng, M.Jiang, Y.T.Li, Z.Y.Wu, C.W.Yan. *J. Mol. Struct.*, **1058**, 97 (2014)
153. X.Li, C.Fang, Z.Zong, L.Cui, C.Bi, Y.Fan. *Inorg. Chim. Acta*, **432**, 198 (2015)
154. S.M.Emam, I.E.T.El Sayed, N.Nassar. *Spectrochim. Acta, Part A*, **138**, 942 (2015)
155. C.Acilan, B.Cevatemre, Z.Adiguzel, D.Karakas, E.Ulukaya, N.Ribeiro, I.Correia, J.C.Pessoa. *Biochim. Biophys. Acta — Gen. Subj.*, **1861**, 218 (2017)
156. K.E.Prosser, S.W.Chang, F.Saraci, P.H.Le, C.J.Walsby. *J. Inorg. Biochem.*, **167**, 89 (2017)
157. F.Zhao, W.Wang, W.Lu, L.Xu, S.Yang, X.M.Cai, M.Zhou, M.Lei, M.Ma, H.J.Xu, F.Cao. *Eur. J. Med. Chem.*, **146**, 451 (2018)
158. J.Deng, P.Yu, Z.Zhang, J.Wang, J.Cai, N.Wu, H.Sun, H.Liang, F.Yang. *Eur. J. Med. Chem.*, **158**, 442 (2018)
159. U.M.Rafi, D.Mahendiran, V.G.Devi, M.Doble, A.K.Rahiman. *Inorg. Chim. Acta*, **482**, 160 (2018)
160. S.S.Massoud, F.R.Louka, G.T.Ducharme, R.C.Fischer, F.A.Mautner, J.Vančo, R.Herchel, Z.Dvořák, Z.Trávníček. *J. Inorg. Biochem.*, **180**, 39 (2018)
161. K.Dhahagani, M.P.Kesavan, G.G.V.Kumar, L.Ravi, G.Rajagopal, J.Rajesh. *Mater. Sci. Eng. C*, **90**, 119 (2018)
162. B.-L.Fei, S.Tu, Z.Wei, P.Wang, C.Qiao, Z.-F.Chen. *Eur. J. Med. Chem.*, **176**, 175 (2019)
163. X.Shi, H.Fang, Y.Guo, H.Yuan, Z.Guo, X.Wang. *J. Inorg. Biochem.*, **190**, 38 (2019)
164. M.Simunkova, P.Lauro, K.Jomova, L.Hudecova, M.Danko, S.Alwasel, I.M.Alhazza, S.Rajcaniova, Z.Kozovska, L.Kucerova, J.Moncol, L.Svorc, M.Valko. *J. Inorg. Biochem.*, **194**, 97 (2019)
165. A.Mirzaahmadi, S.A.Hosseini-Yazdi, E.Safarzadeh, B.Baradaran, E.Samolova, M.Dusek. *J. Mol. Liq.*, **293**, 111412 (2019)
166. Y.Cui, L.Wu, W.Yue, F.Lian, J.Qu. *J. Mol. Struct.*, **1191**, 145 (2019)
167. P.Alper, M.Erkisa, H.M.Genckal, S.Sahin, E.Ulukaya, F.Ari. *J. Mol. Struct.*, **1196**, 783 (2019)
168. K.H.Mashat, B.A.Babgi, M.A.Hussien, M.Nadeem Arshad, M.H.Abdellattif. *Polyhedron*, **158**, 164 (2019)
169. S.K.Pandey, D.P.Singh, S.Pratap, G.Marverti, R.J.Butcher. *Polyhedron*, **170**, 431 (2019)
170. S.C.Manna, S.Mistri, A.Patra, M.K.Mahish, D.Saren, R.K.Manne, M.K.Santra, E.Zangrando, H.Puschmann. *Polyhedron*, **171**, 77 (2019)
171. T.E.Kokina, L.A.Glinskaya, L.A.Sheludyakova, Y.A.Eremina, L.S.Klyushova, V.Y.Komarov, D.A.Piryazev, A.V.Tkachev, S.V.Larionov. *Polyhedron*, **163**, 121 (2019)
172. J.A.Eremina, E.V.Lider, T.S.Sukhikh, L.S.Klyushova, M.L.Perepechaeva, D.G.Sheven', A.S.Berezin, A.Y.Grishanova, V.I.Potkin. *Inorg. Chim. Acta*, **510**, 119778 (2020)
173. C.Icsel, V.T.Yilmaz, Ş.Aydinlik, M.Aygun. *Eur. J. Med. Chem.*, **202**, 112535 (2020)
174. L.M.Balsa, M.C.Ruiz, L.Santa Maria de la Parra, E.J.Baran, I.E.León. *J. Inorg. Biochem.*, **204**, 110975 (2020)
175. S.Li, J.Zhao, Y.Guo, Y.Mei, B.Yuan, N.Gan, J.Zhang, J.Hu, H.Hou. *J. Inorg. Biochem.*, **210**, 111102 (2020)

176. A.Drzewiecka-Antonik, P.Rejmak, M.Klepka, A.Wolska, A.Chrzanowska, M.Struga. *J. Inorg. Biochem.*, **212**, 111234 (2020)
177. O.O.Krasnovskaya, D.A.Guk, A.E.Naumov, V.N.Nikitina, A.S.Semkina, K.Y.Vlasova, V.Pokrovsky, O.O.Ryabaya, S.S.Karshieva, D.A.Skvortsov, I.V.Zhirkina, R.R.Shafikov, P.V.Gorelkin, A.N.Vaneev, A.S.Erofeev, D.M.Mazur, V.A.Tafeenko, V.I.Pergushov, M.Y.Melnikov, M.A.Soldatov, V.V.Shapovalov, A.V.Soldatov, R.A.Akasov, V.M.Gerasimov, D.A.Sakharov, A.A.Moiseeva, N.V.Zyk, E.K.Beloglazkina, A.G.Majouga. *J. Med. Chem.*, **63**, 13031 (2020)
178. R.A.Khan, M.R.Khan, M.Usman, F.Sayeed, H.A.Alghamdi, S.Alrumman, W.Alharbi, N.N.Farshori, M.M.Al-Oqail, M.R.Siddiqui, M.A.Khanjer, A.Alsalme. *Saudi J. Biol. Sci.*, **27**, 2164 (2020)
179. D.H.Cai, C.L.Zhang, Q.Y.Liu, L.He, Y.J.Liu, Y.H.Xiong, X.Y.Le. *Eur. J. Med. Chem.*, **213**, 113182 (2021)
180. Y.-P.Zhang, Z.-Y.Ma, P.-P.Qiao, C.-Y.Gao, J.-L.Tian, J.-Z.Zhao, W.-J.Du, J.-Y.Xu, S.-P.Yan. *J. Mol. Struct.*, **1236**, 130278 (2021)
181. C.Santini, M.Pellei, V.Gandin, M.Porchia, F.Tisato, C.Marzano. *Chem. Rev.*, **114**, 815 (2014)